

Hans RIEGLER

Murine brown adipogenesis and microRNAs

Diploma Thesis



Institute for Genomics and Bioinformatics
Graz University of Technology
Petersgasse 14, 8010 Graz
Head: Univ.-Prof. Dipl.-Ing. Dr.techn. Rudolf Stollberger

Supervisor:

Univ.-Ass. Dipl.-Chem. Dr.rer.nat. Marcel Scheideler

Evaluator:

Univ.-Ass. Dipl.-Chem. Dr.rer.nat. Marcel Scheideler

Graz, April, 2012

Statuary Declaration

I declare that I have authored this thesis independently, that I have not used other than the declared sources / resources, and that I have explicitly marked all material which has been quoted either literally or by content from the used sources.

Date:

Signature:

Abstract

Obesity has become a major health problem and a global burden for society. Its etiology is multifactorial and involves complex interactions while the fundamental cause is a dysbalance in energy homeostasis, with energy uptake exceeding energy expenditure. With the discovery of brown adipose tissue (BAT) a counterpart for white adipose tissue (WAT) was found. BAT is known for energy dissipation by thermogenesis in case of cold stress. *Uncoupling protein 1 (Ucp1)* is considered as hallmark of brown adipocytes as it is responsible for heat production by uncoupling the electron transport chain from ATP production. White and brown adipocytes are found together in visceral and subcutaneous fat depots and transdifferentiation between types of adipocytes is of utmost medical interest to specifically act on energy metabolism. MicroRNAs (miRNAs) are a novel class of non-coding RNAs and have emerged as key post-transcriptional regulators of gene expression.

Aim of this study is to identify and characterize endogenous miRNAs in adipocytes, which are relevant in lipid metabolism and thus pose potential targets for the prevention and treatment of obesity.

miR-26a, a candidate from an earlier screening performed within the "RNA Biology Group" at the Institute for Genomics and Bioinformatics, Graz University of Technology, has already been shown to modulate human brown adipogenesis. Experiments in murine in vitro model systems confirmed 'browning' effects of miR-26a in brown iBACs, but not in white 3T3-L1 adipocytes. Levels of miR-26a increased during murine brown adipogenesis and was found to be even more elevated upon β -adrenergic stimulation.

Furthermore, white 3T3-L1 cells and their ability to perform brown adipogenesis was tested. Enhancement of Ucp1 mRNA by chronic peroxisome proliferator-activated receptor gamma (*Ppar γ*) activation and upon longterm β -adrenergic stimulation can be reported and was even stronger when dexamethasone and IBMX for induction of adipogenesis were omitted.

Finally, a global screening for miRNAs in different biological conditions (WAT, BAT and cold exposed WAT) was performed by miRNA microarray analysis, in order to identify candidates with differential expression.

Kurzfassung

Fettleibigkeit ist mittlerweile ein massives Gesundheitsproblem und eine globale gesellschaftliche Herausforderung. Die Ätiologie ist multifaktoriell und beinhaltet komplexe Wechselwirkungen, die Ursache ist jedoch ein Ungleichgewicht im Energiehaushalt zugunsten der Energieaufnahme. Mit der Entdeckung von braunem Fettgewebe (BAT) wurde ein Gegenspieler zum weißen Fettgewebe (WAT) gefunden. BAT bildet Wärme (Thermogenese) bei Kälte. *Uncoupling Protein 1 (Ucp1)* ist der Marker brauner Fettzellen und die funktionelle Einheit, die Wärme durch die Entkopplung der Elektronentransportkette von der ATP Produktion erzeugt. Weiße und braune Adipozyten findet man gemeinsam in viszeralen und subkutanen Fettdepots, und die Transformation zwischen beiden Fettzelltypen ist die Beeinflussung des Energiestoffwechsels von höchstem medizinischen Interesse. MikroRNAs sind nicht kodierende RNAs und sind als posttranskriptionale Schlüsselregulatoren etabliert.

Das Ziel dieser Studie sind die Identifizierung und Charakterisierung endogener MikroRNAs, welche im Fettmetabolismus von Adipozyten relevant sind, um Ansätze zur Prävention und Behandlung von Fettleibigkeit zu finden.

Für miR-26a, einem Kandidat aus einer früheren Studie der "RNA Biology Group" am Institut für Genomik und Bioinformatik, Technische Universität Graz, konnte bereits eine Wirkung auf die humanen braune Adipogenese gezeigt werden. Experimente mit miR-26a in einem murinen in vitro Modell bestätigten diese Effekte in braunen iBACs, aber nicht in weißen 3T3-L1 Adipozyten. Die endogene miR-26a Expression nahm während der braunen Adipogenese zu und wurde durch β -adrenerge Stimulation noch verstärkt. Tests an 3T3-L1 Zellen, braune Adipogenese zu vollziehen, zeigten eine Erhöhung der *Ucp1* mRNA Expression durch chronische Aktivierung von *Ppar γ* . Einen solcher Effekt konnte auch durch langfristige β -adrenerge Stimulierung erreicht werden, der ohne Verwendung von Dexamethason und IBMX für die Induktion der Adipogenese noch verstärkt wurde. Abschließend wurde eine genomweite MikroRNA-Expressionsstudie mittels Microarrays in WAT, BAT und Kälte exponiertem WAT durchgeführt, in der mehrere MikroRNA-Kandidaten mit differenzieller Expression identifiziert werden konnten.

Aim of this thesis

The aim of this study is to show conserved microRNA-26a (miR-26a) effects in murine brown adipogenesis. Therefore, isolated and immortalized cells from brown adipose tissue (iBACs), white 3T3-L1 and 3T3-F442A cells are characterized for their ability to express *Uncoupling protein 1 (Ucp1)*, the hallmark of brown adipogenesis during adipogenesis and upon β -adrenergic stimulation. A valid brown cell model is investigated for endogenous miR-26a levels, and effects of overexpression and inhibition of miR-26a. White cell models are investigated for enhancement of *Ucp1* levels by chronic peroxisome proliferator-activated receptor gamma (*Ppar γ*) activation, by different induction cocktails (with or without dexamethasone and 1-methyl-3-isobutylxanthine (IBMX)), upon β -adrenergic stimulation and overexpression of miR-26a.

Furthermore, a global miRNA profiling of murine brown adipose tissue is performed, where two biological conditions are examined : WAT vs. BAT and WAT vs. cold exposed WAT (WATce). The aim is to reveal differential expression in both setups, leading to novel miRNA candidates with potential involvement in the distinction between white and brown adipocytes.

Acknowledgements

First I want to thank the state of Austria for studentship, making it possible to study at a university. This diploma thesis in particular was funded by GEN-AU and the Faculty of Electrical and Information Engineering.

Foremost I would like to express my deep gratitude to my supervisor Dr. Marcel Scheideler who guided my whole work in a very wise and clever way while my mentor Dr. Michael Karbiener opened deep insights in biology by always having time and enthusiasm to answer my questions in depth. For technical introduction I want to thank my skillful and patient teacher Claudia Neuhold and all colleagues of the Institute for Genomics and Bioinformatics who introduced me to all the new things, gave advice, reviewed my concepts and also supported work by creating a great and motivating working atmosphere.

Last, I want to thank my nieces and nephews for cheering my mind, sisters and friends having an ear to entrust my thoughts and my parents for setting an example of how things could be done.

CONTENTS

1 Introduction.....	1
1.1 Obesity.....	1
1.2 Adipose tissue	4
1.2.1 Function and mechanism	5
1.2.2 Morphology	8
1.2.3 Transdifferentiation between WAT and BAT	12
1.2.4 Stages in adipocyte differentiation	17
1.2.5 Cell models	23
1.2.6 Transcriptional Control	25
1.3 MicroRNAs.....	29
1.3.1 Biogenesis.....	29
1.3.2 Mode of action.....	31
1.3.3 Target Prediction	35
1.3.4 MicroRNAs in obesity	36
2 Materials and Methods	38
2.1 Materials	38
2.1.1 Standard laboratory equipment.....	38
2.1.2 Instruments	38
2.1.3 Microarrays	39
2.1.4 Analysis of triglyceride accumulation	39
2.1.5 RNA isolation	39
2.1.6 Cell culture	40
2.1.7 quantitative real-time RT-PCR	40
2.1.8 Software and web tools.....	41
2.2 Methods	42
2.2.1 Cell culture	42
2.2.2 Molecular biology and biochemistry	46
2.2.3 Statistical analysis.....	49
3 Results	50
3.1 Murine cell model characterization in brown adipogenesis	50
3.1.1 iBACs as appropriate cell model for murine brown adipogenesis.....	50
3.1.2 3T3-L1 cells and their ability to express <i>Ucp1</i>	53

3.2 Endogenous miR-26a levels in murine brown adipogenesis	55
3.2.1 Endogenous miR-26a levels in iBACs	56
3.2.2 Beta-adrenergic stimulation of miR-26a levels in iBACs.....	56
3.2.3 Beta-adrenergic stimulation of miR-26a levels in 3T3-L1 cells	57
3.3 Exogenous modulation of miR-26a levels in murine adipogenesis	59
3.3.1 Overexpression of miR-26a in iBACs.....	59
3.3.2 Overexpression of miR-26a in 3T3-L1 and -F442A cells	60
3.3.3 Inhibition of miR-26a	62
3.4 Global miRNA profiling in murine adipose tissue.....	63
4 Discussion of Methods	67
4.1 Cell culture experiments	67
4.1.1 Cell models	67
4.1.2 Differentiation of cells.....	67
4.1.3 Transfection of adipocytes	68
4.1.4 Quantitative real time RT-PCR.....	69
4.1.5 Statistics to analyze biological replicates	69
4.2 Microarray	70
5 Discussion of Results	72
5.1 Murine cell models in brown adipogenesis	72
5.2 Endogenous miR-26a levels in murine brown adipogenesis	73
5.3 Exogenous modulation of miR-26a levels in murine adipogenesis	75
5.4 Global miRNA signatures in murine adipose tissue.....	75
6 Literature	76

1 Introduction

1.1 Obesity

Obesity can be defined as abnormal or excessive fat accumulation, possibly impairing health¹. Several approaches for scaling obesity are used: body fat percentage, Body Mass Index (BMI), waist-to-hip-ratio, waist circumference and waist-to-height ratio. Although there is no agreement which index should be used^{2,3,4,5}, BMI is the most considered⁶ scale for obesity and calculated, for both sexes and for all ages of adults, as $(\text{weight} / \text{height}^2)$. WHO defined obesity as BMI equal or greater than 30. Obviously this is a simple classification regarding tools but also for diagnostic conclusions BMI should be only a rough guide¹. In addition, fat distribution plays an important role, as it is established that increased intra-abdominal/visceral fat (central or apple-shaped obesity) promotes a high risk of metabolic disease, whereas increased subcutaneous fat in the thighs and hips (peripheral or pear-shaped obesity) exerts little or no risk⁷.

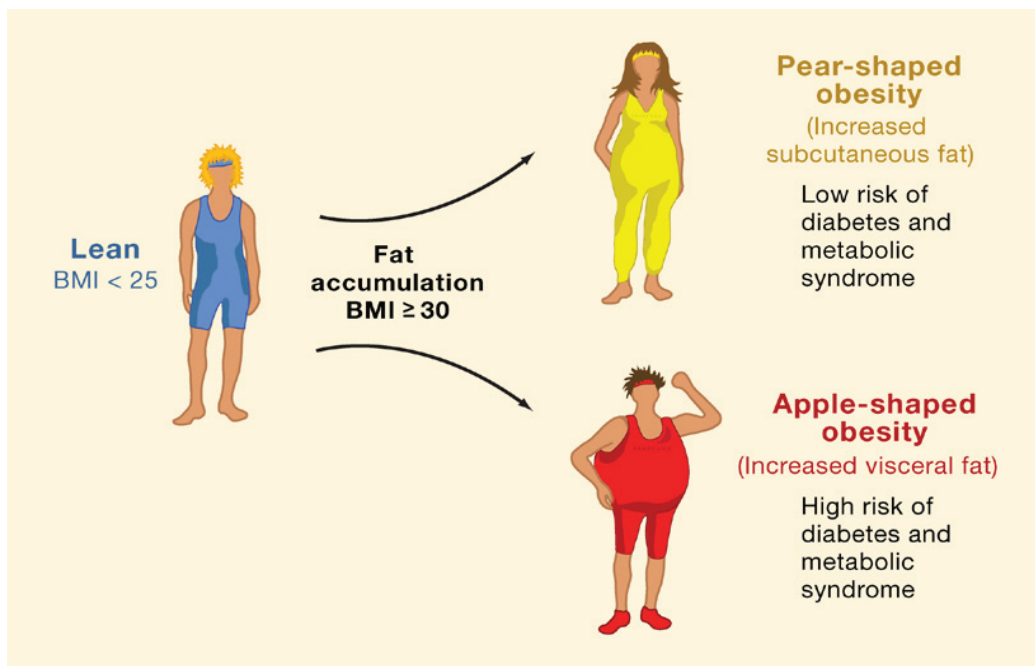


Figure 1. Obesity is the consequence of an excess in fat accumulation⁸ and is defined by a body mass index of ≥ 30 . Fat distribution can be estimated by measurements of the ratio of waist to the hip circumference (WHR). Obese individuals with low WHR, (subcutaneous or pear-shaped obesity) are at low risk for metabolic complications of obesity, whereas individuals with a high WHR (visceral or apple-shaped obesity) are at high risk for these complications⁹.

The fundamental cause of Obesity is a disbalance of energy uptake and expenditure. Further etiology is multifactorial and involves complex interactions among the genetic background, hormones and social environmental factors⁶. Several key factors are listed by the WHO (Table 1) and might be a result of societal changes, lack of supportive policies in sectors such as health, agriculture, transport, urban planning, environment, food processing, distribution, marketing and education¹.

Table 1. Summary of strength of evidence on factors that might promote or protect against weight gain and obesity (WHO, 2003)¹⁰.

Strength of evidence	Decreased risk	Increased risk
Convincing	Regular physical activity High dietary intake of fiber	Sedentary lifestyle High intake of energy-dense foods
Probable	Home and school environments that support healthy food choices for children Breastfeeding	Adverse socioeconomic conditions in developed countries
Possible	Low glycemic index foods	Large portion sizes High proportion of food prepared outside the home (developed countries) Rigid restraint/periodic disinhibition eating patterns
Insufficient	Increased eating frequency	Alcohol

Globally, the World Health Organization reports that obesity has more than doubled since 1980. 1.5 billion adults were estimated to be overweighted in 2008, where 500 million corresponded to obesity and nearly 43 million children (age < 5 years) were overweight in 2010.¹ Although obesity is preventable, 65% of the world's population lives in countries where overweight and obesity kills more people than underweight¹ and 2 to 7% of total health care costs are attributable to obesity¹¹.

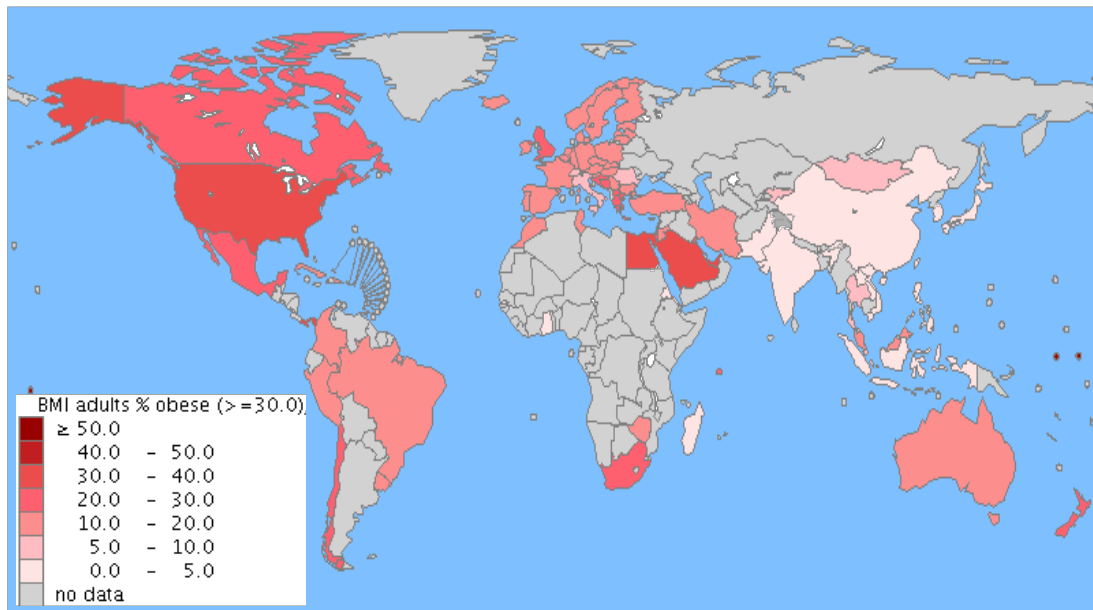


Figure 2. Worldwide obesity distribution (most recent data from 2012).¹² An obese adult is classified as having a Body Mass Index equal or greater than 30.

Obesity is classified as a disease (code E66 of the International Statistical Classification of Diseases and Related Health Problems, 10th revision (ICD-10)) and is associated with many other diseases. Epidemiological studies show the relationship between excess weight, abdominal fatness and risk of a wide range of illnesses^{13,14,15,16}.

Table 2. Approximate relative risk of physical health problems associated with obesity¹⁷.

Relative risk >3	Relative risk 2-3	Relative risk 1-2
Type II diabetes	Coronary heart disease	Cancer Reproductive
Gallbladder disease	Hypertension	hormone abnormalities
Dyslipidemia	Osteoarthritis	Polycystic ovary
Insulin resistance	Hyperuricemia and gout	syndrome Impaired
Breathlessness		fertility Low back pain
Sleep apnea		Increased risk of
		anesthesia complications
		Fetal defects (associated
		with maternal obesity)

Obesity predispose to many follow-up diseases, also due to the fact that the adipose organ is the body's largest endocrine organ revealing broad influence¹⁸.

Minding the fundamental cause of obesity (disbalance of energy uptake and expenditure) two imperative therapeutic ways rise: Either energy uptake is lowered or energy expenditure is increased. There are several approaches differing in

efficiency and side effects. So far, bariatric surgery is the only effective treatment for morbidly obese patients and currently remains the only option for achieving and maintaining weight loss. Bariatric surgical procedures help reducing the caloric intake by modifying the anatomy of the gastrointestinal tract, which, of course, carries inherent risks¹⁹. Usual current treatment modalities include lifestyle modification (e.g. increased physical activity), diet and pharmacological agents. Unfortunately, non-surgical pharmacological interventions have displayed limited efficacy and unpleasant side effects^{19,20}. Hence, a better understanding of the molecular mechanisms linking adipose tissue development, function and expansion is indispensable in order to find and develop novel and valid therapeutic strategies²¹.

1.2 Adipose tissue

Adipose tissue in human is located in many regions of the body. Moreover, two major types of adipose tissue, with opposing functions in energy balance, are established: white and brown adipose tissue.

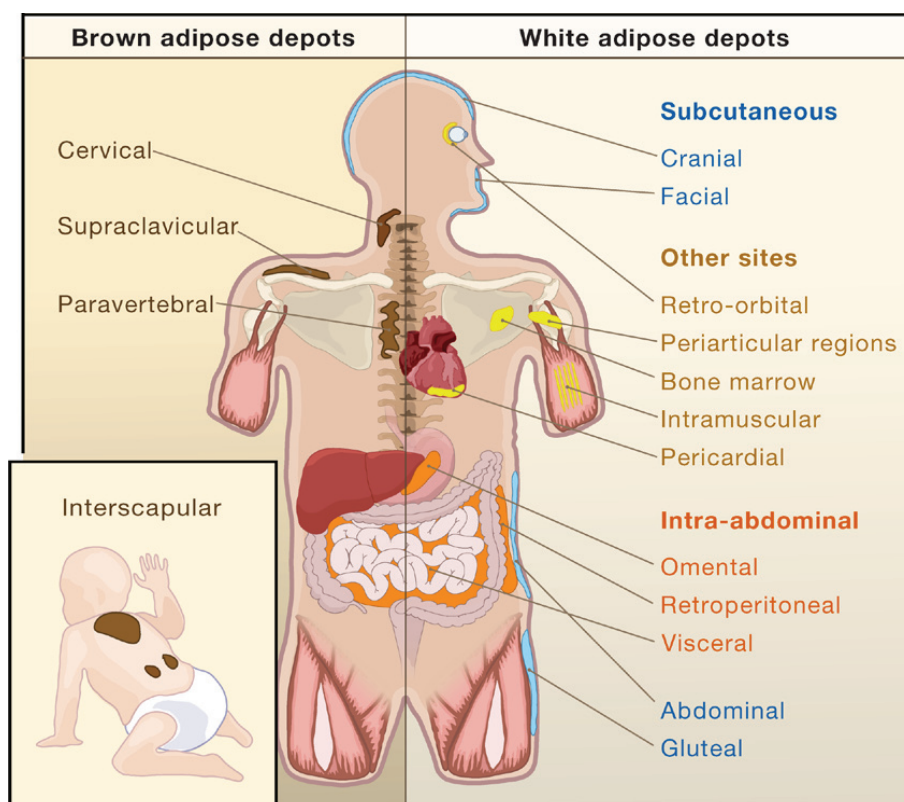


Figure 3. In humans, depots of white and brown adipose tissue are found in areas all over the body,⁸ with subcutaneous and intra-abdominal depots representing the main compartments for fat storage. Brown adipose tissue is abundant at birth and still present in adulthood but to a lesser extent.

1.2.1 Function and mechanism

White adipose tissue (WAT)

The smallest-sized molecules having the greatest energy content are fatty acids, and the cells specializing in their accumulation are white adipocytes²². Classic white fat is known for providing insulation, mechanical support and storage of surplus fuels²³. White adipocytes are highly specialized cells that store large amounts of triglycerides during periods of energy excess. The lipid store of WAT in human is capable to provide energy in form of triglycerides (TG) for several days, while liver's glycogen store (short-term-energy-buffer) is depleted in several hours. When energy uptake by nutrition is higher than energy expenditure, white adipocytes are able to mediate uptake of food-derived free fatty acids (FFA) from the bloodstream by key lipogenic enzymes (lipoprotein lipase (*LPL*), FA transporters and FA binding proteins). FFA are reesterified and stored in form of neutral TG. In addition to FFA uptake, glucose can be imported via glucose transporters (*GLUT4*), transformed to acetyl-CoA (via glycolysis and pyruvate dehydrogenase) and subsequently used for de novo FA synthesis (via fatty acid synthase (*FASN*)). In case of scarce food, a protein cascade (lipases) breaks down TG into glycerol and FFA, to be released into the blood.

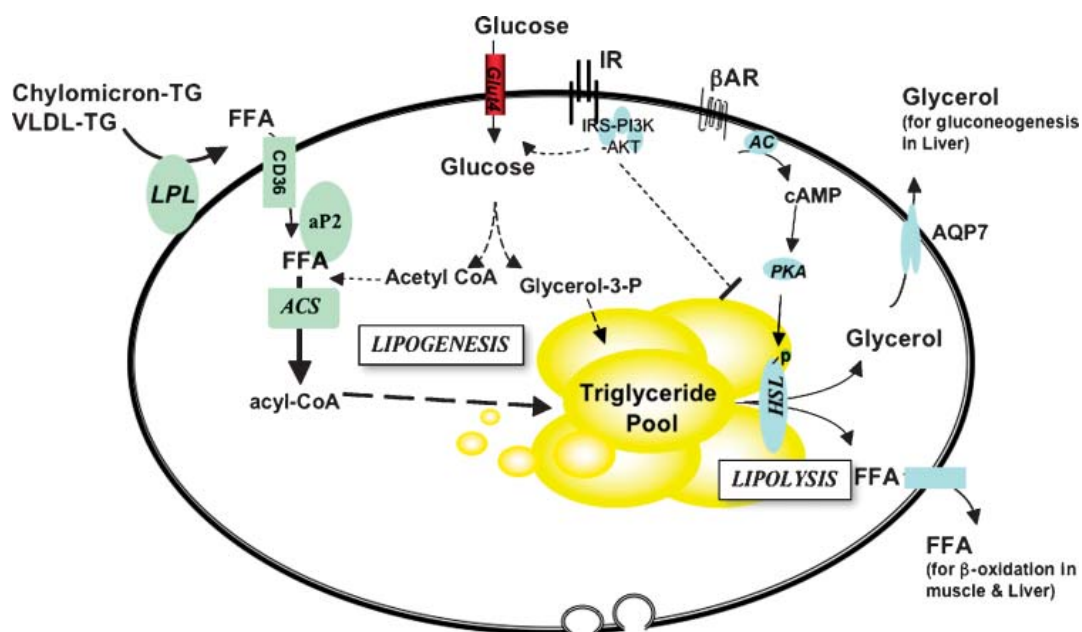


Figure 4. Lipid metabolism in adipocytes.²³ Adipocytes are equipped with the biochemical machinery to function effectively as the body's fuel store. To do this, it must mediate lipogenesis

[conversion of FFA to triglycerides (TG) for storage] and lipolysis (breakdown of triglycerides to FFA and glycerol). It is also sensitive to changing nutritional cues. For example, it is insulin-sensitive [insulin stimulates glucose uptake and lipogenesis and inhibits lipolysis] and subject to adrenergic regulation [stimulates lipolysis and adaptive thermogenesis (brown adipose tissue)]. *AC*, adenylate cyclase; *ACS*, acyl-CoA synthase; *AKT*, AKR mouse thymoma viral proto-oncogene; *AR*, adrenergic receptor; *HSL*, hormone sensitive lipase; *IR*, insulin receptor; *PI3K*, phosphatidylinositol 3-kinase; *PKA*, protein kinase A.

Brown adipose tissue (BAT)

Brown adipose tissue in human adults is present to a low extent and abundant at birth. It plays an important role in all ages for energy storage and body heating. Brown adipocytes store less lipids and have more mitochondria than white adipocytes. Almost all genes expressed in white adipocytes are expressed in brown adipocytes, but they also express some distinct genes, including uncoupling protein-1 (*Ucp1*)²¹. Both types of adipocytes are involved in energy metabolism, although with reverse effects. Brown adipocytes are known for energy dissipation by thermogenesis in case of cold or abundance of energy (free fatty acids). *Ucp1* is the functional core-element of thermogenesis and therefore the hallmark of brown adipocytes.²⁴ Thermogenesis is guided by the sympathetic nervous system^{25,26,27} and release of Norepinephrine onto beta adrenergic receptors to initiate degradation of triglycerides from lipid droplets^{28,29,30,31}, leading into free fatty acids, activating *Ucp1* for thermogenesis^{32,33,34}.

Ucp1 is a member of the mitochondrial carrier protein family uncoupling the respiratory chain by increasing the permeability of the inner mitochondrial membrane³⁵. Protons that have been pumped out to the intermembrane space, usually serving ATP synthase for energy production, are now able to shorten the respiratory chain by channeling through *Ucp1* into the mitochondrial matrix^{36,37}. Electron pumping complexes of the mitochondria are functionally unaffected but continuously loaded performing fast substrate oxidation (but at low rate of ATP production), hence an increased fraction of the food and the oxygen available in the blood is taken up by the tissue and combusted therein, collectively leading to an increased heat production.³⁸ Recent studies may distinguish brown adipocytes in origin (brown vs. brite) or represent an intermediate state of brown adipogenesis

(see views of transdifferentiation, chapter 1.2.3), where function is obviously related to brown by the presence of *Ucp1* protein³⁸.

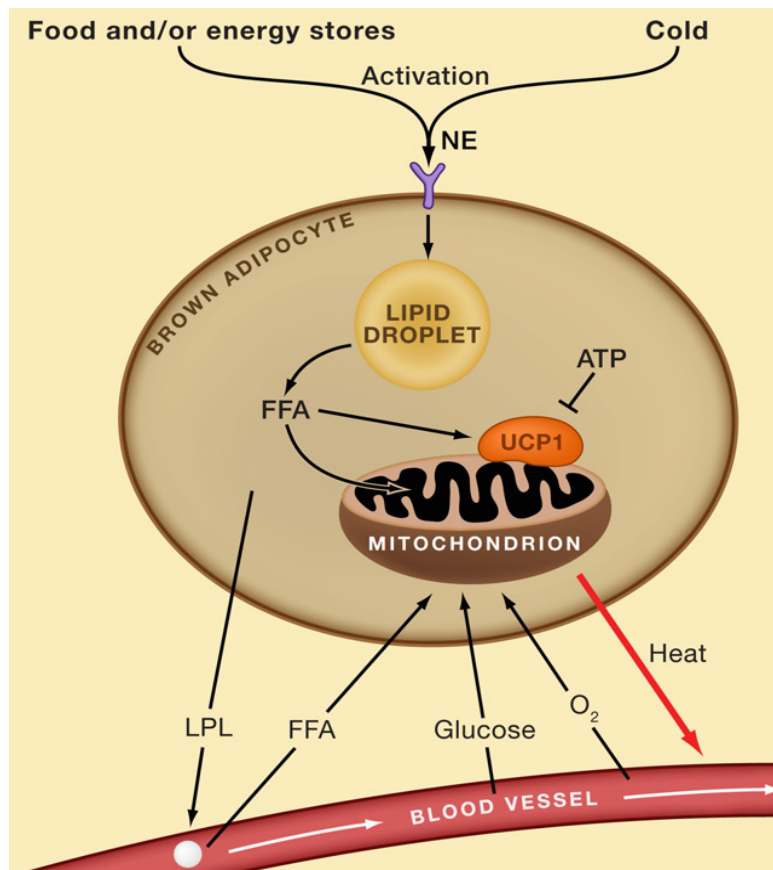


Figure 5. Regulation of the activity and recruitment of brown adipose tissue.³⁹ In the resting state, the protonophoric activity of *Ucp1* in the inner mitochondrial membrane is inhibited by cytosolic purine nucleotides, notably ATP. When brown adipose tissue is activated from centers in the brain affected by environmental temperature or acute food intake (or body energy stores), norepinephrine (NE) is released from the sympathetic nerves innervating the tissue. In the mature brown adipocytes, this leads to hydrolysis of the triglycerides stored in the lipid droplets, and the released fatty acids (FFA) in some way activate *Ucp1*, overcoming the inhibition. Due to the uncoupling activity of *Ucp1*, the combustion of different substrates may now proceed: fatty acids released from triglycerides (fat droplets) in the tissue are initially the main source, but successively the main substrates for heat production are delivered from the circulation. NE induces release of lipoprotein lipase (LPL) that degrades chylomicrons and VLDL in the circulation, and the released fatty acids are combusted, and there is also stimulated glucose uptake into the cells (making active brown adipose tissue visible in fluorodeoxyglucose PET scanning). The combustion of all these substrates demands high oxygen uptake, and the blood leaving the tissue is heated but extremely oxygen depleted. During chronic stimulation, NE also stimulates the progenitor cells in the tissue to proliferate and the brown preadipocytes to differentiate (a process that can also be stimulated by *Pparγ* ligands). NE has also an antiapoptotic effect on the cells. Thus, chronic stimulation will increase the total capacity of the tissue, a process referred to as recruitment.

In general the functional activity of brown adipose tissue in any given physiological condition is determined by two factors:

1. The acute effects of norepinephrine, resulting in stimulation of thermogenesis, through utilization of different degrees of the maximal capacity (“**activity state**”)
2. The total thermogenic capacity found at that particular time in the tissue (“**recruitment state**”)⁴⁰

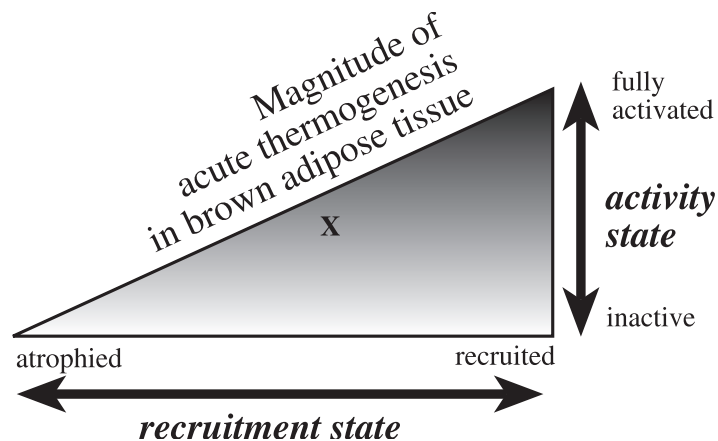


Figure 6. Activity state and recruitment state.⁴⁰ Thermogenesis (here illustrated as gray scale intensity) in brown adipose tissue at a given moment (here illustrated by X) is determined by the degree of activation at that moment (y-axis) and can alter within seconds, but the capacity for thermogenesis is determined by the degree of recruitment of the tissue (x-axis) and needs days or weeks to be significantly altered. The degree of activity is determined by the acute rate of sympathetic stimulation (norepinephrine release) in the tissue, and the recruitment state is mainly determined by the chronic level of sympathetic stimulation.

The capacity is determined in its turn by the total number of brown adipocytes in the tissue plus the degree of differentiation of the tissue, including the mitochondrial density and amount of *Ucp1*³⁸ (also see Stages in adipocyte differentiation, chapter 1.2.4 1.2.4 below).

1.2.2 Morphology

From a original sight adipocytes are divided in three groups (also see Original view of transdifferentiation of WAT and BAT, chapter 1.2.3), while morphologically it is a multi-depot organ called the "adipose organ"⁴¹. It is composed of two main subcutaneous depots (anterior and posterior) and several visceral depots and all depots are composed of two cytotypes such as white and brown adipocytes⁴², with

the possibility of physiologically reversible transdifferentiation²². Morphologically, brite (brown in white) adipocytes are suggested to correspond to an intermediate state²² but are probably not distinguishable by cytotype. At least brown, brite and white adipocytes have a lot in common morphologically with varying degrees of severity. Although the ability to contain triglycerides is uncommon in mammalian cells, adipocytes share it with hepatocytes and striated muscle cells²².

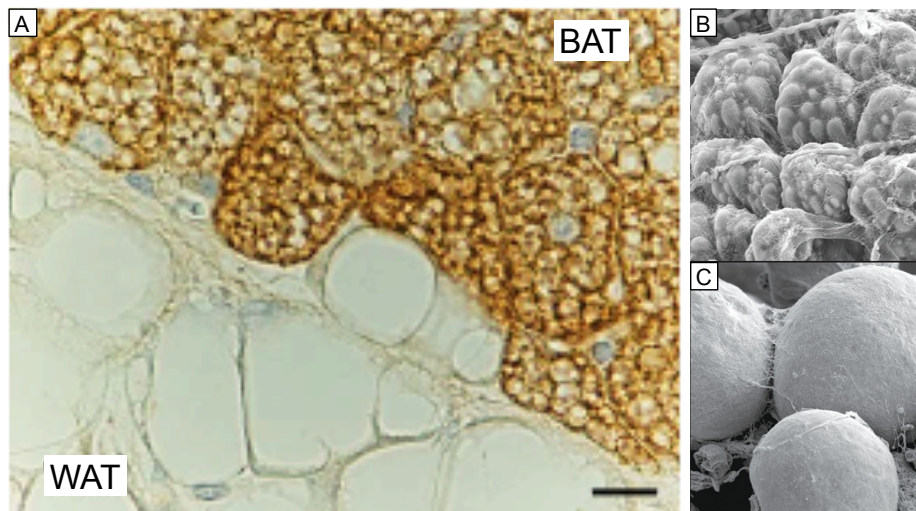


Figure 7. Mouse adipose organ (A)²². Anterior subcutaneous depot, interscapular area. Light microscopy of a section where the transition between brown (BAT) and white adipose tissue (WAT) is visible. Note the different cytoplasmic lipid accumulation: mostly unilocular in WAT and multilocular in BAT. Only BAT is intensely stained by *Ucp1* antibodies (immunohistochemistry ABC method, primary antibody: anti-sheep *Ucp1* dilution 1:4000, Bar = 25 μ m. Scanning electron microscope image of brown (B) and white (C) adipocytes⁴³.

White adipose tissue (WAT)

A crucial feature of WAT subserving accumulation, storage and rapid release of fatty acids is its capacity to expand. Indeed, adipocytes can grow in volume by 6–7 times. From the morphological standpoint, more than 90% of the white fat cell volume is made up of a single, spherical, lipid vacuole separated from the rest of the cytoplasm by a non-membranous electron-dense barrier containing functionally important proteins such as perilipin⁴⁴. The thin cytoplasm contains the nucleus, characteristically squeezed by the large lipid vacuole, a usually under-developed Golgi apparatus, rough endoplasmic reticulum made up of short, isolated cisternae, rare lysosomes, and thin, elongated mitochondria with short, randomly arranged cristae. Numerous pinocytotic vesicles are found at the level of

the outer cytoplasmic membrane, where a distinct basal membrane is also present.²² Several of these features can also be seen during the development of adipocyte precursors, or preadipocytes^{45,46}. The least differentiated preadipocyte stage seems to be the one where the cell is integrated into the wall of WAT capillaries⁴⁷ and even there small adipocytes (measuring 5-10 microns in diameter, roughly one-tenth of the adult diameter) are easily distinguished from any other poorly differentiated cell element by its early displayed morphological features and a high nucleus–cytoplasm ratio since the basal membrane²². A white adipocyte undergoing intense lipolysis acquires a distinctive morphology, with cell projections characterized by the presence of several microvilli-like structures that can be seen since the early phase of lipolysis, when the lipid vacuole is still quite large⁴¹. Cells in a more advanced stage of delipidization may exhibit numerous projections, and the lipid vacuole progressively shrinks. Smooth endoplasmic reticulum becomes abundant and is characteristically arranged around the lipid vacuoles⁴¹.

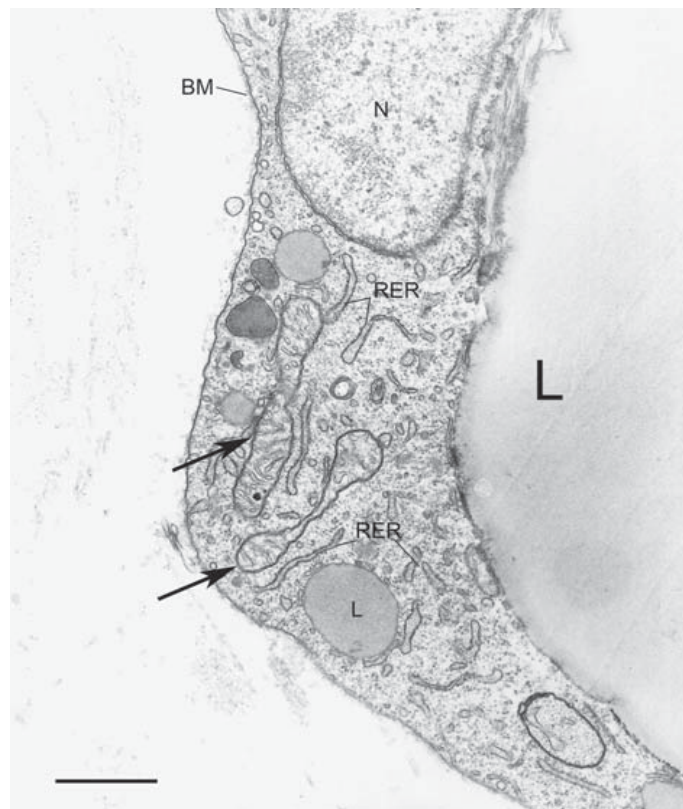


Figure 8. Rat adipose organ: epididymal depot.²² Electron microscopy of the peripheral part of a white adipocyte. Elongated mitochondria with randomly oriented cristae are visible (arrows). N = nucleus; RER = rough endoplasmic reticulum; large L = main lipid droplet; small L = peripheral lipid droplet; BM = basal membrane. Bar = 0.7 μ m.

Brown adipose tissue (BAT)

Long before the discovery of BAT's role, the name adipocyte has been given to this cell type because it contains large amounts of lipids but in contrast to WAT, triglycerides usually serve as an essential substrate for the fundamental function of brown adipocytes²². In fact the purpose of these cells is to perform thermogenesis (see Function and mechanism of BAT, chapter 1.2.1).

Morphologically, brown adipocytes differ from white fat cells essentially in their multilocular cytoplasmic lipids and the numerous special mitochondria. These have a spherical or ovoid shape and are rich in lamellar cristae, which contain a protein, *Ucp1*, subserving their thermogenic activity^{48,49}. Exposure to temperatures below thermoneutrality activates BAT directly, through adrenergic fibers that stimulate thermogenesis via neuro-adipose junctions. Noradrenaline acts via $\beta 3$ receptors⁵⁰. $\beta 3$ agonists have similar pharmacological effects as cold exposure⁵¹. The numerous mitochondria and rich vascularity of the tissue are the main reasons for the brown color of BAT, setting it apart from WAT even on gross inspection. The other organelles of brown adipocytes have similar characteristics as those of white adipocytes, including a distinct basal membrane on the outer side of the plasma membrane. The spherical central nucleus of brown adipocytes is not usually squeezed by the lipid vacuoles in the cytoplasm. Mature brown adipocytes are approximately half the size of white adipocytes. Their nucleus and size therefore denote a lower degree of elasticity and expansibility compared with white fat cells. However, both cell types are characterized by a fairly variable morphology depending on functional status^{41,52}. Brown preadipocytes of classic interscapular BAT are characterized by a structural marker that is almost not found in white preadipocytes, i.e. large mitochondria whose morphology foreshadows that of mature cell mitochondria (pretypical mitochondria)⁵³. Other characteristics are the presence of glycogen granules and the basal membrane. Therefore, these cells are not only clearly distinguishable morphologically from the other cell types in the adipose tissue, but they are also easily discerned from white preadipocytes based on their characteristic pretypical mitochondria.

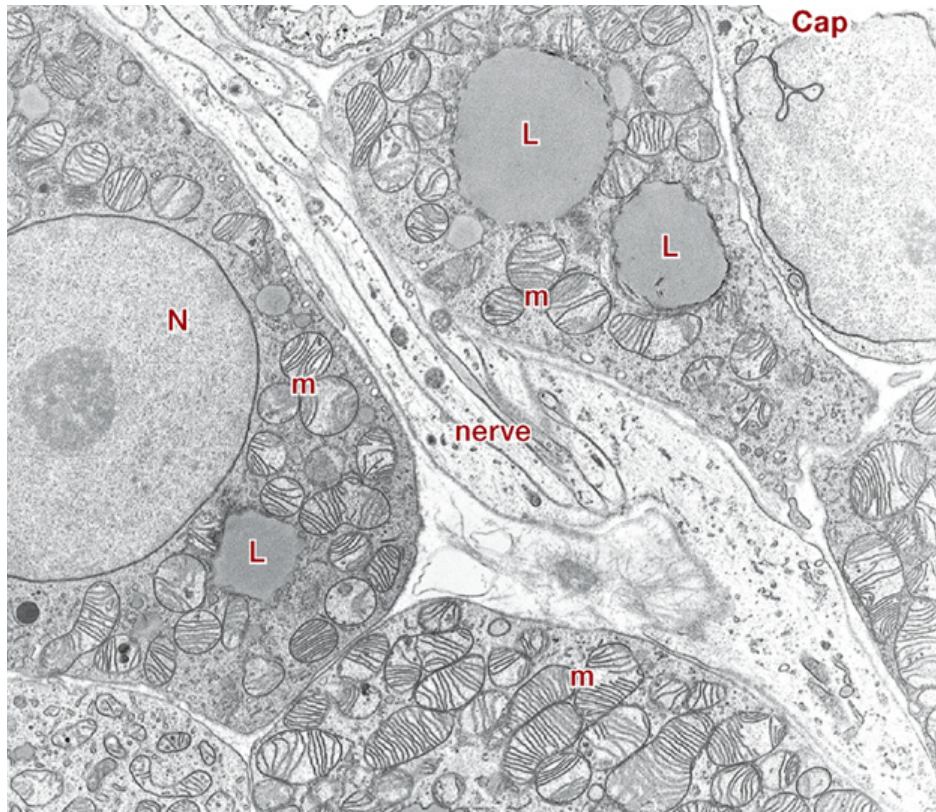


Figure 9. Transmission electron microscopic appearance of BAT.⁴³ Brown adipocytes with the cytoplasm filled with large mitochondria (some indicated as “m”) and small lipid droplets (L). A parenchymal nerve can be seen among the adipocytes. N, nucleus; Cap, capillary.

1.2.3 Transdifferentiation between WAT and BAT

The adipose organ already offers one example of physiological and reversible transdifferentiation beside the transdifferentiation of WAT and BAT, namely the female mammary gland. White-to-brown transdifferentiation is of medical interest, because the brown phenotype of the adipose organ is associated to obesity resistance, and drugs inducing this phenotype curb murine obesity and related disorders.²²

Transdifferentiation as a process is not completely investigated. Morphologists distinguish by function (thermogenic activity) leading to 2 types of adipocytes (brown and white) and suggest further distinction in development, thereby adding an intermediate state of paucilocular lipid droplets (see also figure in chapter Morphological view of Transdifferentiation between WAT and BAT, chapter 1.2.3), probably corresponding to brite or brown adipocytes. Other studies looked at adipocytes by origin, suggesting 3 types of adipocytes (white, brite, brown)^{54,55,56,57}

corresponding to marker genes (see also figure in chapter Original view of Transdifferentiation between WAT and BAT, chapter 1.2.3).

Morphological view

In all mammals including humans, most white and brown adipocytes are found together in visceral and subcutaneous depots (adipose organ) despite, or probably because, their reverse function in energy metabolism. Indeed, they share the same progenitor niche and starting point for white and brown adipogenesis *in vivo*²². A growing body of evidence suggests that the reason for such anatomical arrangement is their plasticity, which under appropriate stimulation allows direct conversion of one cell type into the other according to requirements.

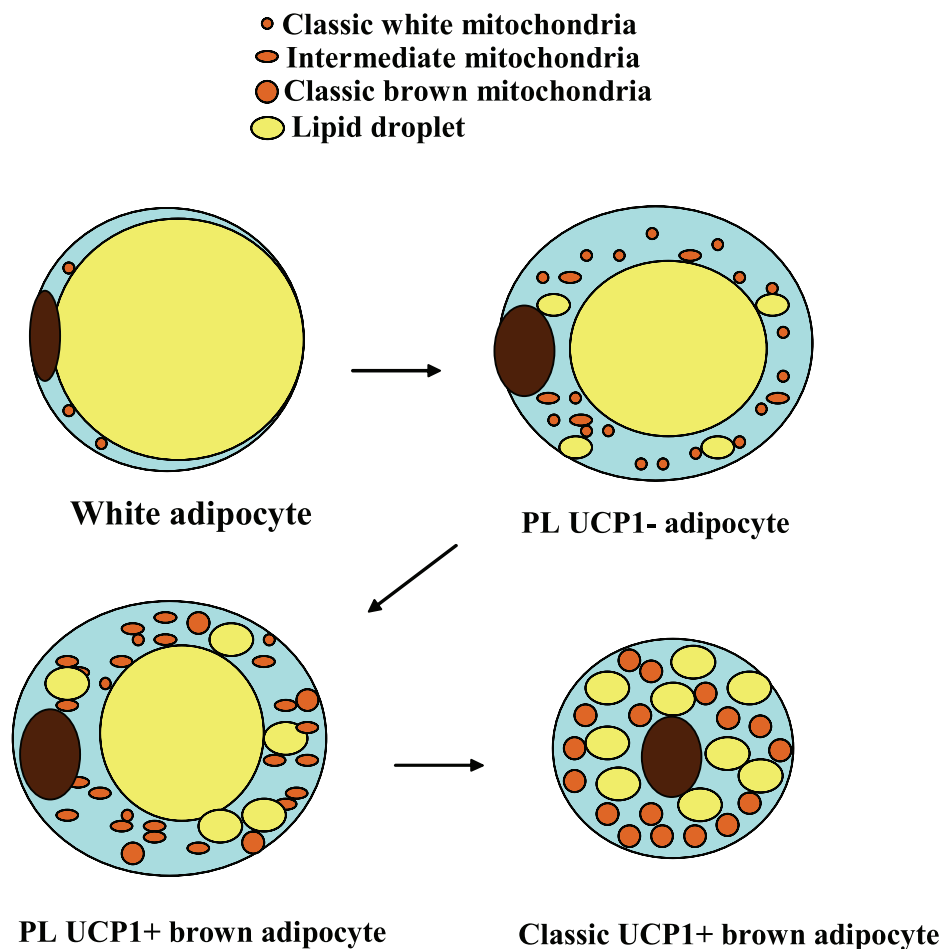


Figure 10. Stages of white to brown transdifferentiation.⁵⁸ Schematic showing the transitional steps of transdifferentiation from white into brown adipocytes. Adipocytes were identified as unilocular (UL; containing a single large vacuole), paucilocular (PL; exhibiting a large vacuole surrounded by at least 5 small lipid droplets), or multilocular (ML; containing more than 5 small homogenous lipid droplets).

Whether transdifferentiation describes direct transformation²² of a differentiated cell into another mature cell with different morphological and functional characteristics in physiological conditions or via an additional step of de-differentiation⁵⁹ is unclear.

Anyway, thermogenically active cells are characterized by numerous, small lipid vacuoles and plentiful spherical mitochondria rich in laminar cristae containing abundant *Ucp1*. The closer the temperature to thermoneutrality, the larger and less numerous the lipid vacuoles; at the same time mitochondria shrink and cristae numbers decrease in parallel with the decreased synthesis of *Ucp1* and its immunoreactivity^{41,38}. The morphology of the under-stimulated brown adipocyte is therefore more akin to that of the white adipocyte. Additionally, quantitative studies have shown that the BAT increase seen in cold-exposed animals corresponds to a reduction in WAT that is unrelated to apoptosis.²²

In animals treated with $\beta 3$ agonists, 80%–95% of newly formed brown adipocytes do not display proliferation markers and present all the morphological stages of white-to-brown transition^{60,61}, which would be a supplement of brite adipocytes idea from morphologists view.

BAT is activated through adrenergic fibers that stimulate thermogenesis, obviously related to the activity of the sympathetic nervous system. The number of such fibers in the adipose organ is proportional to the overall amount of brown adipocytes and hence increases upon cold exposure together, suggesting a role of the sympathetic nervous system playing a role in the phenotypic differentiation of preadipocytes and transdifferentiation of mature adipocyte. Whereby, data suggest that development of new brown adipocytes from preadipocytes appears to be a minor phenomenon⁵⁸.

Immunohistochemically, only in the morphological condition after transdifferentiation from brown to white, the once brown adipocyte is immunoreactive for protein S-100⁶², a protein used to detect white adipocytes⁶². Conversely, leptin cannot be detected in brown adipocytes of cold-exposed animals, but after transdifferentiation to white^{63,64,65}, implying a unidirectional transdifferentiation.⁴¹

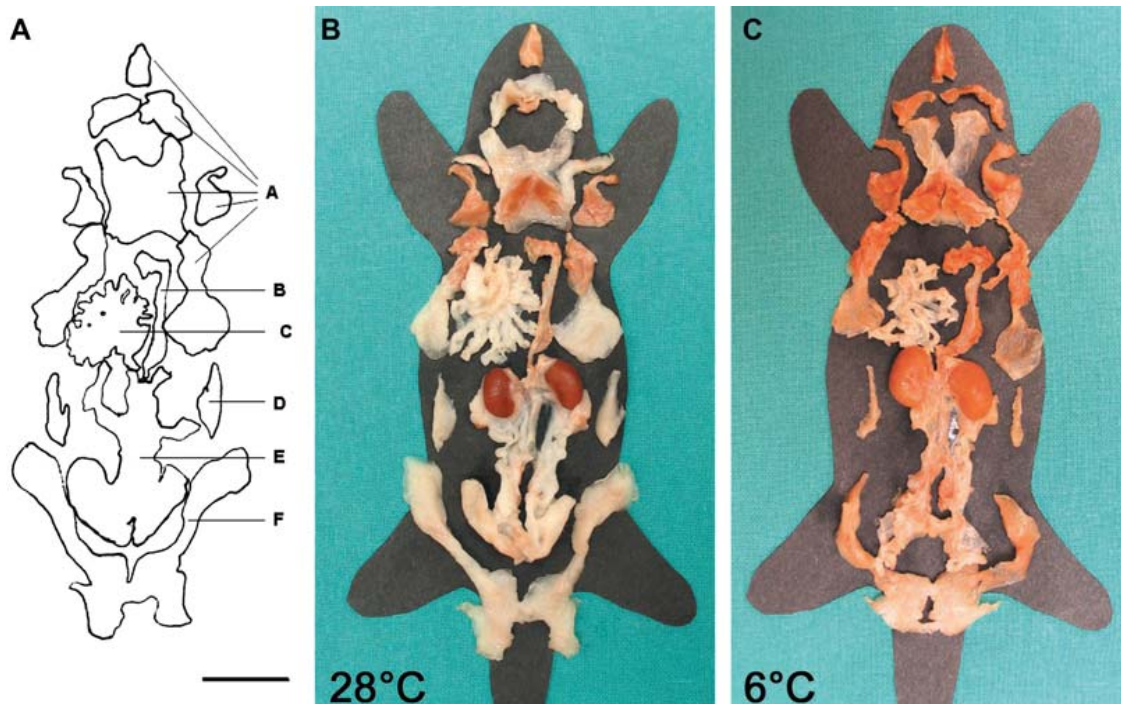


Figure 11. Gross anatomy of mouse adipose organ (adult female Sv129 mice)²². Middle: mouse kept at warm temperature (28°C for 10 days). Right: mouse kept at cold temperature (6°C for 10 days). Note the different colour of the organ, due to the increase of brown adipose tissue and decrease of white adipose tissue contained in the organ. The organ is made up of two subcutaneous depots (A and F): anterior (A) (composed of: deep cervical, superficial cervical, interscapular, subscapular, axillothoracic) and posterior (F) (composed of: dorsolumbar, inguinal, gluteal); and of several visceral depots: mediastinal (B), mesenteric (C), retroperitoneal (D), and abdominopelvic (composed of: perirenal, periovarian, parametrial, perivesical) (E); Bar = 1 cm.

Original view

Brown adipocytes express almost all the genes that are expressed in white adipocytes²¹. Because of their shared ability to accumulate lipids, brown and white adipocytes have classically been considered to be closely related cell types. Interestingly, brown adipocytes and muscle cells share a common origin and in this respect are distinct from white adipocytes. Additionally to classical brown and white adipocytes, brite (brown in white) adipocytes were observed and characterized^{66 54}.

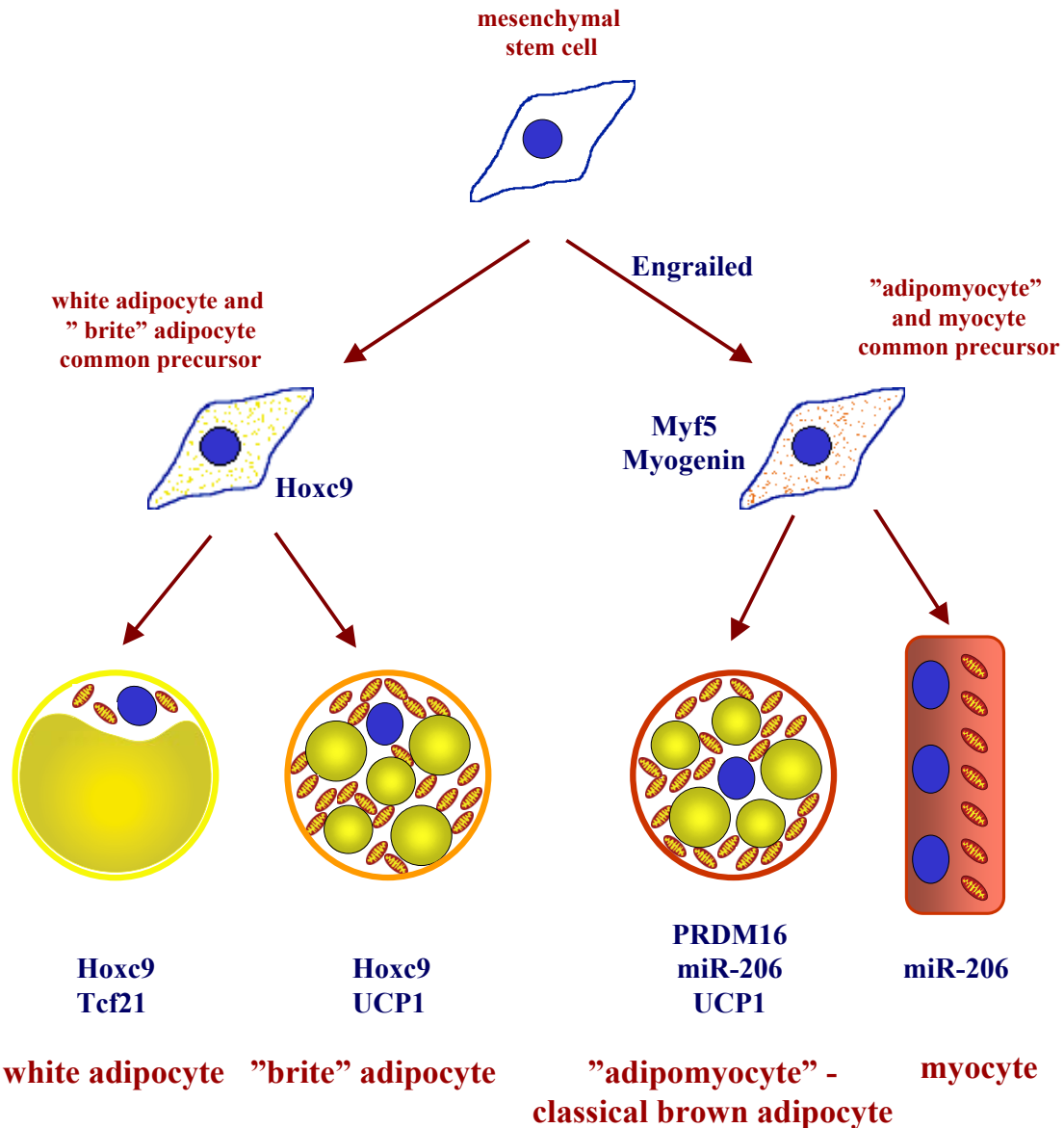


Figure 12. Subtypes of adipocytes and their origins.⁵⁴ Based on literature^{55,56,67}, (at least) three types of adipocytes should be distinguished: the classical brown adipocytes (the "adipomyocytes"), the "brite" adipocytes (i.e. the brown-adipocyte-like adipocytes induced in white adipocyte cultures), and the genuine white adipocytes. The "adipomyocytes" share their origin with myocytes, while "brite" and white adipocytes have a different origin.

In 2006, Atit and colleagues⁵⁵ observed that cells deriving from the central dermomyotome, molecularly defined as cells that at some time in their development had expressed the homeobox transcription factor Engrailed 1 (En1), developed into three types of tissue: dermis, muscle and brown adipose tissue (WAT was not developed at that time), thus implying a close developmental relationship between brown adipocytes and myocytes. Additionally, in 2007 cell cultures of precursors from BAT - but not cultures of WAT precursors - initially

demonstrated a remarkable expression of genes that had always been considered to be muscle specific; thus these brown adipocytes expressed a myogenic signature that was not shared by the white adipocytes, clearly indicating different origins of WAT and BAT⁵⁶. Also muscle specific microRNAs (myomirs) were expressed and maintained in brown adipocytes but not in white adipocytes⁶⁸. Further it was demonstrated that cells expressing the myogenic transcription factor *Myf5* during development could develop into muscle or BAT, but never into WAT⁶⁷. At least, a clear distinction between brown adipocyte and myocyte could be done by expression of PRDM16^{67,69,70}.

However, a not insignificant expression of the "brown-fat specific" uncoupling protein-1 (*Ucp1*) can be found in vivo depots considered to be WAT, in response to chronic β -adrenergic stimulation^{57,71,72,61,73} or in response to chronic *Ppar γ* -agonist stimulation^{74,75,76,77,78,79}. In situ, the adipocyte is exposed to distinctive but different external agents (neuronal transmitter substances, hormones, cytokines, etc.) giving rise to the idea that there is a second origin of brown like adipocyte, finally proven by primary cultures of white- and brown-fat precursor cells. Primary cultures of the most "pure" white-fat depot, those obtained from epididymal WAT^{72,80}, treated with the potent *Ppar γ* ligand rosiglitazone, promoted *Ucp1* gene expression⁵⁴. A subset of white adipocytes was initiated to express a broad but nonetheless incomplete array of classical brown-adipocyte marker genes, able to perform norepinephrine-induced thermogenesis. Obviously, brite (brown in white) adipocytes distinguish molecularly and developmentally from classical brown adipocytes but demonstrating thermogenesis.⁵⁴

1.2.4 Stages in adipocyte differentiation

The least differentiated preadipocyte stage seems to be the one where the cell is integrated into the wall of adipose capillaries. Tang et al.⁴⁷ demonstrated that the majority of adipocytes descend from a pool of proliferating progenitors that are already committed, either prenatally or early in postnatal life. These progenitors reside in the mural cell compartment of the adipose vasculature⁴⁵ and show specific molecular markers⁸¹. Thus, the adipose vasculature appears to function as a progenitor niche and starting point for white and brown adipogenesis in vivo.²²

Generally assuming a unidirectional process of a less specialized cell becoming committed, several stages, from the earliest steps of cellular differentiation in

mesodermal germ layer of stem cells to mature adipocytes, are passed. During adipocyte differentiation, acquisition of the adipocyte phenotype is characterized by chronological changes in the expression of numerous genes, primarily taking place at the transcriptional level⁸². Viewed in a simple way, genes contributing to adipogenesis are activated and inhibitory genes to adipogenesis or simply unnecessary for adipose cell function are repressed, involving a highly regulated and coordinated cascade of transcription factors⁸³ and microRNAs⁸⁴. Several cell lines in human and murine adipogenesis are established to study adipocyte differentiation⁸⁵.

Overview of stages

There are two major phases of adipogenesis²¹:

1. **Determination** involves the commitment of the pluripotent stem cell to a preadipocyte. Although morphologically there is no difference, the cell has lost its potential to differentiate into other cell types after this phase.
2. During **differentiation** the preadipocyte acquires the machinery to become a mature adipocyte. Lipid transport and synthesis, insulin sensitivity and secretion of adipocyte specific proteins has to be ensured during early changes of gene expressions, late events and terminal differentiation.

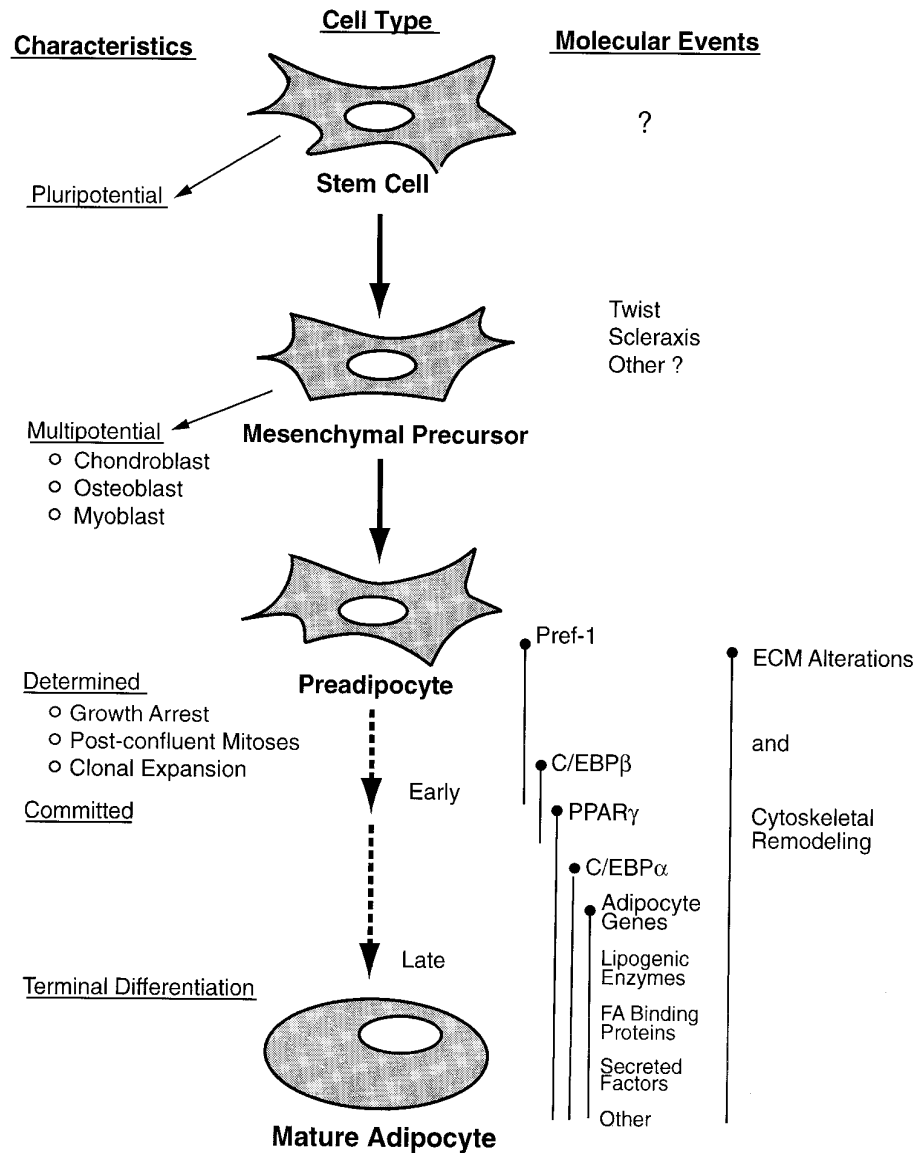


Figure 13. Overview of stages in adipocyte differentiation⁸². Our current understanding of adipocyte differentiation indicates that a pluripotent stem cell precursor gives rise to a mesenchymal precursor cell with the potential to differentiate along mesodermal lineages of myoblast, chondroblast, osteoblast, and adipocyte. As discussed in text, given appropriate environmental and gene expression cues, preadipocytes undergo clonal expansion and subsequent terminal differentiation. Selected molecular events accompanying this process are indicated to right, with their approximate duration reflected by the solid line. *Ppar γ* , peroxisome proliferator activated receptor- γ ; *C/ebp*, CCAAT/enhancer binding protein; *pref-1*, preadipocyte factor- 1; ECM, extracellular matrix; FA, fatty acid.

Although both phases are crucial, molecular regulation of terminal differentiation is more extensively characterized than commitment because most studies have used cell lines that have a restricted potential to differentiate into other cell types.

One major characteristic of preadipose cell lines, as well as primary preadipocytes during differentiation, is **growth arrest**, termed "day zero". Interestingly not cell confluence or cell-cell contact per se appears to be required⁸⁶ but mainly two transcription factors acting cooperatively (*C/ebpa* and *Pparγ* described in detail in chapter 1.2.6 Transcriptional control). Induction cocktails containing Insulin, dexamethasone and 1-methyl-3-isobutylxanthine (IBMX) at day zero are used to shift cells to the next step of commitment: one or two post confluent population doublings, to amplify the population of committed cells (clones)⁸⁶. Although some of the checkpoint proteins for mitosis also regulate aspects of adipogenesis²¹, mitotic clonal expansion is not performed by all cell lines (e.g. primary preadipocytes derived from human adipose tissue) and its must for differentiation is controversial⁸⁷. Although it is helpful to schematize the stages of adipocyte differentiation into a hierarchy of molecular events, an accurate chronology of the **earliest steps in adipocyte differentiation** has not been elucidated. Growth arrest and clonal expansion are accompanied by complex changes in the pattern of gene expression that can differ with the cell culture models and the specific differentiation protocols employed.⁸² Expression of lipoprotein lipase (LPL) mRNA has often been cited as an early sign of adipocyte differentiation^{88,89,90,91}, LPL is secreted by mature adipocytes and plays a central role in controlling lipid accumulation^{92,93}. However, LPL expression occurs spontaneously at confluence and is independent of the addition of agents required for adipocyte differentiation^{94,95}. During adipocyte differentiation cells convert from a fibroblastic to a spherical shape (not associated with lipid accumulation), beside a switch of collagen gene expression^{96,97}, it is likely that these morphological changes also influence the expression of two families of transcription factors, *C/ebp* and *Ppar*, increasing their expression levels since this event and remaining high during lifetime (see Transcriptional control)

Another transcription factor induced very early during adipocyte differentiation is sterol regulatory element binding protein-1c (*Srebp-1c*)/adipocyte determination and differentiation factor 1 (ADD1), a bHLH-leucine zipper protein that is involved in cholesterol metabolism⁹⁸.

Late events during terminal differentiation of adipocytes are accompanied by increased de novo lipogenesis and acquired sensitivity to insulin. The activity, protein, and mRNA levels for enzymes involved in triacylglycerol metabolism

increase 10- to 100-fold^{99,100,101}. Glucose transporters¹⁰², insulin receptor number, and insulin sensitivity increase. During adipocyte differentiation, there is a loss of β 1-adrenergic receptors and an increase in the β 2- and the β 3-subtypes; this results in an increase in total adrenergic receptor number^{103,104,105,106}. As mentioned in early steps in adipocyte differentiation, *Ppar γ* and *C/ebp α* remain at high levels all time as increasing and activating several genes during terminal differentiation (see also chapter "Transcriptional Control")

Finally, experiments with BALB/c 3T3 mesenchymal stem cells indicate that cells that have progressed beyond a specific stage in the differentiation process are committed to subsequent terminal differentiation and can neither dedifferentiate nor reenter mitosis^{107,108}. However, recent evidence indicates that the precise stage beyond which adipocytes can be considered terminally differentiated is not clearly defined and at least partially differentiated human preadipocytes are still capable of cell division as assessed histologically and by flow cytometry¹⁰⁹.

As described above (events of terminal differentiation), β -adrenergic receptors in general increase during differentiation, where stimulation of BAT affects proliferation and differentiation (e.g. quantity of *Ucp1* protein and mitochondria)⁴⁰ resulting in brown adipogenesis as shown in the figure below.

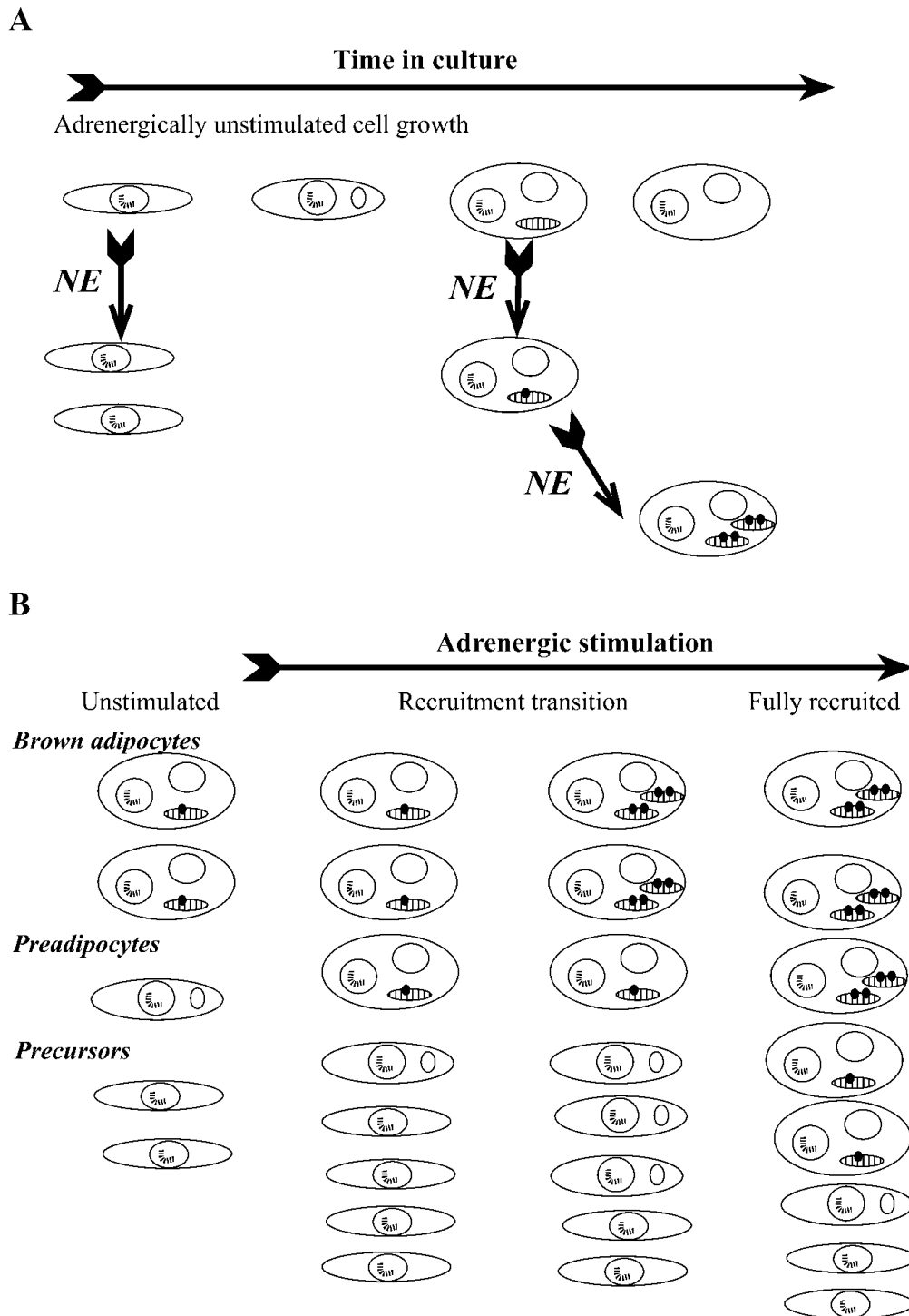


Figure 14. The composite effects of chronic adrenergic stimulation in brown adipose tissue.³⁸ In a cell culture system (A), the effects of a recruitment modifier (here norepinephrine) can be dissected into effects on, e.g., cell proliferation (left) and differentiation (right) and distinguished from “spontaneous” cell differentiation. However, in the tissue (B), the starting material is a composite of cells in different degrees of development, and it also includes different cell types, e.g., endothelial cells, in addition to the brown precursors, preadipocytes, and adipocytes. The small black dots in the hatched mitochondrial structures symbolize *Ucp1*.

1.2.5 Cell models

To assess mechanisms of cell function in general and, more specifically, molecular mechanisms of disease, cell lines are of pivotal significance and considered an integral part of biomedical research.¹¹⁰ In endocrine research, attention has recently focused on fat cell metabolism and function, as adipose tissue appears to be of crucial importance for the development of different components of the insulin resistance syndrome.^{111,112} To date, a variety of different adipocyte cell lines are in common use. Four main approaches have been employed to generate these lines: 1) cloning cells susceptible to adipogenic conversion by serial passage of embryonic fibroblasts, 2) treating embryonic fibroblasts with a DNA methylation inhibitor, 3) isolation of precursor cells from bone marrow, and 4) isolation and subcloning of adipogenic cells from various tumors including those from transgenic mice carrying simian virus 40 (SV40) transforming genes. A similar fifth way of cell immortalization by direct infection of proliferating primary cells with the SV40 large T antigen is part of an advanced technique to create novel adipocyte cell lines from different mouse models.¹¹⁰

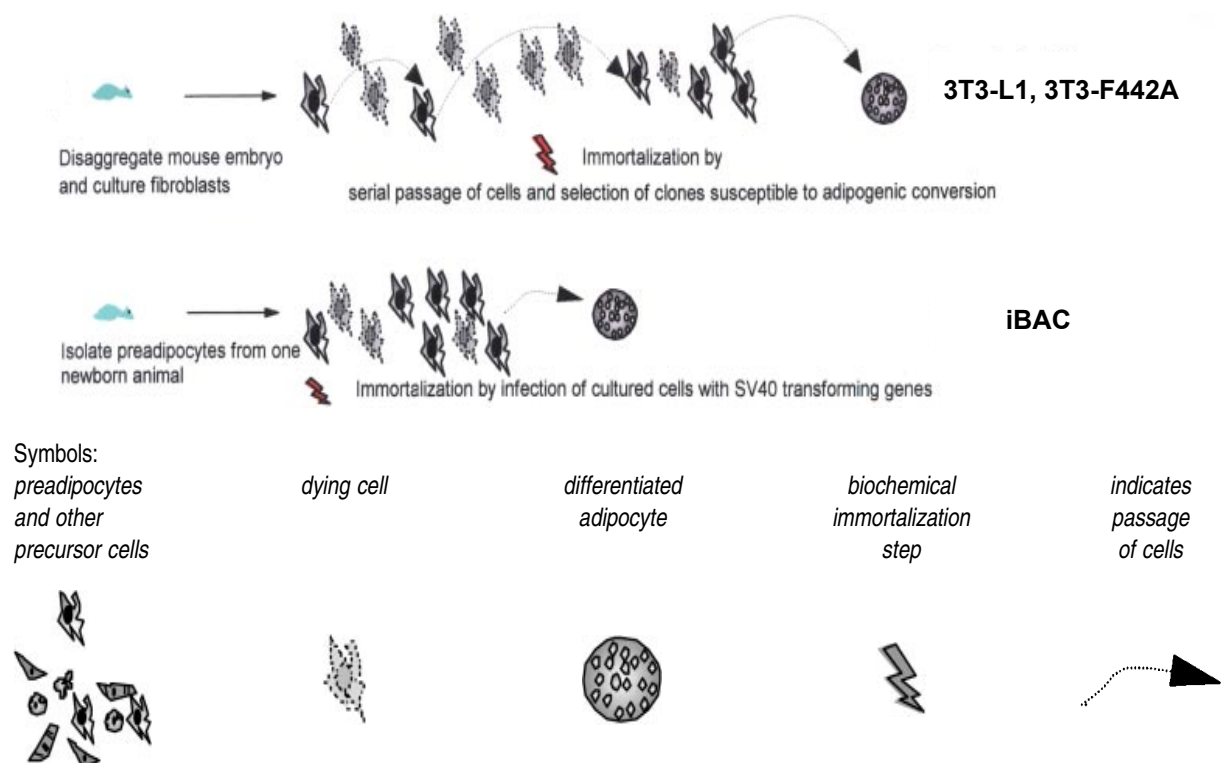


Figure 15. Schematic illustration of immortalization methods for the generation of adipose cell lines¹¹⁰.

3T3-L1 and 3T3-F442A, cell models for white adipogenesis

3T3-L1 and 3T3-F442A cells have derived from fibroblasts isolated from disaggregated Swiss mouse embryos, immortalized by continuous passaging and subcloned according to their differentiation capacity^{113,114}, while 3T3-F442 cells have a higher susceptibility to adipose conversion. These cell lines can be differentiated over a period of 10 to 15 days. Clonal expansion was validated as a prerequisite for differentiation (at least for 3T3-L1 cells)¹¹⁵ and many of the key players in mitotic clonal expansion and the adipocyte terminal differentiation program have been extensively characterized by utilization of both preadipocyte cell lines^{89,116,117,21}. Adipose conversion of 3T3-L1 and 3T3-F442 cells is also reviewed in detail by Max Lafontan⁸⁵ but remains typical as described in chapter "Morphology". Although these cell lines are aneuploid⁸⁵, triglyceride storage, a good responsiveness to lipogenic and lipolytic factors as well as increase in the basal rate of oxygen consumption were observed¹¹⁸. 3T3-L1 and 3T3-F442A cells are considered to be valid models for white adipose tissue although, when fully differentiated, they do not display unilocular intracellular fat stores but multilocular fat droplets typical of brown fat cells¹¹⁰.

Immortalized brown adipocyte cell lines (iBAC)

Fibrostromal fraction of interscapular brown fat from newborn or late fetal mouse is used for cell isolation. This tissue can easily be localized at this developmental stage exhibiting its maximum growth¹¹⁹. Immortalization is performed during first proliferation in culture with the retroviral vector pBabe encoding the SV 40 T antigen, probably resulting in a closer approach to in vivo than cloning cells from mice by serial selection, a process of immortalization whose biology is poorly understood, extending over several months. Differentiation procedure is similar to the standard differentiation of 3T3-L1 cells and full differentiation is reached after 8-10 days.¹¹⁰ Mature iBACs develop high *Ucp1* mRNA levels (approximately 70% of in vivo) and are sensitive upon β -adrenergic stimulation (induction of mRNA and protein)¹¹⁹. Insulin stimulation of the major signaling components is provided^{119,120,121,122} and results in a robust and diverse metabolic response¹²³ providing a valid cell model for brown adipogenesis.

1.2.6 Transcriptional Control

Brown adipogenesis is in many cases similar to white adipogenesis, both requiring the key actors peroxisome proliferator-activated receptor γ (*Ppar γ*) and CCAAT-enhancer-binding proteins (*C/ebps*), although there are different necessities and sufficiencies for *C/ebps* in each tissue.²¹ Detailed review of molecular regulation of white versus brown adipogenesis can be found in the literature²⁴.

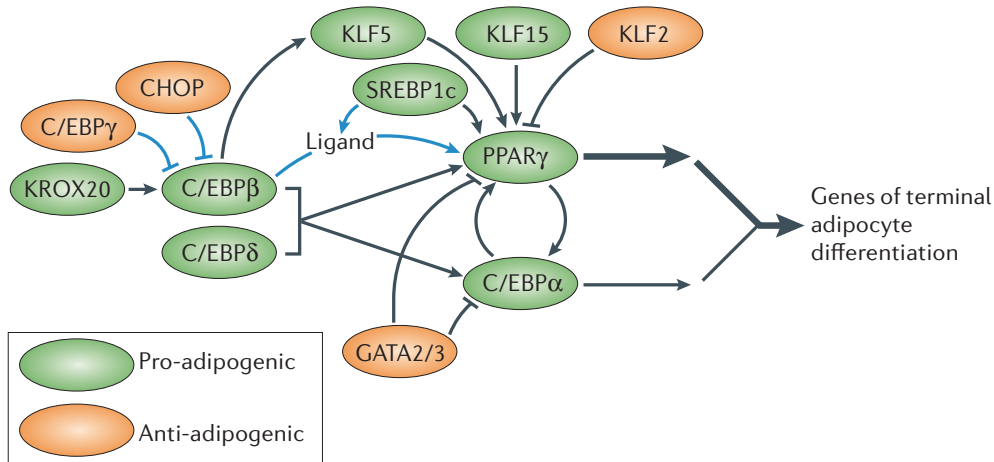


Figure 16. A complex transcriptional cascade regulates adipogenesis.²¹ Peroxisome proliferator-activated receptor γ (*Ppar γ*) lies at the core of the transcriptional cascade that regulates adipogenesis. The expression of *Ppar γ* is regulated by several pro-adipogenic (green) and anti-adipogenic (orange) factors. *Ppar γ* itself is activated by an as-yet-uncharacterized ligand. CCAAT-enhancer-binding protein α (*C/ebp α*) is regulated through a series of inhibitory protein–protein interactions. Some transcription-factor families have several members that participate in adipogenesis, such as the Krüppel-like factors (KLFs). Black lines indicate effects on gene expression, whereas blue lines represent effects on protein activity.

Ppar γ and ligands

Peroxisome proliferator- activated receptor γ (*Ppar γ*), the "master regulator" of adipogenesis, is a member of the nuclear-receptor superfamily, and is both necessary and sufficient for adipogenesis^{117,124,125}. *Ppar γ* is required for the formation of both WAT and BAT in vivo^{126,127,128,129}. TZDs (thiazolidinediones) are ligands for *Ppar γ* , and powerfully promote white and brown adipogenesis in vitro^{130,131}. Moreover, they increase expression of *Ucp1* in cultured brown^{131,132,133} and partially in white (brite)^{54,134,135} adipocytes. TZD as well as non TZD *Ppar γ* ligands can induce *Ucp1* expression in BAT^{133,136,77}, BAT hyperplasia^{131,136} as well as the appearance of brown adipocytes and *Ucp1* expression in WAT

depots^{77,75,137}. Strikingly, TZD treatment induces mitochondrial biogenesis in white adipocytes in vitro and in vivo and results in mitochondrial remodeling to a cristae-rich morphology^{137,138}. This effect is possibly due to the ability of TZDs to induce expression of PGC-1 α in white and brown adipocytes in vitro and in vivo^{77,79,139,140}. Beside PGC-1 α a number of SPPARMs (selective *Ppar γ* modulators) have been developed recently^{141,142,143,144}.

***C/EBP* family**

C/ebps, a family of transcription factors interacting with CCAAT motifs (CCAAT-enhancer-binding proteins), containing a basic transcriptional activation domain and adjoining leucine zipper domains for dimerization. The different members of *C/ebp* family can form homo- and hetero-dimers. Members of this family were the first transcription factors demonstrated to play a major role in adipocyte differentiation⁸² also interacting very close⁸³ with *Ppar γ* , the indispensable¹²⁶ major transcription factor in adipogenesis.

C/ebp α and *Ppar γ* are involved in growth arrest after clonal expansion of preadipocytes, necessary for adipocyte differentiation¹⁴⁵. *C/ebp α* itself is autoregulated¹⁴⁶ and acts in a "feed-forward" fashion⁸³ (also see Figure 16) with *Ppar γ* , inducing each other and promoting downstream gene expression cooperatively (e.g. adipocyte fatty acid binding protein aP2 (*Fabp4*)¹⁴⁷). Low levels of these two transcription factors during clonal expansion of preadipocytes may be sufficient to mediate growth arrest⁸², increasing dramatically during adipocyte differentiation and remain high for the whole life of the mature adipocyte⁸³.

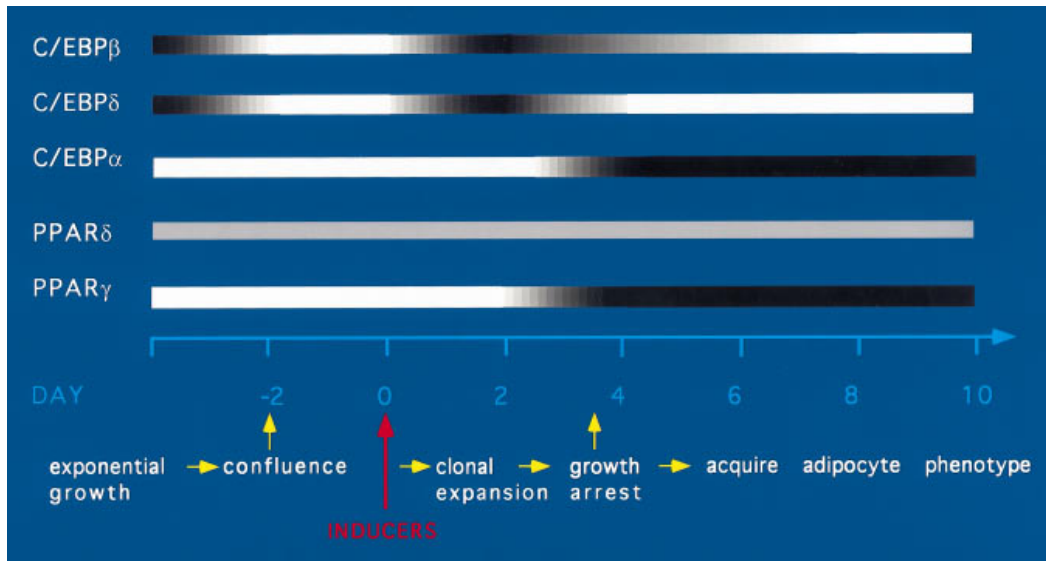


Figure 17. Expression of C/EBP and Ppar family members during differentiation of 3T3-L1 preadipocytes.¹¹⁶ The magnitude of expression is indicated by the intensity of the horizontal band corresponding to each transcription factor.

C/ebpα is highly expressed in adipose tissue¹⁴⁸, slightly before the expression of adipocyte specific genes^{149,150,116}. In some instances, constitutive expression of *C/ebpα* is sufficient to induce differentiation of 3T3-L1 cells in the absence of hormonal agents, and expression of antisense *C/ebpα* mRNA in 3T3-L1 preadipocytes prevents differentiation^{151,152}. Moreover, *C/ebpα* can efficiently promote adipogenesis in a variety of mouse fibroblastic cells, including those that have little or no spontaneous capacity to develop into adipocytes¹⁵³. Inhibition of *C/ebpα* in 3T3-L1 cells impairs adipocyte differentiation¹⁵¹. A global knockout of *C/ebpα* in vivo resulted in perinatal lethality in mice¹⁵⁴. Mutation of *C/ebp* binding site in several adipocyte genes abolishes transactivation^{155,156,157,147}. Together, these findings provide evidence that *C/ebpα* is both, required and sufficient to induce adipocyte differentiation.

C/ebpα plays an important role in differentiation since final growth arrest, its protein is not detectable in undifferentiated preadipocytes¹⁵⁸ and not responsible for converting preadipocytes into adipocytes¹⁴⁵. Two other isoforms *C/ebpβ* and *C/ebpδ* seem to be involved in earlier stages of adipocyte differentiation. *C/ebpβ* and *C/ebpδ* are expressed at high levels in actively dividing preadipocytes⁹¹, and upon achieving first growth arrest at confluence, expression of both decreases. Interestingly, expression levels of these two *C/ebp* isoforms increase a second time, after induction of differentiation by treating confluent preadipocytes with

induction cocktail⁹¹, subsequently entering post confluent mitosis leading to second (final) growth arrest (mediated by *C/ebpα*). Particularly, levels of *C/ebpβ* are influenced by IBMX (also termed MIX) and *C/ebpδ* by Dexamethason¹⁵⁸, two components of standard differentiation cocktail. The temporal expression indicates a cascade whereby early induction of *C/ebpβ* and δ leads to induction of *C/ebpα*²¹, but also *Pparγ* by heterodimerization¹⁵⁹, additionally confirmed by *C/ebpβ*- and *C/ebpδ* deficient MEFs which do not express *C/ebpα* and *Pparγ*²¹.

Interactions and temporally changing levels of *C/EBPs* during proliferation and determination of adipocytes reveals involvement in commitment. Indeed, ablation of *C/ebpα* blocks development of most white adipose tissue¹⁵⁴ and conversely mice lacking either *C/ebpβ* or δ have normal WAT, although their BAT shows reductions in lipid accumulation and *Ucp1* expression¹⁶⁰. *C/ebpβ* is a transcriptional regulator of *Ucp1*¹⁶¹ (also suggested for *C/ebpδ*¹⁶¹), responsive to β -adrenergic stimulation¹⁶² (also true for *C/ebpδ*¹⁶¹) and plays a major role in development of BAT¹⁶³. Actually overexpression of *C/ebpβ* is able to reprogram white 3T3-L1 cells, expressing brown marker genes¹⁶⁴.

1.3 MicroRNAs

MicroRNAs (miRNAs) comprise a large family of ~21 nucleotide long RNAs that have emerged as key post-transcriptional regulators of gene expression in metazoans and plants, and have revolutionized our comprehension of the post-transcriptional regulation of gene expression^{165,166}. In mammals, miRNAs are predicted to control the activity of ~50% of all protein-coding genes. Functional studies indicate that miRNAs participate in the regulation of almost every cellular process investigated so far and that changes in their expression are associated with many human pathologies.¹⁶⁷

1.3.1 Biogenesis

miRNAs are processed from precursor molecules (pri-miRNAs), which are either transcribed by RNA polymerase II from independent genes or represent introns of protein-coding genes. The pri-miRNAs fold into hairpins, which act as substrates for two members of the RNase III family of enzymes, Drosha and Dicer. The product of Drosha cleavage, an ~70-nucleotide pre-miRNA, is exported to the cytoplasm where Dicer processes it to an ~20-bp miRNA/miRNA* duplex. One strand of this duplex, representing a mature miRNA, is then incorporated into the miRNA-induced silencing complex (miRISC). As part of miRISC, miRNAs basepair to target mRNAs and induce their translational repression or deadenylation and degradation. Argonaute (AGO) proteins, which directly interact with miRNAs, and glycine-tryptophan protein of 182 kDa (GW182) proteins, which act as downstream effectors in the repression, are key factors in the assembly and function of miRISCs. In their role in miRNA maturation both Drosha and Dicer are assisted by a number of cofactors or accessory proteins, with some playing an important regulatory function.¹⁶⁷

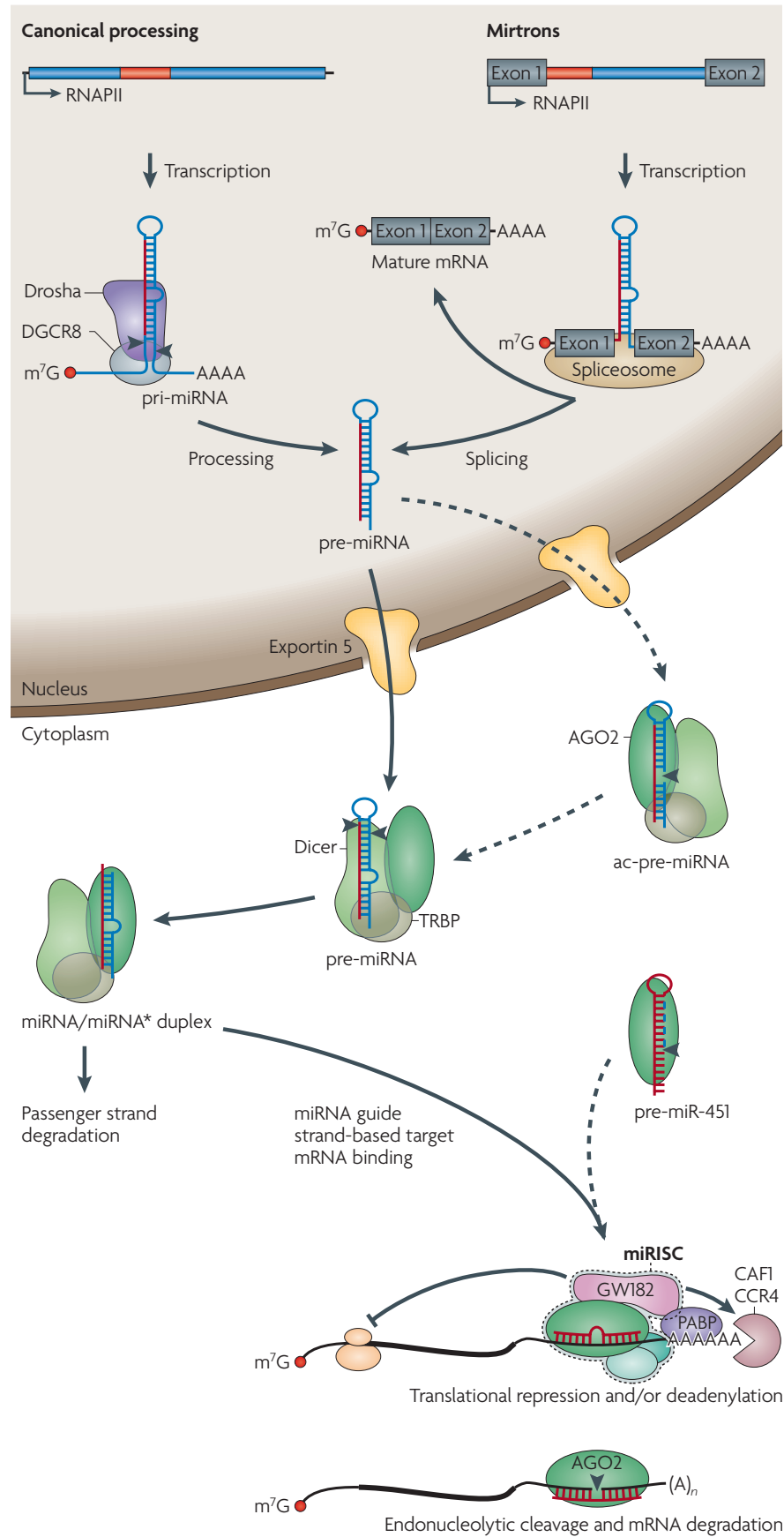


Figure 18. MicroRNA biogenesis.¹⁶⁷ MicroRNAs (miRNAs) are processed from RNA polymerase II (RNAPII)-specific transcripts of independent genes or from introns of protein-coding genes^{166,168}.

Primary precursor (pri-miRNA) processing occurs in two steps, catalyzed by two members of the RNase III family of enzymes, Drosha and Dicer, operating in complexes with dsRNA-binding proteins (dsRBPs), for example DGCR8 and transactivation-responsive (TAR) RNA-binding protein (TRBP) in mammals. In the first nuclear step, the Drosha–DGCR8 complex processes pri-miRNA into an ~70-nucleotide precursor hairpin (pre-miRNA), which is exported to the cytoplasm. Some pre-miRNAs are produced from very short introns (mirtrons) as a result of splicing and debranching, thereby bypassing the Drosha– DGCR8 step. In either case, cleavage by Dicer, assisted by TRBP, in the cytoplasm yields a ~20-bp miRNA/miRNA* duplex. In mammals, argonaute 2 (AGO2), which has robust RNaseH-like endonuclease activity, can support Dicer processing by cleaving the 3' arm of some pre-miRNAs, thus forming an additional processing intermediate called AGO2-cleaved precursor miRNA (ac-pre-miRNA)¹⁶⁹. Processing of pre-miR-451 also requires cleavage by AGO2, but is independent of Dicer and the 3' end is generated by exonucleolytic trimming^{170,171}. Following processing, one strand of the miRNA/miRNA* duplex (the guide strand) is preferentially incorporated into an miRNA-induced silencing complex (miRISC), whereas the other strand (passenger or miRNA*) is released and degraded. Generally, the retained strand is the one that has the less stably base-paired 5' end in the miRNA/miRNA* duplex. miRNA* strands are not always by-products of miRNA biogenesis and can also be loaded into miRISC to function as miRNAs^{172,173,174,175}.

1.3.2 Mode of action

Post-transcriptional regulation by miRNAs is done either by directing target transcript cleavage or by translational inhibition^{176,177} (see Figure 19a). 21643 mature miRNA products, in 168 species have now been identified in the microRNA database¹⁷⁸, implying that miRNAs mediate a vast network of unappreciated regulatory interactions in species. However, the *in vivo* functions and biologically relevant target genes are thus far known only for a few miRNAs.

Target recognition

It was reported that putative targets of most plant miRNAs were found simply by searching for highly complementary sequences in mRNA coding sequences or untranslated regions¹⁷⁹. Highly complementary miRNA-binding sites mediate biologically relevant negative regulation and limited G:U pairing, bulged nucleotides, and/or mismatches between miRNA and target are tolerated.¹⁸⁰ It is now believed that most plant miRNA targets, or at least those with extensive complementarity to miRNAs, have been identified^{181,182}.

Animal miRNAs do not generally exhibit extensive complementarity to endogenous transcripts (see Figure 19b) and it is much more challenging to find target genes.

Loss-of-function phenotypes showed that miRNA candidates obviously regulate the timing of developmental transitions, and genetic interactions although this implicates a coherent set of genes as regulatory targets. A study in flies¹⁸³ was the first “informatic” determination of animal miRNA targets and made two vital observations. First, it was invariably the 5' end of the miRNA that is complementary to the 3' UTR regulatory motif, with a stretch of more than seven nucleotides of contiguous pairing in each case (see Figure 19b). Second, base-pairing within this region is canonical, with no G:U base-pairs seen. The importance of the 5' miRNA end for target recognition was further suggested by the finding that, in many cases, miRNAs could be grouped according to their homologous 5' ends.¹⁸⁰

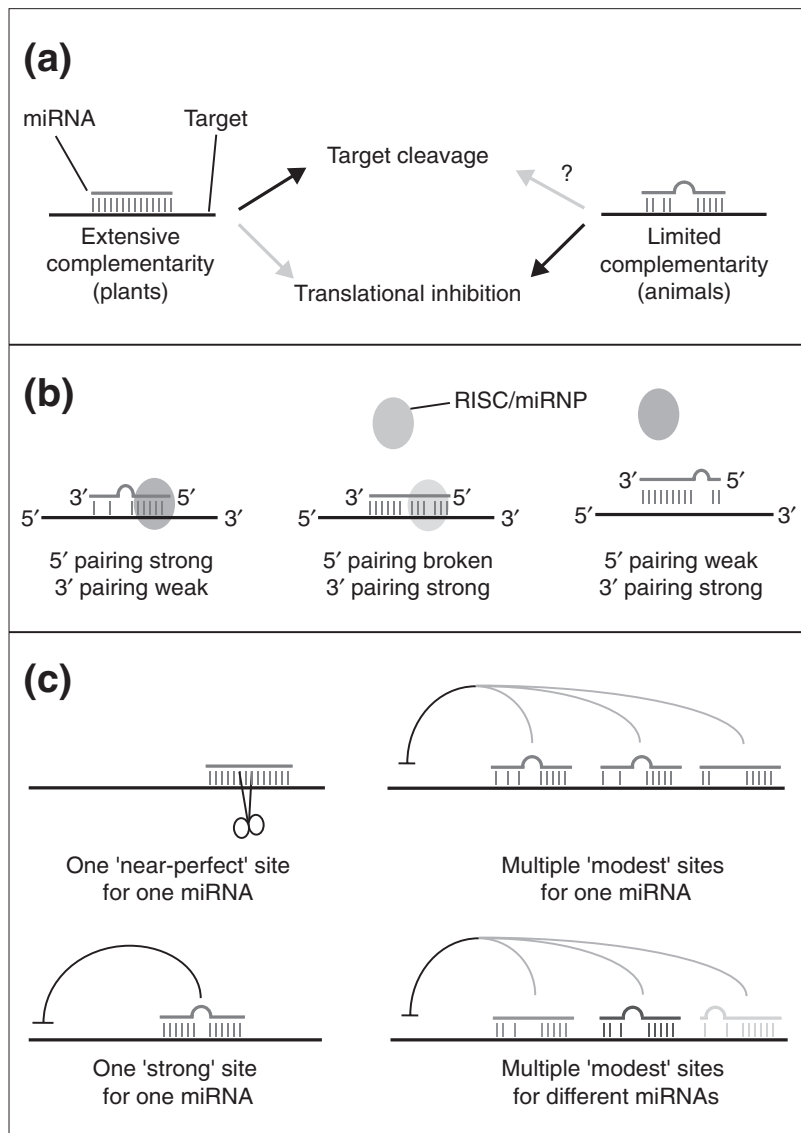


Figure 19. Complementarity of miRNAs and their targets.¹⁸⁰ (a) Two classes of miRNA-binding site. Some miRNA-binding sites have extensive, near-perfect complementarity to miRNAs (left),

whereas other miRNA-binding sites display only limited pairing to a miRNA (right). In many cases, the former leads to target cleavage while the latter causes translational inhibition (black arrows), although converse examples have also been described (gray arrows). Plant miRNAs commonly show extensive pairing to targets, whereas this is exceedingly uncommon for animal miRNAs. (b) Strong canonical base-pairing to the 5' end of a miRNA (nucleotides 2-8) is important for regulation of sites with limited complementarity. This is presumably due to specific recognition of the 5' end of the miRNA-target duplex by components of the RISC/miRNP complex (oval). It should be noted that RISC/miRNP may have physical contact along the entire miRNA:target duplex. An approximately seven-nucleotide duplex with the 5' end of a miRNA may in fact be sufficient for target recognition (left). Imperfect 5' pairing renders most sites nonfunctional, although in some cases, site functionality is 'rescued' by sufficiently extensive 3' pairing (middle). Sites that lack strong 5' pairing are nonfunctional, regardless of the degree of 3' pairing (right). (c) Examples of different configurations of miRNA-binding sites. Individual sites need to be considered within the milieu of other miRNA-binding sites present on a given transcript. Single sites can suffice for target cleavage (upper left) or strong translational inhibition (lower left), but these are typically 'near-perfect' or 'strong' sites that present extended complementarity to the miRNA. Multiple 'modest' sites that maintain 5' pairing to the miRNA can act synergistically and together confer strong regulation (upper right). Some transcripts contain multiple binding sites for different miRNAs (designated in different shades), which might also function synergistically (lower right).

Gene silencing

To perform their regulatory functions miRNAs assemble together with argonaute family proteins into miRNA-induced silencing complexes (miRISCs). Within these complexes, miRNAs guide Argonaute proteins to fully or partially complementary mRNA targets, which are then silenced posttranscriptionally¹⁸⁴.

Despite remarkable progress in our understanding of miRNA biogenesis and function, the mechanisms used by miRNAs to regulate gene expression remain under debate. Published studies indicate that miRNAs repress protein expression in four distinct ways: (1) cotranslational protein degradation; (2) inhibition of translation elongation; (3) premature termination of translation (ribosome drop-off); and (4) inhibition of translation initiation (see Figure 20).¹⁸⁵

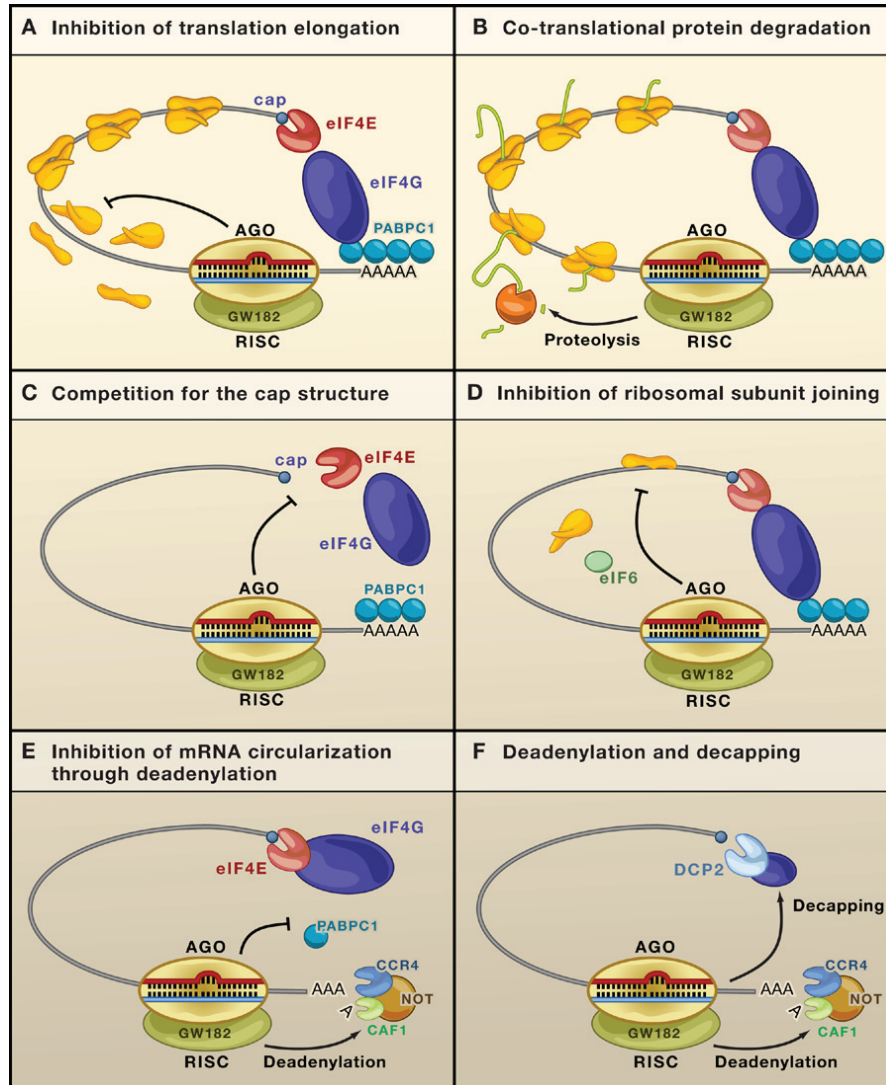


Figure 20. Mechanisms of miRNA-Mediated Gene Silencing¹⁸⁵. (A) Postinitiation mechanisms. MicroRNAs (miRNAs; red) repress translation of target mRNAs by blocking translation elongation or by promoting premature dissociation of ribosomes (ribosome drop-off). (B) Cotranslational protein degradation. This model proposes that translation is not inhibited, but rather the nascent polypeptide chain is degraded cotranslationally. The putative protease is unknown. (C–E) Initiation mechanisms. MicroRNAs interfere with a very early step of translation, prior to elongation. (C) Argonaute proteins compete with eIF4E for binding to the cap structure (cyan dot). (D) Argonaute proteins recruit eIF6, which prevents the large ribosomal subunit from joining the small subunit. (E) Argonaute proteins prevent the formation of the closed loop mRNA configuration by an ill-defined mechanism that includes deadenylation. (F) MicroRNA-mediated mRNA decay. MicroRNAs trigger deadenylation and subsequent decapping of the mRNA target. Proteins required for this process are shown including components of the major deadenylase complex (CAF1, CCR4, and the NOT complex), the decapping enzyme DCP2, and several decapping activators (dark blue circles). (Note that mRNA decay could be an independent mechanism of silencing, or a consequence of translational repression, irrespective of

whether repression occurs at the initiation or postinitiation levels of translation.) RISC is shown as a minimal complex including an Argonaute protein (yellow) and GW182 (green). The mRNA is represented in a closed loop configuration achieved through interactions between the cytoplasmic poly(A) binding protein (PABPC1; bound to the 3' poly(A) tail) and eIF4G (bound to the cytoplasmic cap-binding protein eIF4E).

Literature reveals many mechanisms and it is hard to reconcile the different reported modes of miRNA regulation of gene expression. Perhaps these different modes reflect different interpretations and experimental approaches. Another possibility is that miRNAs do indeed silence gene expression via multiple mechanisms. Finally, miRNAs might silence gene expression by a common and unique mechanism; and the multiple modes of action represent secondary effects of this primary event.¹⁸⁵

1.3.3 Target Prediction

The common initial step for target prediction algorithms is to assess and rank-order target 3' UTR complementarity to a miRNA by either duplex free energy and/or number of paired nucleotides, typically with some requirement or reward given to pairing to the 5' portion of the miRNA. The output of independent analyses of common datasets varies significantly, as the various algorithms perform and evaluate RNA foldings in different ways, make different allowances for bulges and loops in the duplexes, and promote 5' pairing to different extents. Simple 'matching' of miRNAs to mRNAs in a single genome is ineffectual, since individual, genuine animal miRNA regulatory sites do not display a statistically significant amount of complementarity¹⁸⁶. Confidence in a given target increases if it is conserved between species. Another strategy is to concern oneself primarily with targets that contain multiple sites, which can be factored in as a cumulative score for a given 3' UTR.¹⁸⁰

Several computational prediction tools for miRNA-target interactions exist, e.g. miRBase Targets, miRanda, PicTar, PITA and TargetScan. Considering that miRNAs are able to act in concert, capable of molecular pathway modulation¹⁸⁷, DIANA-mirPath is a useful tool. This software performs an enrichment analysis of multiple miRNA target genes comparing each set of miRNA targets to all known KEGG pathways.¹⁸⁸

1.3.4 MicroRNAs in obesity

miRNAs appear to play regulatory roles in many biological processes associated with obesity, including adipocyte differentiation, insulin action and fat metabolism. Recent studies show miRNAs are dysregulated in obese adipose tissue. During adipogenesis miRNAs can accelerate or inhibit adipocyte differentiation and hence regulate fat cell development. In addition miRNAs may regulate adipogenic lineage commitment in multipotent stem cells and hence govern fat cell numbers. The potential of miRNA based therapeutics targeting obesity is reviewed in literature⁸⁴ as well as recommendations for future research which could lead to a breakthrough in the treatment of obesity.

miRNAs and adipocyte differentiation

To date studies have profiled miRNA expression during adipogenic differentiation predominantly in the mouse 3T3-L1 cell-line^{189,190,191,192,193} but also in human multipotent adipose-derived stem cells^{194,195,196}. Studies have used miRNA arrays in combination with validation by Northern blot or RT-qPCR, but with no universally accepted miRNA array platform there is little agreement between studies on candidate miRNAs¹⁹⁷. Some miRNAs appear to be negative regulators of adipocyte differentiation while some miRNAs are capable of accelerating adipocyte differentiation^{197,20}.

miRNAs and multipotent mesenchymal stem cells during adipogenesis

Studies in mouse and human in the last years have reported miRNA expression is altered during adipogenic lineage commitment of multipotent mesenchymal stem cells (MSC)^{190,198,199,200,201,202,203,204,196}. Positive modulation of adipogenic lineage commitment in the multipotent MSC population could contribute to adipocyte hyperplasia in obesity. However to date the contribution of multipotent MSCs to increased adipose tissue mass in obesity is largely unknown.

miRNAs in brown adipogenesis

All studies to date agree that the absence of brown adipose tissue is correlated with obesity²⁰⁵. Recent findings suggest brown adipocytes to be derived from

distinct precursors (also see original view of transdifferentiation), although these findings are discussed. miR-455 which is expressed at low levels in white preadipocytes and white mature adipocytes is reported to be upregulated during brown pre-adipocyte differentiation⁶⁸. In addition, miR-1, miR-133a and miR-206 which are highly expressed in skeletal muscle²⁰⁶ are reported to be absent from white adipocytes but are expressed in brown pre-adipocytes and mature adipocytes⁶⁸. Recently miR-193b-365 (a brown fat enriched microRNA cluster) was reported to be essential for brown fat differentiation²⁰⁷, where miR-26a induces brown adipogenesis in hMADS cells (human multipotent adipose-derived stem cells) leading to a brite phenotype¹⁹⁶.

Further studies in miRNAs, differentially regulated in brown, white and brite adipocytes and upon β -adrenergic stimulation could identify useful therapeutic targets to treat obesity. Understanding brown adipogenesis and miRNAs interaction, energy expenditure could be increased by enhanced recruitment and further activation of brown and brite adipocytes.

2 Materials and Methods

2.1 Materials

2.1.1 Standard laboratory equipment

product name	company / product number
PIPETMAN Neo P2N	Gilson / F144561
PIPETMAN Neo P10N	Gilson / F144562
PIPETMAN Neo P20N	Gilson / F144563
PIPETMAN Neo P100N	Gilson / F144564
PIPETMAN Neo P200	Gilson / F123601
PIPETMAN Neo P1000	Gilson / F123602
PIPETBOY acu	VWR / 612-0928
0.2mL PCR Tubes	Biozym / 710980
1.5mL Microcentrifuge Tubes	Sarstedt / 72.690.001
2mL Microcentrifuge Tubes	Biozym / 710190
1.5mL Safe-Lock Tubes	Eppendorf / 0030 123.328
15mL PP Centrifuge Tubes	Corning / 430791
50mL PP Centrifuge Tubes	Greiner Bio-One / 227261
10 µLPipette Tips	Biozym / 720031
100 µLPipette Tips	Greiner Bio-One / 685290
1000 µLPipette Tips	Corning / 4868
10 µLFilter Tips	Biozym / 693010
100 µLFilter Tips 4050	Biopointescientific / 342-
1mL SafeSeal-Tips	Biozym / 691000
CELL STARR Serological Pipette,5mL	Greiner Bio-One / 606107
CELL STARR Serological Pipette,10mL	Greiner Bio-One / 607180
CELL STARR Serological Pipette,25mL	Greiner Bio-One / 760107
Pasteur Pipettes without swab L=150mm	ROTH/4518.1
Pasteur Pipettes without swab L=230mm	ROTH/4522

2.1.2 Instruments

product name	company
Microcentrifuge 5415R	Eppendorf
CR 4 22 Centrifuge	Jouan
6K16 High Volume Refrigerated Centrifuge	Sigma
MS1 Minishaker	IKA Works
MR2001K Magnetic Stirrer & Hotplate	Heidolph
Explorer Analytical Balance	OHAUS
DNA120 SpeedVac R	ThermoSavant
Thermomixer Compact	Eppendorf
Water Bath	GFL

Transsonic 420	Elma
CO2-Incubator CB210	Binder
Safeflow 1.2	BIOAIR
OT340 Hotplate	medite
CKX41 Inverted Light Microscope	Olympus
C-4040ZOOM Digital Camera	Olympus
NanoDrop ND-1000	Thermo Scientific
PTC-225 PCR Cycler	MS Research
ABI PRISM 7000 Sequence Detection System	Applied Biosystems
Mini Orbital Shaker SSM1	Stuart
Tecan HS 400 Hybridization Station	Tecan
GenePix 4000B Scanner	Axon Instruments
Arpege40 liquid N2 tank	Air Liquide

2.1.3 Microarrays

product name	company / product number
miRCURY™ LNA microRNA Array ready-to spot probe set	Exiqon / 208010-A
Nexterion HiSens E slides	Schott / 1125813
DEPC-treated H2O	Roth / T143.3
miRCURY LNATM microRNA Hy3/Hy5 Power Labeling Kit	Exiqon/ 208032
miRCURY LNATM microRNA Hy3/Hy5 Hi-Power Labeling Kit	Exiqon/ 208035
Bovine Serum Albumin	PAA / K45-001
Sodium Citrate Tribasic Dihydrate	Sigma / C7254
NaCl	Roth / 3957.2
Sodium Dodecyl Sulfate	Sigma / 4360.2
miRCURY LNATM Array, 2x Hybridisation Buffer	Exiqon / 208020

2.1.4 Analysis of triglyceride accumulation

product name	company / product number
Formaldehyde Solution 36.5%	Sigma / F8775
Phosphate Buffered Saline (PBS)	Invitrogen / 10010015
Oil Red O ICN	Biomedicals / I155984
2-Propanol	Roth / 7343.1
Aqua Bidestillata Sterilis (ddH2O)	Fresenius Kabi /
0698961/01A	
Triglycerides Kit	Thermo Scientific / TR22203
Glycerol ≥98%	Roth / 7530.1

2.1.5 RNA isolation

product name	company / product number
TRIzol Reagent	Invitrogen / 15596018
Chloroform ≥99%	Sigma / C2432

2-propanol	Roth / 7343.1
Ethanol absolute	AustrAlco / UN1770
DEPC-treated H2O	Roth / T143.3

2.1.6 Cell culture

product name	company / product number
Phosphate Buffered Saline (PBS)	Invitrogen / 10010015
Dulbecco's Modified Eagle Medium (DMEM) 1g/l Glucose	Lonza / BE12-707F
Dulbecco's Modified Eagle Medium (DMEM) 4.5 g/l Glucose	Invitrogen / 41966029
Fetal Bovine Serum Pan	Biotech / P30-3300
L-Glutamine (200mm)	Invitrogen / 25030024
HEPES Buffer Solution (1M)	Invitrogen / 15630-122
Trypsin, 0.5% (10x) with EDTA	Invitrogen / 15400054
Normocin	Invivogen / ant-nr-2
Penicillin-Streptomycin	Invitrogen / 15140122
3-Isobutyl-1-methylxanthine (IBMX)	Sigma I-7018
3,3',5-Triiodo-L-thyronine sodium salt (T3)	Sigma T-6397
Dexamethasone	Sigma D-4902
Trypan Blue Solution – 0.4%	Sigma / T8154
Insulin solution human	Sigma I-9278
Rosiglitazone	Beecham Laboratory Research, Contact at GSK: Jo Forsythe Dole, PhD / (BRL49653)
Hemocytometer	Neubauer / T728.1
Cell culture 6-well Multiwell Plates	Greiner Bio-One / 657160
Cell culture 12-well Multiwell Plates	Greiner Bio-One / 665180
Dimethylsulfoxide (DMSO)	Sigma / 472301
2mL Cryotubes	Lactan / E3091
Nuclease-free H2O	Exiqon / 203400-02
Aqua Bidestillata Sterilis (ddH2O) 0698961/01A	Fresenius Kabi /
HiPerFect Transfection Reagent	QIAGEN / 301707
miRIDIAN Mimic hsa-miR-26a 0005	Dharmacon / C-300499-05-
miRIDIAN Mimic Negative Control #1 01-20	Dharmacon / CN-001000-
anti-hsa-miR-26a antisense oligonucleotide	Exiqon / 138463- 00
non-targeting control antisense oligonucleotide	Exiqon / EQ 866923
0.22 µm Syringe Filters	Biochrom / P99722
20mL Sterile Syringes	Lactan / RC539.1

2.1.7 quantitative real-time RT-PCR

product name	company / product number
--------------	--------------------------

RQ RNase-Free DNase	Promega / M6101
100mm dNTP Set	Invitrogen / 10297018
Random Hexamer Primers	Invitrogen / 48190011
Oligo dT(12-18) Primers	Invitrogen / 18418012
RNase OUTTM Recombinant Ribonuclease Inhibitor	Invitrogen / 10777019
SuperScript II Reverse Transcriptase Kit	Invitrogen / 18064014
Aqua Bidestillata Sterilis (ddH2O)	Fresenius Kabi /
0698961/01A	
Platinum SYBR Green qPCR	Invitrogen / 11744500
SuperMix-UDG w/ROX	Invitrogen / 11744500
1 kb Plus DNA Ladder	Invitrogen / 10787-018
100 bp DNA Ladder	Invitrogen / 15628-019
6x DNA Loading Dye	Fermentas / R0611
PCR SingleCap 8-SoftStrips 0.2 ml	Biozym / 710980
hsa-miR-26a, LNATM PCR Primer Set	Exiqon / 204724
5S rRNA (hsa, mmu) PCR Primer Set, UniRT	Exiqon / 203906
Universal cDNA Synthesis Kit	Exiqon / 203300
SYBR Green Master Mix, Universal RT	Exiqon / 203400
ROX Reference Dye, 1mm	Roche / 04673549001
MicroAmp Optical 96-Well Reaction Plates	Applied Biosystems / N801-0560
MicroAmp Optical Adhesive Film	Applied Biosystems / 4311971

Primer

gene / RefSeq ID	forward primer (5'→3')	reverse primer (5'→3')	amplicon (bp)
FABP4 / NM_001442	TGTGCAGAAATGGGATGGAAA	CAACGTCCCTTGGCTTATGCT	132
FASN / NM_004104	TGAACTCCTTGGCGGAAGAGA	GTAGGACCCCGTGAATGTCA	153
GLUT4 / NM_001042	CGTCGGGCTTCCAACAGATA	CACCGCAGAGAACACAGCAA	92
PGC1 α / NM_013261	ACAACACTTACAAGCCAAACCA	GCCTGCAGTTCCAGAGAGTT	136
PPAR γ / NM_138712	AGCCTCATGAAGAGCCTTCCA	TCCGGAAGAAACCCTTGCA	120
RB1 / NM_000321	TGGACTTCCAGAGGTTGAAAAT	CGTGGTGTCTCTGTGTTTCA	147
RIP140 / NM_003489	TTGGAGACAGACGAACTGA	TCTACGCAAGGAGGAGGAGA	143
S6K1 / NM_003161	CCATATGAACTTGGCATGGA	TTCCATAGCCCCCTTACC	131
UCP1 / NM_021833	GTGTGCCCAACTGTGCAATG	CCAGGATCCAAGTCGCAAGA	95
mRb1 / NM_009029	TGAGAGACCGACATTTGGACCAGA	AACACGTTTAAAGGTCTCCTGGGC	143
mRip140 / NM_173440	TCAGGCTGAGGCAGACGATAC	CCTCGCAACTTCCTTAGCACA	125
mS6K1 / NM_028259	TGGACCATGGGGGAGTTGGACC	AGCCCCCTTACCAAGTACCCGA	144
mUcp1 / NM_009463	TGAACCCGACAACCTCCGAA	GGCCTTACCTTGATCTGAA	138

2.1.8 Software and web tools

ABI Prism 7000, Version 1.1, Applied Biosystems
 QPCR 1.0
 ArrayNorm 1.7.6b
 Genesis 1.7.6

2.2 Methods

2.2.1 Cell culture

Cultivation and passaging of cells

For experiments 3T3-L1, 3T3-F442A and BAT-cells were used. Proliferation medium (PM) was adapted to each cell line (see Table 3) and stored at 4 °C. Cells were proliferated in T75 cell culture flasks and incubated at 37 °C in humidified atmosphere with 5% CO₂. At cell densities between 50-80% cells were split, considering the regarded maximum of passages for valid experiments.

For passaging old medium was aspired, cells were washed with PBS and incubated with trypsin. After 3-5 minutes, controlling detachment via microscope, trypsin was inactivated by adding at least 5 ml PM. Obtained cell suspension was split and completed with PM to a final volume of 10 ml for each T75 flask. Finally each flask was pivoted to reach a good distribution of proliferating cells.

All procedures outside the incubator were kept as short as possible, cells were temporarily stored at a hotplate and reagents were preheated in a waterbath (37°C).

Table 3. Overview of cell models and treatment during cultivation

	Used Passages	Proliferation-medium (PM)	Split ratio during proliferation	Seeding density	Days to confluence since seeding	Induction-medium	Maintenance-medium
3T3-L1	P22-P24	high glucose, 10 % FBS (07F0483K), 5ml L-Glut, 5ml P/Strp, 1ml Normo, 10 mM Hepes Buffer	1:2 - 1:10	20.000 c/w or 1 T75 for 50 wells (12-well plate)	2-3	PM and 0,5mM IBMX +/- 1mM dex +/- 2ug/ml insulin +/- rosiglitazone (1µM)	PM and +/- 2ug/ml insulin +/- rosiglitazone (1µM)
3T3-F442A	P18-P24	s. 3T3-L1 PM	1:5 - 1:30	70.000 c/w or 1 T75 for 18 wells (12-well plate)	2	PM and +/- rosiglitazone (100nM)	PM and +/- rosiglitazone (100nM)
iBAC	P3, P9-P13	3T3-L1 PM but 20 mM Hepes Buffer	1:10-1:16	20.000 c/w or 1 T75 for 72 wells (12-well plate)	4	PM and 1 nM T3 500 nM dex 0.5 mM IBMX 125 µM indomethacin	PM and 1 nM T3

dex ... dexamethasone

IBMX ... 1-methyl-3-isobutylxanthine

Normo ... normocin

P/Strp ... penicillin/streptomycin

FBS ... fetal bovine serum

L-Glut ... L-glutamin

Determination of cell concentration and viability

50 µl of cell suspension and 10 µl Trypan Blue were mixed by pipetting and transferred to the interspace of a hemocytometer. The concentration was determined by counting n unstained cells in f determined fields, indicating a certain volume V with n viable cells.

$$c = \frac{n}{V} = \frac{n}{f} * 12000 \quad [\text{cells/ml}]$$

n ...viable cells in f fields (each 1 mm²)

f ...counted fields

12000 is a scaling factor including the geometry of the interspace to calculate the volume, the dilution factor due to mixing with Trypan Blue (6:5) and the conversion of units ($1000 \text{ mm}^3 = 1 \text{ cm}^3 = 1 \text{ ml}$).

Transfection and adipocyte differentiation

Cells were seeded in 12-well plates with PM to reach confluence in about 2-4 days (depending on cell line, see Table 3). At confluence cells were transfected and at least 24h later the adipogenic differentiation program was started by adding the induction cocktail to medium (Induction Medium). Medium was regularly changed every other day or earlier due to an obvious drop in pH. For details see figures of experimental setups in iBACs (Figure 21), 3T3-L1 (Figure 22) or 3T3-F442A (Figure 23) cells.

Transient Transfection of cells was performed using HiPerFect Transfection Reagent according to manufacturer's instruction. At confluence medium was changed and 1h later the transfection mixture was added dropwise while swaying the plate. The medium was not changed for at least 1 day.

For the transfection mixture stock solutions of oligonucleotides ($20 \mu\text{M}$) were thawed on ice and diluted with nuclease-free H_2O to $2 \mu\text{M}$ working solutions. Working solutions were mixed with DMEM and HiPerFect by vortexing and incubated at room temperature for 10 min.. For the transfection procedure pipettes with filter tips were used and RNase-away was used to clean all working materials.

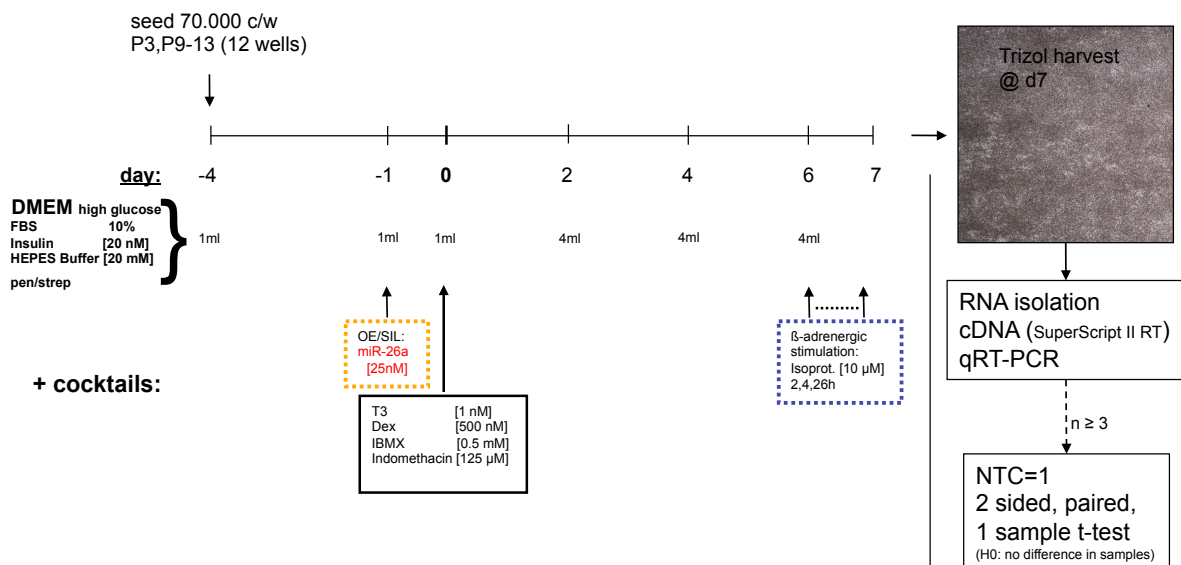


Figure 21. Experimental setups in iBACs

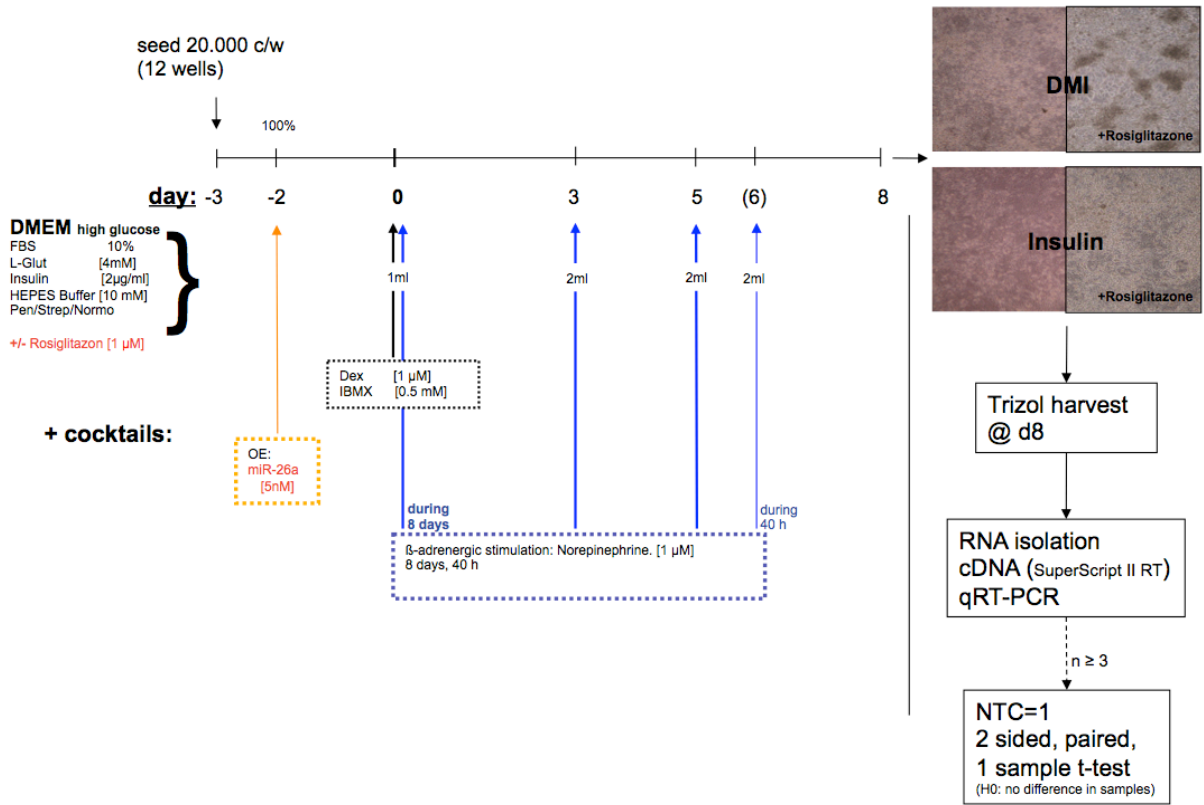


Figure 22. Experimental Setups in 3T3-L1 cells

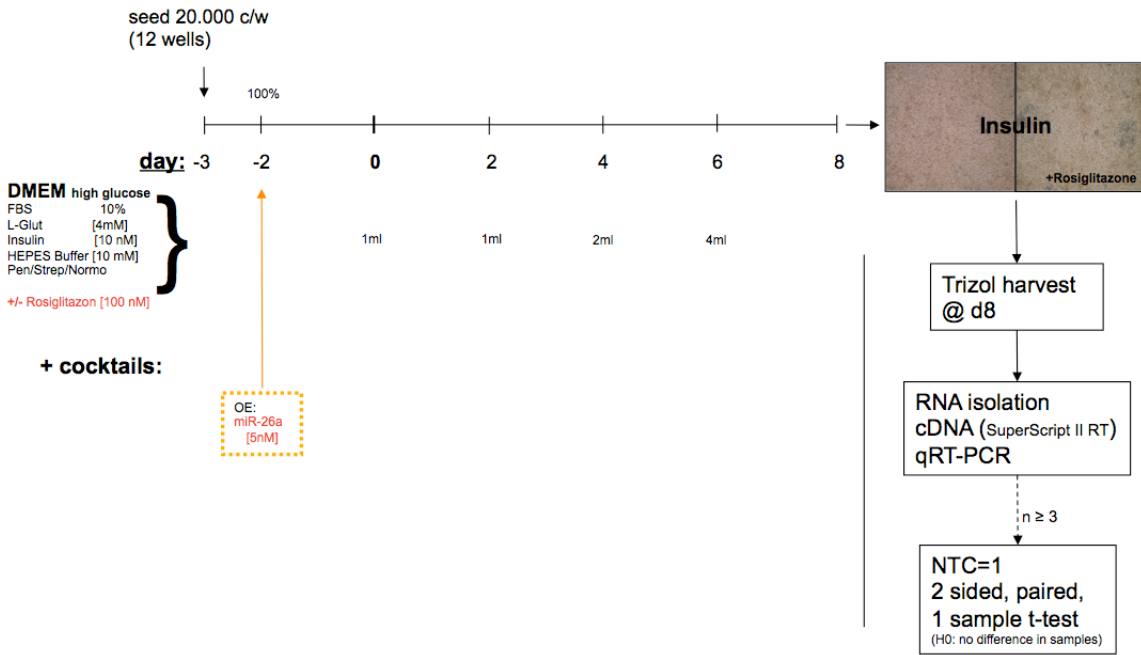


Figure 23. Experimental setup in 3T3-F442A cells

2.2.2 Molecular biology and biochemistry

Oil Red O staining

Medium was aspirated from all wells (12-well plate) and cells were washed immediately with 1 mL PBS per well, fixed in 3.6% formaldehyde (in PBS) for 15 min., again washed with PBS and stained by incubation with Oil Red O (30 min.). The Oil Red O working solution was prepared by diluting 0,5 g Oil Red O (Sigma) in 100 mL isopropanol (diluted with water (3:2) and filtrated). 1 mL Oil Red O solution per well was added. After incubation fixed cells were washed with PBS and prevented from drying with either water or 50% glycerol solution.

RNA isolation

RNA-isolation was performed according to SOP MET023_03 (adjusted to used materials).

Briefly medium was aspirated, cells were washed with PBS and 0,4 ml Trizol was added per well of a 12-well plate. Trizol-samples were stored at -80 °C.

For RNA-isolation frozen samples were thawed at room temperature for about 30 minutes. Meanwhile, the centrifuge was cooled to 4°C and the air hood was cleaned with RNase away.

80 µl Chloroform was added to the samples, the mixture was shaken vigorously and incubated for 3 minutes at room temperature. Samples were centrifuged (17 min., 4°C, 12000*g) splitting the conglomerate into phases.

The aqueous phase was pipetted into fresh 1,5 ml Safe-Lock tubes and 200 µl 2-propanol. After vortexing and incubating samples were centrifuged (20 min., 4°C) resulting in pellets at the bottom of the tubes. After removing the supernatant 400 µl ethanol was added to wash the RNA-pellet by centrifugation (8 min., 4°C, 7600*g). Again there should be a pellet, depending on the amount of RNA, at the bottom of the tube. After removing the ethanol-supernatant the RNA was air dried until only the borders of the pellet became invisible. By adding 20-60 ml of DEPC-treated H₂O (depending on pellet size), pipetting and incubating at 55 °C for 10 min, RNA-strands were well distributed. Purity (260/280 ratio at 1.8 - 2.0) and concentration (300 ng/µl < c < 1000 ng/µl) were determined by spectrophotometry using NanoDrop ND1000. Isolated and measured samples were stored at -80 °C.

For validation RNA was once checked on an Agilent Bioanalyzer 2100 according to manual.

MicroRNA expression profiling

Microarrays were generated by an in-house established microarray production platform and kindly provided by Dr. Marcel Scheideler. EXIQON Labeling kits (see Materials) were used according to manufacturer's recommendations, hybridization was performed on a Tecan HS400 hybridization station according to SOP MET030_01.

Prearrangements

Hybridization station chambers were controlled and cleaned with compressed air. Seals were stored in ddH₂O for 24 h to soak, or changed if fragile. Nitrogen bottle for hybridization station was checked for filling level and pressure was adjusted to 2.85 bar. Buffers were prepared, ultrasonicated and preheated if necessary (s. Table in SOP MET030_01). Labeling kit components (except enzymes) were thawed, Cy3/5 additionally light protected. RNA samples were thawed on ice and aliquoted to 1 µg total RNA per condition (2 conditions per chamber) plus 1 µg for dye swaps.

Labeling

Labeling was arranged in two steps: First, removal of 5' phosphates from the terminal of the miRNAs for cleavage on spotted probe. Second, enzymatically labeling of a single fluorophore per RNA-molecule for detection.

Step one: Mastermix I (0,5 µl CIP Buffer/sample, 0,5 µl CIP enzyme/sample, 1 µl nuclease-free H₂O) was prepared, added to each sample and all samples were incubated in 2 steps (30 min. at 37 °C, 5 min. at 95 °C), followed by snap cooling (2-15 min. on ice).

Step two: 1,5 µl of Cy3- or Cy5-fluorescent dye and mastermix II (3 µl labeling buffer/sample, 2 µl DMSO/sample, 1 µl labeling enzyme/sample) were added to each sample and incubated in two steps (2 h at 16 °C, 15 min. at 65 °C). Labeled RNA-samples were spun down and ready for hybridization (max. stored for 1,5 h at 4 °C).

Hybridization

Hybridization was started with rinsing the system with ddH₂O and connecting the degassed buffers to the right channels, followed by the "Prime" routine. miRNA

microarray slides were placed into the provided chambers and the hybridization protocol was started.

Preprocessing

After hybridization miRNA microarray chips were scanned with a GenePix 4000B microarray scanner, images were analyzed and preprocessed with GenePix Pro 4.1 software. Data was normalized with ArrayNorm and displayed in heat maps using Genesis software.

Quantitative real-time RT-PCR

For quantification of mRNA levels, RNA samples were thawed on ice, DNase digested and cDNA synthesis was performed. RNASE-Free DNase Kit and Superscript II Reverse Transcriptase Kit were used according to manufacturer's recommendations.

RNA samples were diluted to equal levels of 0,1-1 µg total RNA in 6.2 µl DNase free H₂O. For DNase digestion mastermix I (0.8 µl 10x reaction buffer/sample, 1 µl DNase enzyme/sample) was added and incubated at 30 °C for 30 min., followed by adding 1 µl DNase Stop solution.

For cDNA synthesis mastermix II (1 µl dNTP mix(10mM)/sample, 1 µl Oligo(dT)₁₂₋₁₈ primers (500 ng/µl)/sample, 1 µl random hexamer primers (250 ng/µl)/per sample) was added and incubated at 65 °C for 5 min. Subsequently mastermix III (4 µl 5x FS buffer/sample, 2 µl 0.1 M DTT/sample, 1 µl Rnase OUT/sample) was added and incubated (42 °C, 2 min), followed by adding 1 µl Superscript II Reverse Transcriptase. 3 steps of incubation were performed (10 min at 25 °C, 50 min at 42 °C, 15 min at 70 °C) and cDNA samples were ready to be stored at -20 or quantitative real-time reverse transcriptase PCR (qRT-PCR).

For qRT-PCR, cDNA stocks were diluted to 1 ng/µl (8 ng/µl for weak mRNA-levels) final RNA concentration. Forward and reverse primers were combined to 800 nM primer mix working solutions. Technical triplicates were performed by pipetting 4,5 µl primer mix working solution, 4,5 µl cDNA working solution and 9 µl of SYBR Green qPCR Super Mix-UDG w/ROX into Optical 96-well Reaction Plates. Amplification and measurement was done with an ABI PRISM 7000 Sequence Detection System using the following program: 2 min at 50 °C, 10 min at 95 °C, 40 cycles of 2 min at 60 °C and 15 s at 95 °C; followed by a dissociation protocol (60-95 °C)

Quantification of miRNA-26a was performed by using miRCURY LNA Universal RT microRNA PCR system according to manufacturer's recommendations. For determination of precise amounts of total RNA, samples were diluted to about 50 ng/ μ l, measured by spectrophotometry using NanoDrop ND1000 and diluted in DEPC-H₂O to 20 ng/ μ l to a final volume of 14 μ l. After adding the RT-mastermix (4 μ l 5x reaction buffer/sample and 2 μ l Enzyme Mix/sample) all samples were incubated in 2 steps (42 °C at 60 min, 95 °C at 5 min) using the PTC-225 PCR cycler. RT results were diluted 1:80 in a solution of 381 nM ROX reference dye and nuclease free H₂O. 1.8 μ l of prepared primer mastermixes (forward and reverse primers in 220 μ l DEPC-H₂O) for miRNA-26a or 5S-rRNA plus 9 μ l SYBR Green Master Mix and 7.2 μ l of diluted cDNA sample (ROX and nuclease free H₂O) were used for each qRT-PCR reaction pipetted in an Optical 96-well Reaction Plate. Setup for qRT-PCR run at the ABI PRISM 7000 Sequence Detection System was identical as for the conventional SYBR Green method described above.

All qRT-PCR raw data was stored and analyzed using the QPCR application with Analyzer Miner Cq and efficiency calculation algorithms

2.2.3 Statistical analysis

Cell culture of one experiment was performed with non-targeting control (NTC) and target (e.g. miR-26a) in different wells (equally processed) of one plate with cells from the same passage. RNA isolation and cDNA synthesis of target and NTC were performed in concert. Three technical replicates of target and NTC (cDNA) were used for one quantitative real-time RT-PCR run, results represent means of valid technical replicates with error bars denoting standard errors of the mean (SEM).

Two experiments where cells differ at least in one passage denote two biological replicates. Two sided paired one sample Students t-tests (referenced to NTC) were performed to disproof H₀ (H₀: no difference in samples), when 3 biological replicates were available. Results of t-tests represent means of quantitative real-time RT-PCR results with error bars denoting SEM. H₀ was rejected when calculated p-values were below 0.05 and marked with a star.

3 Results

3.1 Murine cell model characterization in brown adipogenesis

To test miR-26a effects in murine brown adipogenesis and upon beta-adrenergic stimulation a prior quantification had to be done. As there is a large variety of murine cell models, and miR-26a has effect in transdifferentiation¹⁹⁶, two cell lines have been characterized in the context of brown adipocyte differentiation. One cell line is the classical white adipocyte model system, 3T3-L1, while the other is a cell line isolated from brown adipose tissue of newborn mice, called iBAC¹¹⁰. The expression of uncoupling protein 1 (*Ucp1*) is one of the most prevalent characteristics of brown adipocytes¹¹⁰. As *Ucp1* is known to be the key functional element of brown adipogenesis, it serves as marker gene for brown adipogenesis²⁰⁸.

3.1.1 iBACs as appropriate cell model for murine brown adipogenesis

iBACs are cells isolated from brown adipose tissue of newborn mice, kindly provided by Patrick Seale. They were proliferated and immortalized by infection with the simian virus 40 (SV40) large T antigen. iBACs¹¹⁰ are known to express all subtypes of adrenergic receptors and have potency to enhance *Ucp1* levels. In order to confirm that iBACs differentiate into brown and not white adipocytes, the *Ucp1* mRNA levels during 11 days of adipocyte differentiation were determined using an adipogenic cocktail including insulin, dex, IBMX, T3 and indomethacin. Indeed, *Ucp1* mRNA levels were dramatically induced in iBACs during adipogenic differentiation, with an almost 1000-fold increase between day 0 and day 7 (Figure 24). Maximum *Ucp1* mRNA levels with a 1250-fold increase were reached at day 10 compared to day 0 as reference time point.

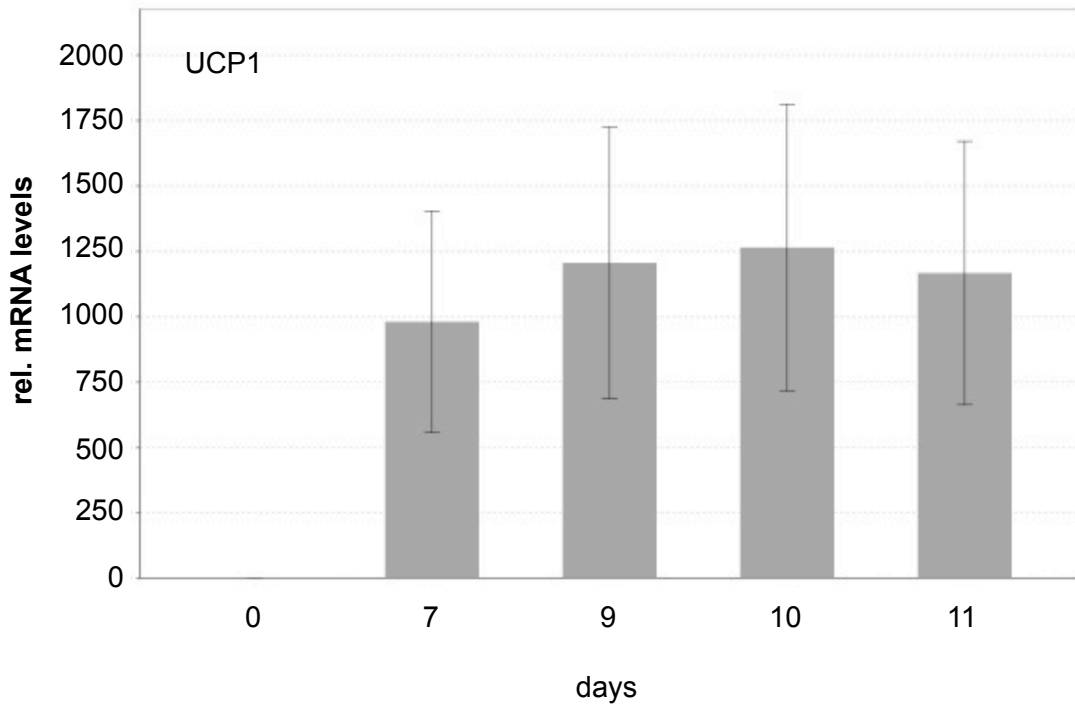


Figure 24. *Ucp1* mRNA levels during adipogenesis of iBACs. iBACs were seeded in 12-well plates (20.000 cells/well), induction cocktail (final solution: 1 nM T3, 500 nM dex, 0.5 mM IBMX, 125 μ M Indomethacin) was added to 1 ml medium (10% FBS, 20nM insulin, 20 nM HEPES buffer, pen/strep) at confluence of cells. Medium (4 ml) was changed every second day. Cells were harvested at indicated timepoints, total RNA was prepared and RT-PCR was performed. *Ucp1* mRNA was normalized to *Hmbs*. Number of independent replicates n=1. Error bars denote standard error of the mean (technical replicates).

Another characteristic of brown adipocytes is the responsiveness of *Ucp1* expression to β -adrenergic stimulation²⁰⁹ which can be performed using isoproterenol. As expected, β -adrenergic stimulation of differentiated iBACs via isoproterenol for 2 h induced *Ucp1* expression at day 7, moreover 4 h stimulation even enforced *Ucp1* expression (Figure 25A). The same effect could be observed upon 4 to 4.75 h isoproterenol treatment of iBACs at day 10 and 11 (Figure 25B). No increase in *Ucp1* levels could be observed in differentiated iBACs when stimulated with isoproterenol at day 9 and harvested 26h later. As it is not expected that these cells do not react on isoproterenol treatment specifically on day 9, these results suggest that *Ucp1* mRNA levels are rapidly induced within a few hours by isoproterenol treatment but also decrease to basal levels within 26h.

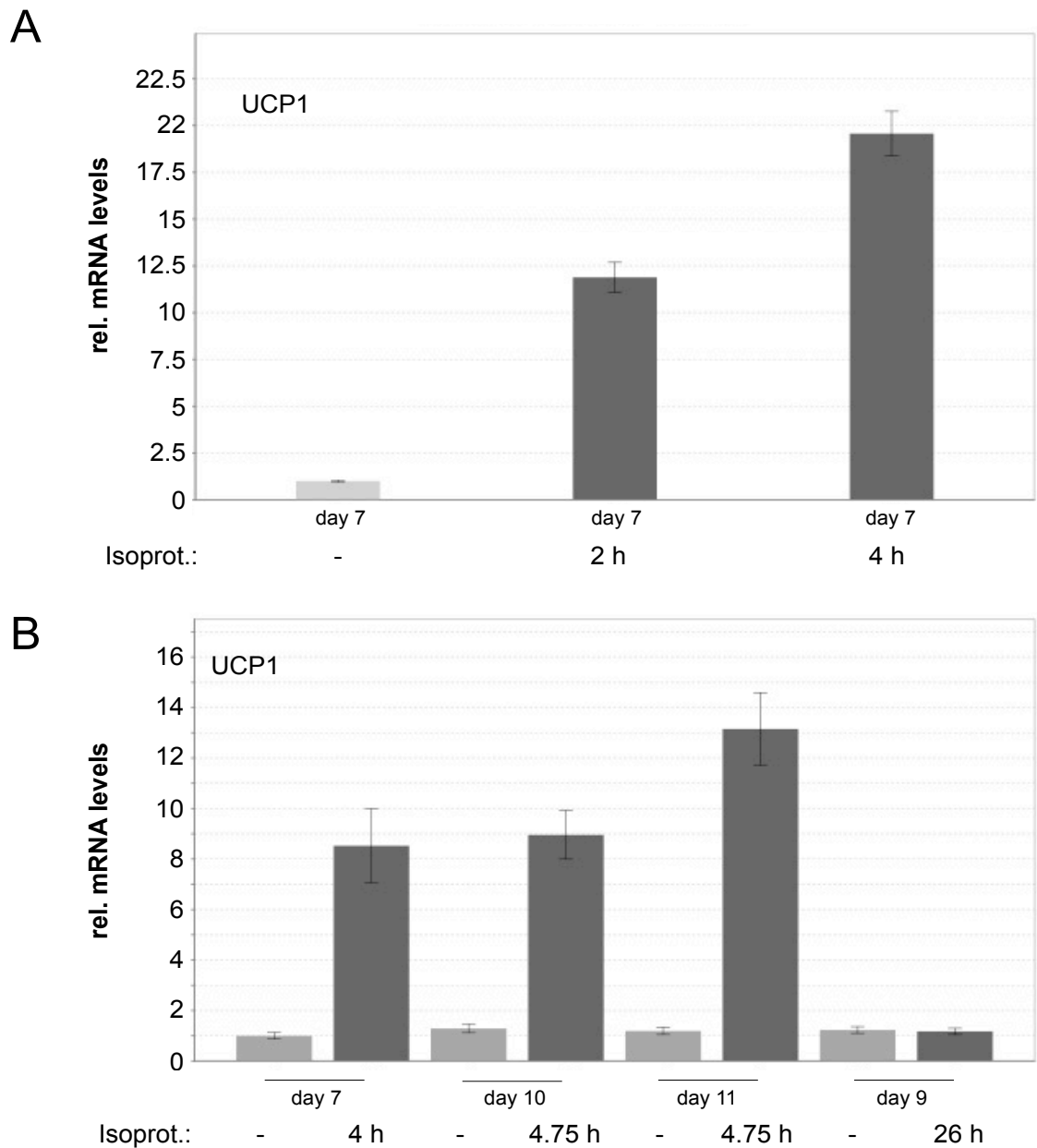


Figure 25. *Ucp1* mRNA levels upon β -adrenergic stimulation of iBACs adipocytes. iBACs were differentiated until day 7/9/10/11, 10 μ M isoproterenol was added to standard medium and a change of medium was performed 2/4/4.75/26 h before harvest. Total RNA was prepared and RT-PCR was performed. *Ucp1* mRNA was normalized to *Hmbs*. Number of independent replicates n=1. Error bars denote standard error of the mean (technical replicates).

Furthermore, comparing iBACs *in vitro* with brown adipose tissue *in vivo* revealed that β -adrenergic stimulated iBACs reached *Ucp1* levels similar to the *in vivo* situation (Figure 26).

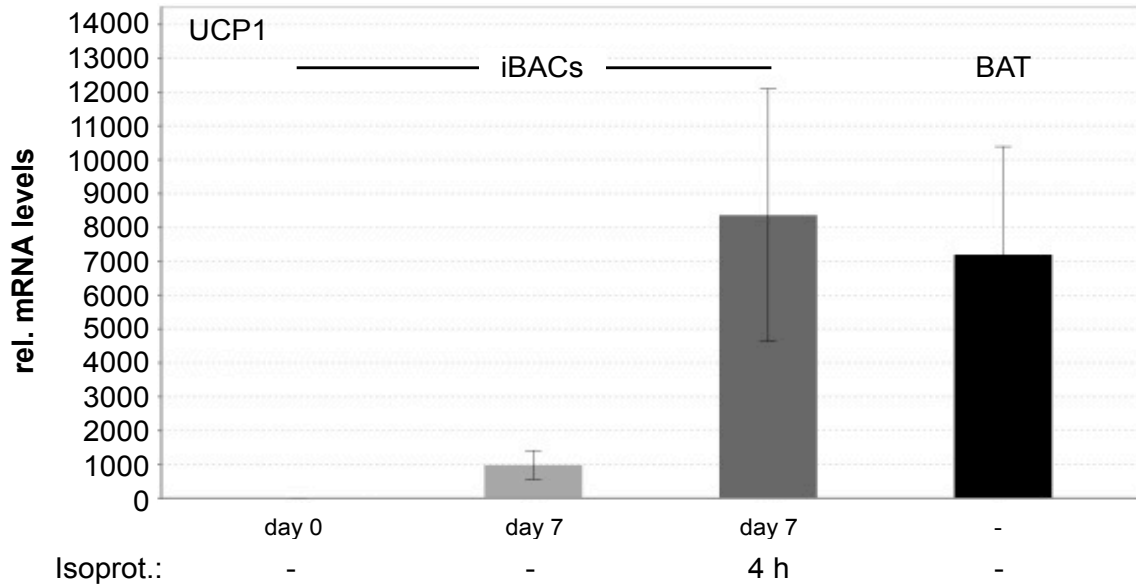


Figure 26. Comparison of *Ucp1* mRNA levels between iBACs *in vitro* and BAT *in vivo*. iBACs were differentiated until day 7, medium was changed at day 2, 4 and 6; For β -adrenergic stimulation, an additional medium change was performed, isoproterenol (10 μ M) was added, and cells were harvested 4 h later. Total RNA was prepared and RT-PCR was performed. *Ucp1* mRNA was normalized to *Hmbs*. Number of independent replicates $n=1$. Error bars denote standard error of the mean (technical replicates).

Altogether, iBACs massively induce *Ucp1* mRNA levels during adipocyte differentiation, and β -adrenergic stimulation can even enforce this *Ucp1* induction to *in vivo* levels. Thus, iBACs have been considered as murine model for brown adipogenesis.

3.1.2 3T3-L1 cells and their ability to express *Ucp1*

It has been shown in human¹³⁴ and mouse⁶⁶ that white preadipocytes have the ability to develop a brown phenotype known as *brite* (brown-in-white) adipocytes. However, this has not been shown for 3T3-L1 cells so far. However, we were interested to quantify *Ucp1* levels in 3T3-L1 cells under various experimental conditions due to previous results by others:

1. Literature shows, chronic treatment of precursors from the pure white (epididymal) adipose tissue depot⁵⁴ with the *Ppar γ* agonist rosiglitazone were not only able to promote *Pgc1 α* expression and mitochondriogenesis but also demonstrated a norepinephrine-augmentable *Ucp1* gene expression⁶⁶. Indeed, chronic rosiglitazone treatment of differentiating 3T3-L1 cells led to enhanced

Ucp1 mRNA levels. 5 biological replicates demonstrated an increase (3-fold, $p=0.0528$) in *Ucp1* mRNA levels during permanent $PPAR\gamma$ activation by rosiglitazone (Figure 27, first two bars).

2. It was shown in literature that *Ucp1* mRNA levels of BAT in cold-exposed (4 °C) *C/ebp β ^{-/-}* mice were significantly higher than in wild type mice¹⁶¹. *C/ebp β* levels were known to be enhanced by IBMX¹⁵⁸, a component of the differentiation cocktail for starting adipogenesis (induction cocktail). To affect *C/ebp β* levels of 3T3-L1 of in vitro model, cells were differentiated without dexamethasone (dex) and IBMX. Permanent $PPAR\gamma$ activation by rosiglitazone was performed like before (1). Compared to standard differentiation conditions (with dex and IBMX), the absence of dex and IBMX showed decreased lipid accumulation (see Figure 22), increased *Ucp1* mRNA levels (see Figure 27, compare left and right group), and rosiglitazone treatment could even enforce effect on *Ucp1* (14-fold, $p<0.05$) (Figure 27, first two bars in the right group).

3. β -adrenergic stimulation in brown and brite adipocytes led to an increase in *Ucp1* expression²¹⁰. For continuous and long-term β -adrenergic stimulation, norepinephrine was applied during the whole differentiation process, while for short-term stimulation only once, 40 h before harvest. As short or long β -adrenergic stimulation alone had no potent effect on *Ucp1* induction, there was indeed an induction in *Ucp1* mRNA levels upon combined long-term treatment with the $PPAR\gamma$ activating ligand rosiglitazone (Figure 27, right and left group of bars).

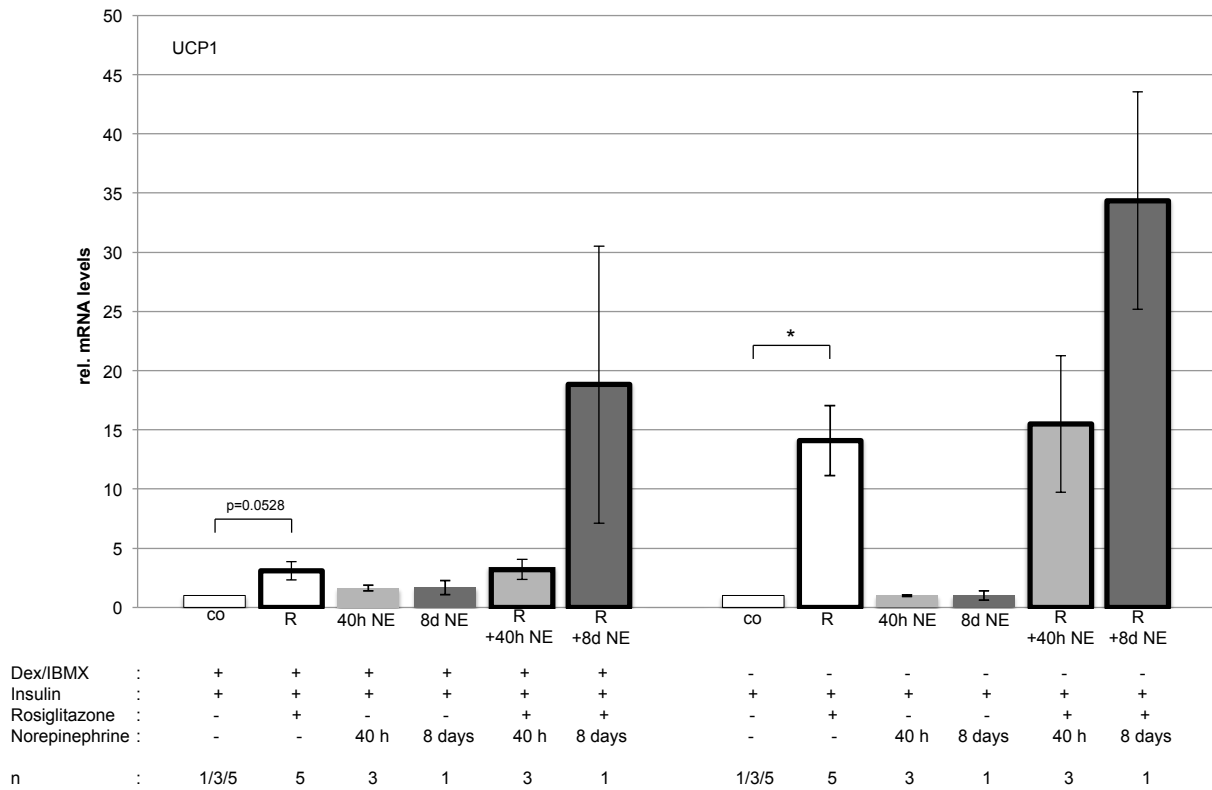


Figure 27. *Ucp1* mRNA levels in 3T3-L1 adipocytes at day 8 upon treatment with norepinephrine, rosiglitazone, or both (day 8). Cells were seeded in 12-well plates (20.000 cells/well), cocktails were added to medium as described below the bars. Induction cocktail was added at confluence (day 0), medium changes were performed at day 3, 5 and additional (only for +40 h NE cells) at day 6. Cells were differentiated until day 8. Optionally, for permanent norepinephrine treatment, norepinephrine was added to standard medium at every medium change, while for a single stimulation, 1 μ M norepinephrine was added 40 h before cell harvest. Total RNA was prepared and RT-PCR was performed. *Ucp1* mRNA was normalized to *TFII β* . Error bars denote standard error of the mean. Two sided, paired, one sample Student's t-tests were performed for biological replicates ($n > 1$), $p < 0.05$ indicated by *.

3.2 Endogenous miR-26a levels in murine brown adipogenesis

Based on previous work within the RNA Biology Group at the Institute for Genomics and Bioinformatics, Graz University of Technology, miR-26a – conserved between mouse and human - has been identified to induce human brown adipogenesis¹⁹⁶ and to be induced in WAT upon β -adrenergic stimulation in mice¹⁹⁶.

3.2.1 Endogenous miR-26a levels in iBACs

Therefore, we were interested in whether miR-26a is also present and differentially expressed in iBACs as a murine brown adipocyte model system (see chapter 3.1.1. iBACs as appropriate cell model for murine brown adipogenesis). Using miRNA qRT-PCR, relative miR-26a levels could be determined. Interestingly, miR-26a levels significantly increased during differentiation between day 0 and day 7 (Figure 28).

3.2.2 Beta-adrenergic stimulation of miR-26a levels in iBACs

Further, we were interested in whether miR-26a was responsive to β -adrenergic stimulation. Indeed, isoproterenol mediated β -adrenergic stimulation of mature brown iBACs adipocytes for 4 h (evidence for 2h) resulted in a further significant increase of miR-26a levels compared to controls (4 biological replicates). These results suggest a functional role for miR-26a in murine brown adipogenesis (Figure 28).

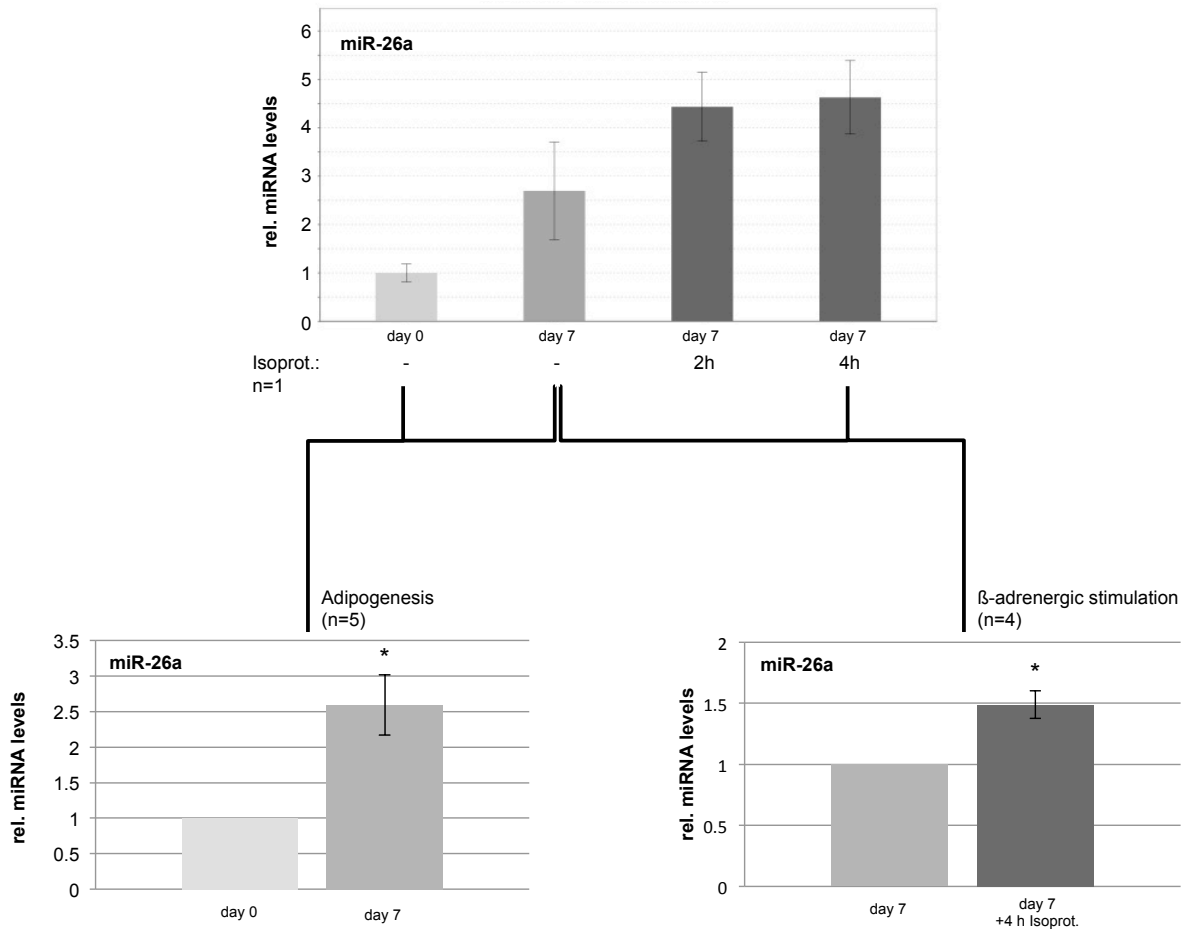


Figure 28. miR-26a level increase during brown adipogenesis and responsiveness to β -adrenergic stimulation in iBACs. Cells were stimulated to undergo adipocyte differentiation at day of confluence (day 0); adipogenesis was performed until day 7. For β -adrenergic stimulation, a medium change was performed with adding 10 μ M isoproterenol 4h (2h) before harvesting. After preparing total RNA, RT-PCR was performed and miR-26a abundance was normalized to RNU5G. Two sided, paired, one sample Student's t-tests were performed for biological replicates ($n > 1$), $p < 0.05$ indicated by *.

3.2.3 Beta-adrenergic stimulation of miR-26a levels in 3T3-L1 cells

In 3T3-L1 adipocytes, permanent *PPAR γ* stimulation (see chapter 3.1.2.) enhanced *Ucp1* mRNA levels (even stronger during differentiation without dexamethasone and IBMX) and enabled β -adrenergic sensitivity. Consequently, we were interested in whether miR-26a levels were also responsive to β -adrenergic stimulation in 3T3-L1 cells. Therefore, 3T3-L1 cells were differentiated

with an induction cocktail containing insulin but without dex and IBMX, and treated permanently with rosiglitazone until day 7. Interestingly, 40h norepinephrine treatment stimulated miR-26a levels to a 3.5 fold increase (Figure 29). However, long-term β -adrenergic stimulation could not enforce this stimulation. (for further remarks see discussion of results chapter 5.2)

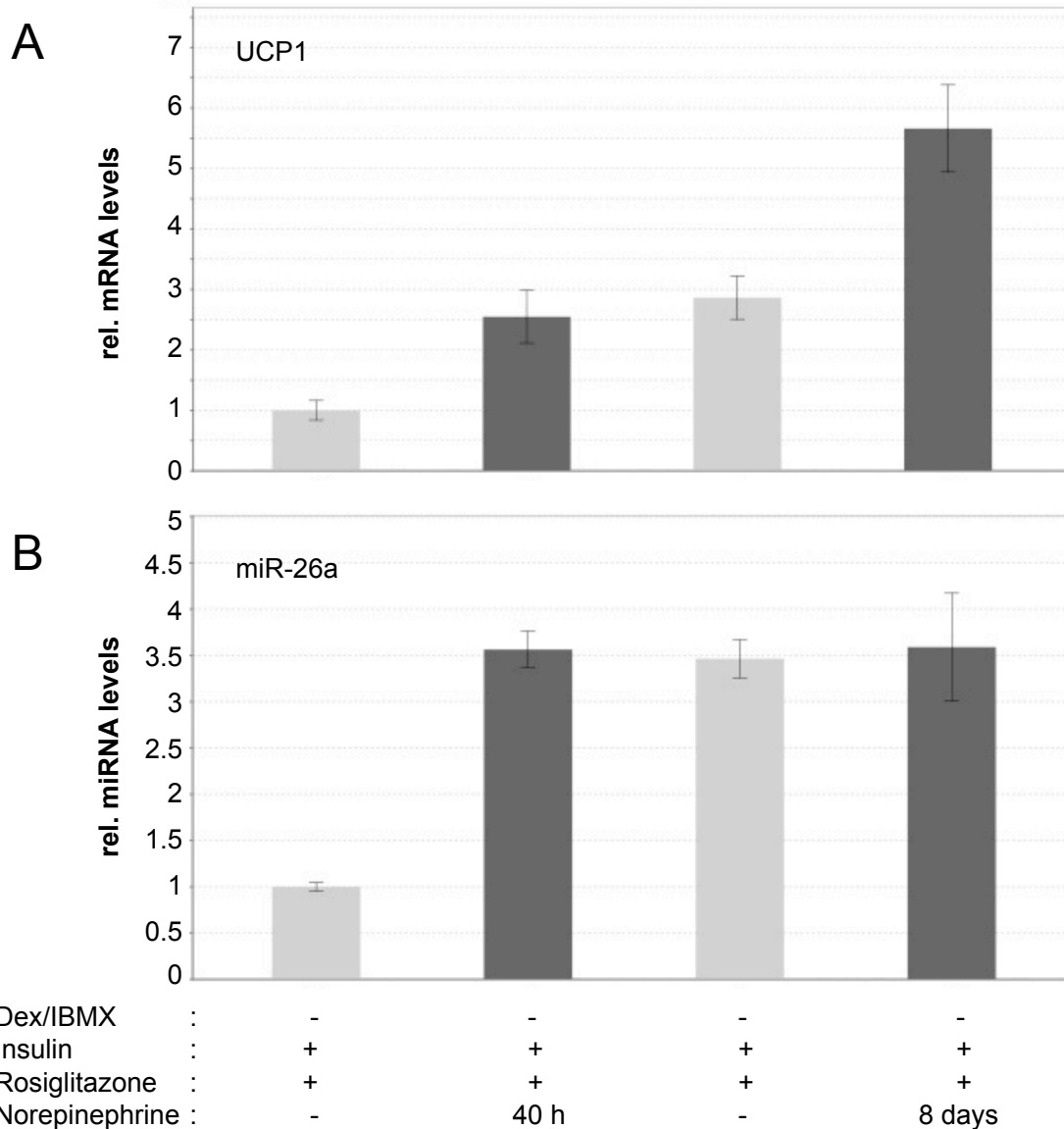


Figure 29. miR-26a responsiveness to β -adrenergic stimulation in one biological replicate of 3T3-L1 cells. Cells were seeded in 12-well plates (20.000 cells/well), cocktails were added to medium as described below bars of panel B. Induction cocktail was added at confluence (day 0), changes of medium were performed at day 3 and 5. Cells were differentiated until day 7 and Trizol harvested. Total RNA was prepared and RT-PCR was performed where miR-26a abundance was normalized to RNU5G and *Ucp1* mRNA was normalized to *TFII β* . Error bars denote standard error of the mean (3 technical replicates).

3.3 Exogenous modulation of miR-26a levels in murine adipogenesis

Knowing about the involvement of miR-26a in murine brown adipogenesis (as described above) there was interest in the effect on genes. Transient transfections of miR-26a (overexpression) and anti-miR-26a antisense oligonucleotides (silencing) were performed at day 0, mRNA of brown marker genes were measured in mature adipocytes (day 7).

3.3.1 Overexpression of miR-26a in iBACs

Increasing levels of miR-26a in iBACs during brown adipogenesis and β -adrenergic stimulation (iBACs as appropriate cell model for murine brown adipogenesis) implies the role of miR-26a in murine brown adipocytes. It has already been shown in hMADs, a human "brite" cell model¹³⁴, that overexpression of miR-26a leads to a more brown phenotype¹⁹⁶. Postulating miR-26a as an accelerator of brown adipogenesis¹⁹⁶, there was interest in its effect on higher basal *Ucp1*⁵⁴ levels of brown adipocytes. Transient overexpression of miR-26a in iBACs (Figure 30C) showed significant increase of *Ucp1* mRNA levels at day 7 (Figure 30A), meaning miR-26a is able to increase *Ucp1* levels of brown adipocytes to an even higher level.

Further effects of miR-26a in murine adipocytes on PGC-1a, another brown marker gene, could not be confirmed (Figure 30B).

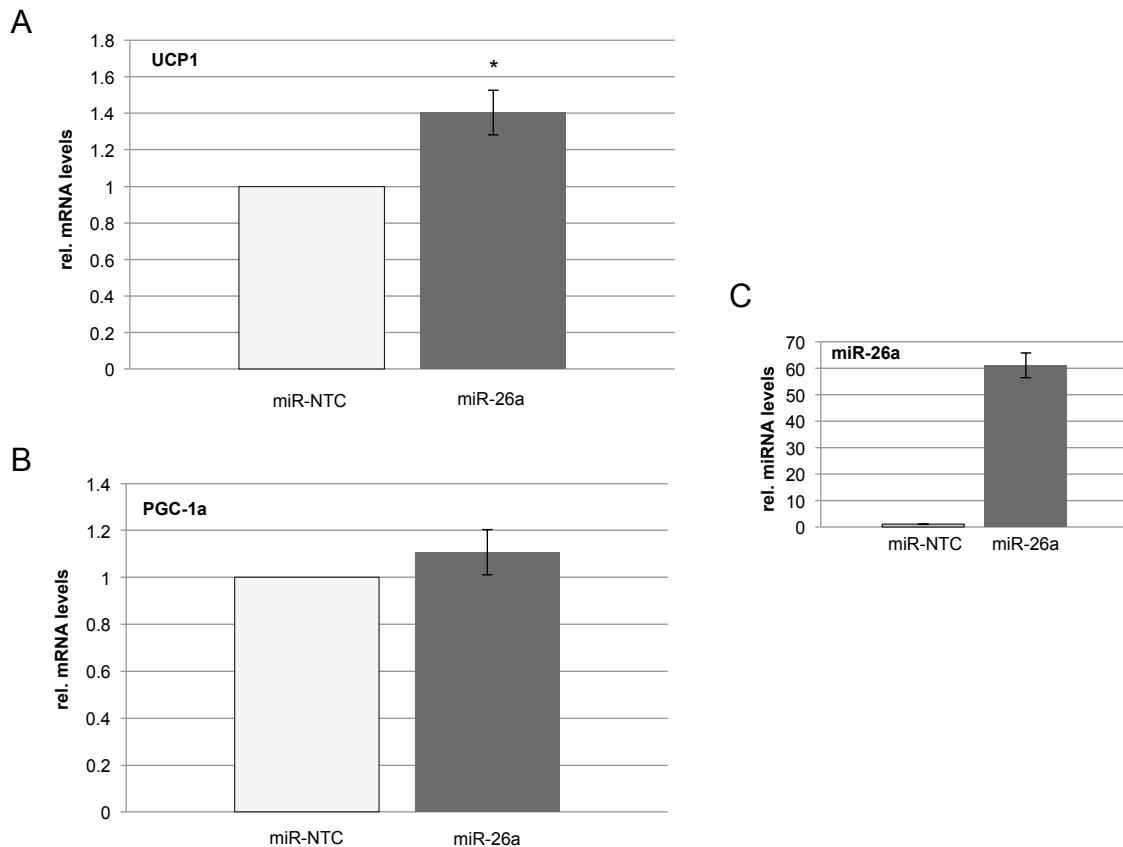


Figure 30. miR-26a initiates increase of *Ucp1* mRNA levels during adipogenesis (no or weak effect on *PGC-1a*). Cells were seeded in 12-well plates (20.000 cells/well). Transient transfection of miR-26a or non-targeting control mimics (25 nM) were performed 1 day before confluence. Differentiation of cells was performed until day 7. Total RNA was prepared and RT-PCR was performed. *Ucp1* (panel A) and *PGC-1a* (panel B) were normalized to HMBS. miR-26a abundance (panel C) 3 days after transient transfection (day 2) was normalized to RNU5G, Error bars denote standard error of the mean. Two sided, paired, one sample Student's t-tests were performed for biological replicates ($n>1$), $p < 0.05$ indicated by *.

3.3.2 Overexpression of miR-26a in 3T3-L1 and -F442A cells

Transient overexpression of miR-26a (5nM) in white adipocytes (3T3-L1 and 3T3-F442A cells) had no measurable effect on *Ucp1*, neither during differentiation with dexamethasone and IBMX (3 biological replicates in 3T3-L1 cells) nor without (3 biological replicates in 3T3-L1, 7 biological replicates in 3T3-F442A cells). Transient transfection of miR-26a in 3T3-L1 cells showed nearly 30-fold changes in miR-26a levels (Figure 31) compared to non-targeting control cells at day 0, and 2-fold changes in 3T3-F442A cells at day 2 (Figure 32).

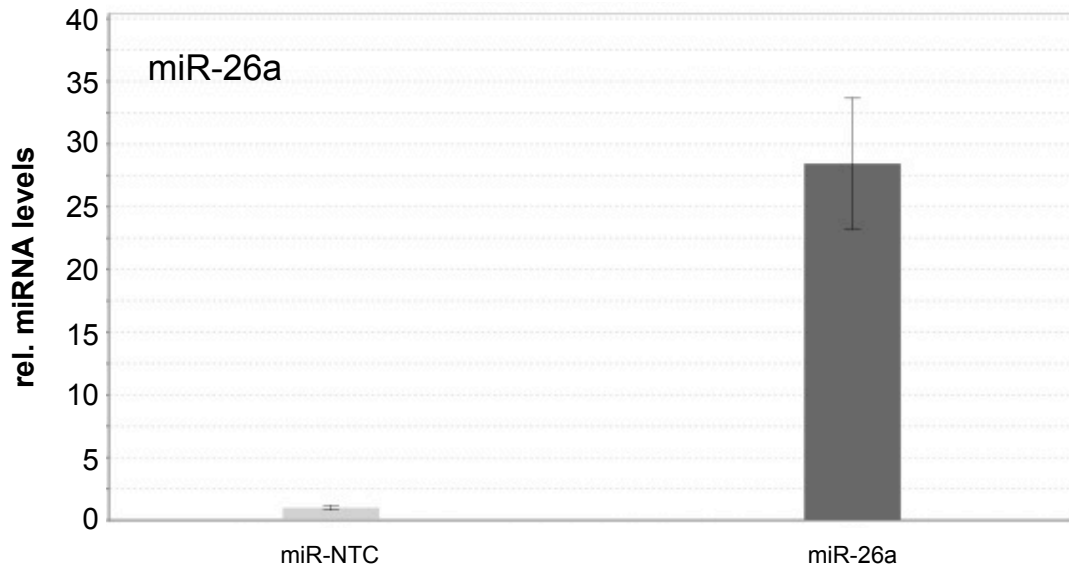


Figure 31. miR-26a levels 2 days after transient transfection (5nM). 3T3-L1 cells were seeded in 12-well plates (20.000 cells/well). Transient transfection of miR-26a or non-targeting control mimics (5 nM) were performed 2 days before confluence. Cells were harvested at confluence (day 0). Total RNA was prepared and RT-PCR was performed where miR-26 abundance was normalized to RNU5G. Error bars denote standard error of the mean.

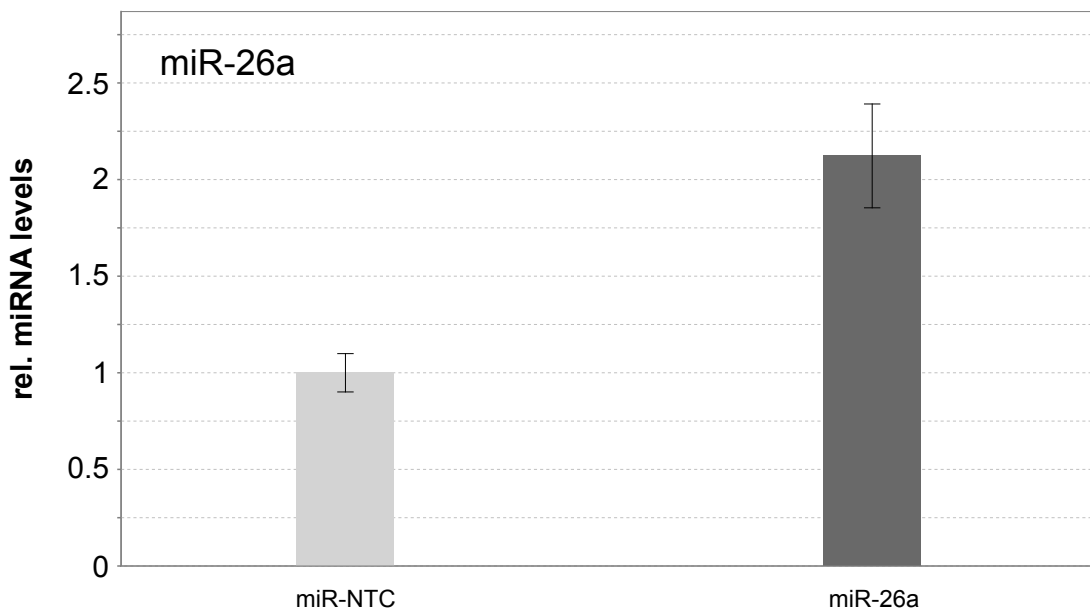


Figure 32. miR-26a levels 4 days after transient transfection (5nM) and permanent PPAR γ activation. 3T3-F442A cells were seeded in 12-well plates (20.000 cells/well). Transient transfection of miR-26a or non-targeting control mimics (5 nM) were performed 2 days before confluence. Induction cocktail was added at confluence (day 0). Medium was changed at day 2, 4 and 6; rosiglitazone was added to medium (100 nM) since day 0. Cells were differentiated until day 2 and harvested. Total RNA was prepared and RT-PCR was performed where miR-26 abundance was normalized to RNU5G. Error bars denote standard error of the mean.

3.3.3 Inhibition of miR-26a

Based on previous work within the RNA Biology Group at the Institute for Genomics and Bioinformatics, Graz University of Technology, establishment of miR-26a dependence in brown adipocyte gene expression programming of hMADs cells¹⁹⁶, initiated interest in further silencing experiments in murine cells. Inhibiting endogenous miR-26a levels by transient transfection of antisense oligonucleotides before induction of adipogenesis showed a weak decrease of *Ucp1* mRNA levels (0.8-fold) at day 7 (Figure 33A).

Experiments in iBACs and hMADs showed that silencing of miR-26a shifts cells to a more white phenotype. Silencing of miR-26a in 3T3-L1 (and -F442A) cells, models for white adipogenesis and therefore weak *Ucp1* mRNA levels, were not performed.

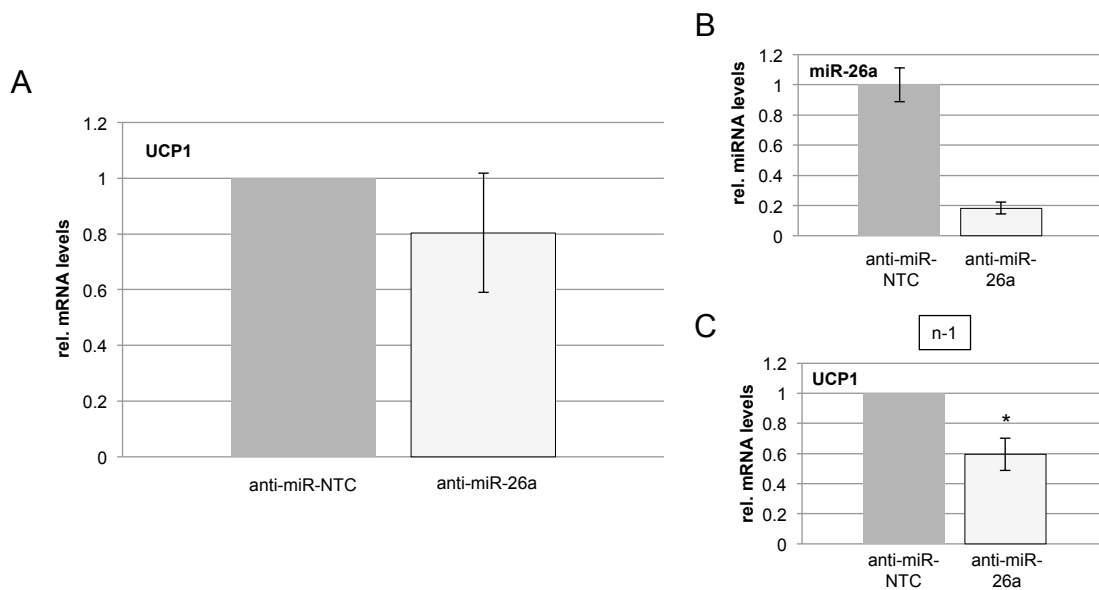


Figure 33. *Ucp1* expression mediated by silencing miR-26a at day 7. Cells were seeded in 12-well plates (20.000 cells/well). Transient transfection of anti-miR-26a antisense oligonucleotide or the respective non-targeting control at identical concentrations (25 nM) were performed 1 day before confluence. Differentiation of cells was performed until day 7. After harvest, total RNA was prepared and RT-PCR was performed (*Ucp1* mRNA normalized to HMBS and miR-26a abundance normalized to RNU5G). Error bars denote standard error of the mean. Two sided, paired, one sample Student's t-tests were performed for biological replicates ($n > 1$), $p < 0.05$ indicated by *. (A) all biological replicates merged ($n = 4$). (B): miR-26a abundance, 3 days after transient transfection (day 2). (C) 3 biological replicates ($n = 1$) merged (also see discussion of results chapter 5.3).

3.4 Global miRNA profiling in murine adipose tissue

Differentially expressed genes during adipocyte and osteoblast differentiation in hMADs were observed²¹¹ and recently miRNAs with differential expression during adipocyte differentiation of hMADs and MEFs¹⁹⁶. Further interest for differential expressed miRNAs in murine adipose tissue in BAT and cold exposed WAT (each referenced to WAT at room temperature) led to a new setup for hybridization (Figure 34).

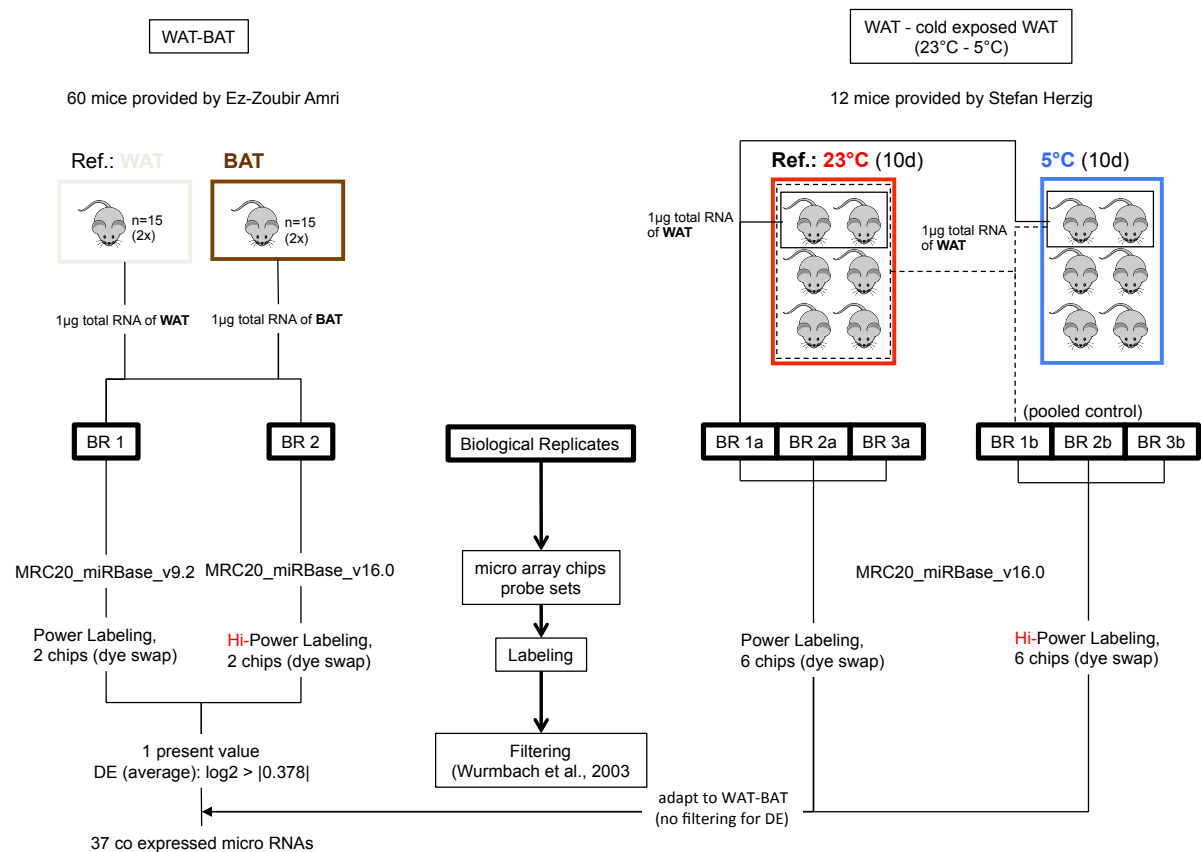


Figure 34. Setups for hybridization. Two principal setups for hybridization (WAT versus BAT and WAT versus cold exposed WAT (WATce)) were performed twice. One biological replicate of WAT versus BAT (BR 1) was already performed by Michael Karbiener. BR 2 was performed with the recent probe set (MRC20_miRBase_v16.0) and a more sensitive labeling kit (Hi-Power labeling). WAT (23 °C) versus cold exposed WAT (5 °C), was also hybridized twice but in 3 biological replicates. For control of experiment clustering different merging strategies of reference mice were done, paired (BR 1-3a) and merged (BR 1-3b). Average of WAT-BAT was filtered for differential expression of 10.3781 and present values of WAT-WATce hybridizations were adapted. Finally, filtering for co expression of principal setups was performed.

Filtering the averages of biological replicate 1 (BR1) and BR2 for differential expressions greater than 10.3781^{212} revealed 63 differentially expressed miRNAs in one principal setup (not shown). Final merging and filtering for co expression in the two principal setups resulted in 36 differentially expressed miRNAs (Figure 35), detecting weaker average differential expressions in WAT-WATce. Further investigations, using DIANA mirPath for analysis of multiple microRNAs, revealed a list of pathways interacting with differentially expressed miRNAs (Table 4 , Table 5).

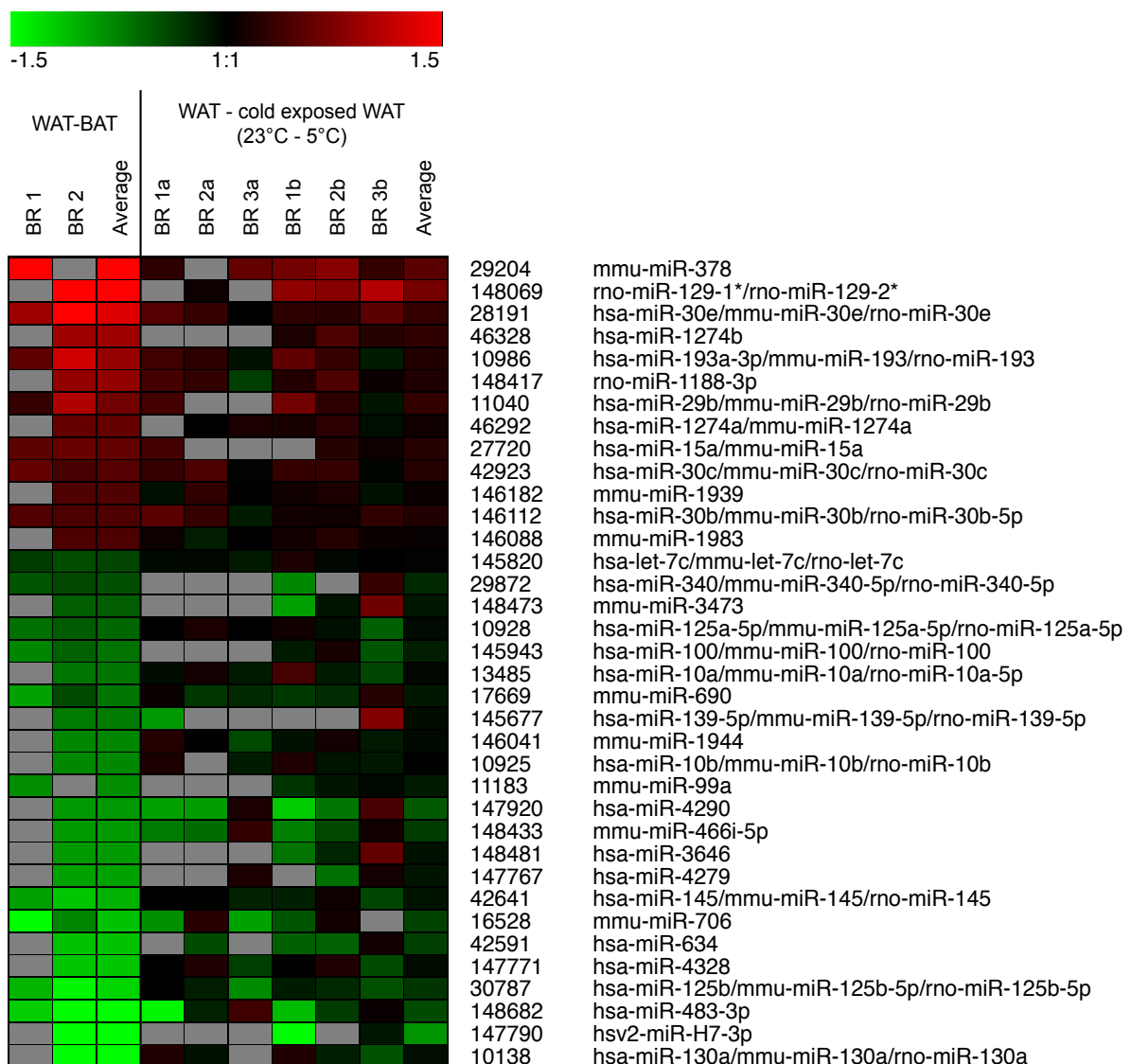


Figure 35. Differential expressed microRNAs in BAT and cold exposed WAT (referenced to WAT). BAT was isolated from 30 mice (kindly provided by Ez-Zoubir Amri). For WATce, 6 mice were exposed to 5 °C, after 10 days WAT was isolated (kindly provided by Stefan Herzig). WAT

from mice kept at room temperature were used for reference in the same amounts as target conditions.

Table 4. Pathways interacted by upregulated miRNAs in BAT and cold exposed WAT (referenced to WAT at roomtemperature). Differentially upregulated (and co expressed in 2 principal setups) miRNAs were fed to DIANA mirPath for interpretation of the involvement in biological processes. 6 of 13 candidates were available in DIANA mirPath database, showing pathways of involvement (filtered for Union p-value < 0.05).

KEGG Pathway	Union		miR-378		miR-30e		miR-193		miR-29b		miR-30c		miR-30b	
	# of Genes	p-value												
Axon guidance	37	2.7904E-14	2	0.46766643	18	7.1386E-06	8	1.9168E-08	16	3.5633E-08	18	6.395E-06	18	7.9686E-06
Focal adhesion	47	3.0453E-13	1	0.83527021	16	0.05447573	8	3.3298E-05	27	4.3118E-16	16	0.05181892	16	0.05669893
Glioma	21	1.5006E-10	0	-	9	0.00222055	3	0.01690747	11	5.0696E-09	9	0.00211225	9	0.0023344
Regulation of actin cytoskeleton	46	1.9657E-10	0	-	26	1.625E-06	8	0.00011279	15	0.00400585	26	1.4269E-06	26	1.8692E-06
ErbB signaling pathway	25	6.861E-10	0	-	12	0.00043944	6	3.9279E-07	9	0.00086741	12	0.00040973	12	0.00047131
Renal cell carcinoma	21	6.5749E-09	0	-	7	0.10860911	4	0.00069611	10	2.3526E-06	7	0.10539922	7	0.11080316
Prostate cancer	24	2.2271E-08	2	0.22763769	9	0.05502322	3	0.08458486	12	6.3477E-07	9	0.05286573	9	0.05669893
T cell receptor signaling pathway	24	1.3339E-07	1	0.87809543	12	0.00153381	3	0.10331218	11	2.983E-05	12	0.00144449	12	0.00162866
Colorectal cancer	20	1.327E-05	0	-	8	0.11648416	5	6.007E-05	9	0.00075409	8	0.11304153	8	0.12003163
Small cell lung cancer	20	2.2772E-05	1	0.92311635	7	0.31348618	2	0.4965853	12	3.8118E-07	7	0.30727874	7	0.31981902
VEGF signaling pathway	17	4.6317E-05	0	-	9	0.00790705	1	0.8025188	9	6.1899E-05	9	0.00752142	9	0.00831246
Melanoma	17	4.6317E-05	0	-	7	0.11765484	2	0.34300852	10	3.0818E-06	7	0.11417762	7	0.12003163
Long-term potentiation	16	4.7253E-05	0	-	12	3.1756E-06	1	0.85214379	3	0.85214379	12	2.8734E-06	12	3.4747E-06
Pancreatic cancer	17	8.1086E-05	1	0.98019867	6	0.34300852	3	0.03579311	8	0.00113627	6	0.33621649	6	0.34645581
Chronic myeloid leukemia	17	0.00017689	1	1	9	0.01499558	2	0.39062784	5	0.22537266	9	0.01440759	9	0.01576442
Heparan sulfate biosynthesis	7	0.00021822	1	0.29229258	2	0.59452055	0	-	4	0.00035266	2	0.58860497	2	0.60049558
Huntington's disease	9	0.0002436	1	0.48675226	3	0.40252422	1	0.70468809	4	0.01099846	3	0.39851904	3	0.40656966
Phosphatidylinositol signaling system	16	0.00025101	0	-	10	0.00137404	3	0.03142976	4	0.48190899	10	0.00129402	10	0.00145901
Acute myeloid leukemia	14	0.00028874	1	0.86070798	5	0.37157669	4	0.00012218	4	0.28083162	5	0.36787944	5	0.37908304
Endometrial cancer	13	0.00029753	0	-	5	0.25410696	3	0.00603608	7	0.00033546	5	0.25157855	5	0.25924026
Non-small cell lung cancer	13	0.00029753	0	-	8	0.00242967	1	0.97044553	6	0.00479587	8	0.00231117	8	0.00255424
MAPK signaling pathway	40	0.00043944	2	0.89583414	22	0.01215518	7	0.01015286	13	0.1755204	22	0.01144732	22	0.01303653
GnRH signaling pathway	19	0.00073118	1	0.86935824	8	0.22537266	4	0.0086517	8	0.01690747	8	0.22090998	8	0.23221622
Inositol phosphate metabolism	12	0.00073916	0	-	9	0.00010837	2	0.15107181	2	0.87809543	9	0.00010104	9	0.00011622
ECM-receptor interaction	17	0.00103848	0	-	5	0.92311635	1	0.71177032	13	5.3295E-09	5	0.91393119	5	0.93239382
Gap junction	18	0.00104891	0	-	8	0.17204486	1	0.66365025	10	0.00019944	8	0.16696017	8	0.1755204
B cell receptor signaling pathway	14	0.00105946	1	0.90483742	7	0.06329177	0	-	8	0.00022263	7	0.06142121	7	0.06521929
Ubiquitin mediated proteolysis	22	0.00388746	1	0.69767633	17	6.1283E-05	1	0.86070798	4	0.98019867	17	5.6009E-05	17	6.7729E-05
Oxidative phosphorylation	2	0.00609675	0	-	1	0.05393369	1	0.77105159	0	-	1	0.05502322	1	0.05339704
Leukocyte transendothelial migration	19	0.00744658	0	-	10	0.09632764	1	0.71177032	8	0.05130331	10	0.09348073	10	0.09926125
Type II diabetes mellitus	10	0.00900478	0	-	6	0.03688317	2	0.12745397	3	0.46301307	6	0.03579311	6	0.03800643
Insulin signaling pathway	22	0.00995182	0	-	10	0.33287108	5	0.00660453	8	0.18451952	10	0.32627979	10	0.33959553
Long-term depression	14	0.01067341	0	-	9	0.01499558	1	0.76337949	5	0.22537266	9	0.01440759	9	0.01576442
Tight junction	21	0.011109	3	0.07207846	12	0.05130331	1	0.86935824	9	0.04880122	12	0.04929168	12	0.05339704
Fc epsilon RI signaling pathway	14	0.01240073	0	-	7	0.17906615	3	0.04595926	7	0.01440759	7	0.1755204	7	0.18451952
Calcium signaling pathway	26	0.01795296	1	0.75578374	19	0.000978	2	0.83527021	6	0.86070798	19	0.00090281	19	0.00105946
Purine metabolism	5	0.02305206	0	-	2	0.06587475	1	0.95122942	2	0.26982006	2	0.06720551	2	0.06457035
Melanogenesis	16	0.02625234	1	0.85214379	7	0.4916442	4	0.00995182	5	0.52204578	7	0.48675226	7	0.05157607
Natural Killer cell mediated cytotoxicity	18	0.02625234	0	-	12	0.01484637	1	0.74081822	8	0.06142121	12	0.0141223	12	0.01560756
mTOR signaling pathway	10	0.02872464	0	-	5	0.25410696	0	-	5	0.0395575	5	0.25157855	5	0.25924026

Table 5. Pathways interacted by downregulated miRNAs in BAT and cold exposed WAT (referenced to WAT at room temperature). Differentially downregulated (and co expressed in 2 principal setups) miRNAs were fed to DIANA mirPath for interpretation of the involvement in biological processes. 14 of 23 candidates were available in DIANA mirPath database, showing pathways of involvement (filtered for Union p-value < 0.05).

KEGG Pathway	Union		let-7c		miR-340		miR-125a		miR-100		miR-10a		miR-690	
	# of Genes	p-value												
MAPK signaling pathway	75	7.6614E-14	24	1.4557E-06	0	-	18	1.5887E-05	1	0.87809543	4	0.2671353	5	0.62500227
Axon guidance	44	9.7867E-12	10	0.02351775	1	0.07502004	5	0.54335087	0	-	5	0.00034915	8	1.4813E-05
O-Glycan biosynthesis	13	4.2127E-07	4	0.00909528	0	-	4	0.00067554	0	-	1	0.51685133	0	-
Focal adhesion	49	1.6088E-06	16	0.00101791	1	0.17377394	5	0.86070798	1	0.97044553	3	0.40252422	6	0.08126824
Colorectal cancer	27	2.2156E-06	7	0.05286573	0	-	3	0.87809543	2	0.00416933	0	-	4	0.03370868
Glioma	21	1.0757E-05	7	0.00504176	0	-	2	0.89583414	2	0.00052611	2	0.1451482	0	-
Renal cell carcinoma	22	2.8375E-05	5	0.22537266	0	-	3	0.63762815	0	-	3	0.00744658	2	0.60653066
TGF-beta signaling pathway	26	3.4657E-05	8	0.01759747	0	-	4	0.4538448	0	-	3	0.02843882	0	-
Regulation of actin cytoskeleton	49	3.8302E-05	13	0.07427358	1	0.20189652	6	0.99004983	0	-	3	0.48675226	6	0.12618578
Chronic myeloid leukemia	23	4.5856E-05	8	0.00416933	0	-	3	0.7344696	0	-	2	0.23457029	1	0.68386141
ErbB signaling pathway	25	5.6572E-05	5	0.4538448	0	-	3	0.89583414	1	0.52729242	3	0.02399284	3	0.23930892
GnRH signaling pathway	26	0.00021822	5	0.61878339	0	-	5	0.2143811	1	0.58274825	1	0.77105159	2	0.91393119
Oxidative phosphorylation	3	0.00054758	0	-	0	-	1	0.33959553	0	-	0	-	1	0.89583414
Wnt signaling pathway	34	0.00065557	10	0.06203851	0	-	4	0.86935824	1	0.8025188	5	0.00114769	5	0.07730474
Prostate cancer	23	0.00134683	6	0.21653567	0	-	4	0.4538448	2	0.00540733	2	0.32955896	2	0.83527021
Adherens junction	20	0.00137404	7	0.01984109	0	-	4	0.26447726	1	0.44932896	1	0.92311635	2	0.65704682
Long-term potentiation	18	0.00169512	2	0.95122942	1	0.00798652	4	0.16863815	1	0.38674102	1	1	2	0.53794444
Glycan structures - biosynthesis 1	27	0.00240549	9	0.03080741	0	-	7	0.0395575	2	0.01849971	1	0.67705687	1	0.93239382
mTOR signaling pathway	15	0.00331267	4	0.25924026	0	-	4	0.07136127	1	0.29819728	0	-	3	0.0395575
Pancreatic cancer	19	0.00344787	8	0.00273944	0	-	4	0.25410696	0	-	0	-	2	0.64403642
Acute myeloid leukemia	16	0.0043831	4	0.36059494	0	-	3	0.44485807	1	0.34300852	0	-	1	0.71177032
Neuroactive ligand-receptor interaction	20	0.00568457	5	0.16863815	0	-	2	0.082085	1	0.86935824	2	0.72614904	2	0.53794444
Melanoma	18	0.0066709	8	0.00204983	0	-	2	0.77880078	1	0.43171052	1	0.94176453	0	-
Autoimmune thyroid disease	1	0.00856561	1	0.57694981	0	-	0	-	0	-	0	-	0	-
T cell receptor signaling pathway	22	0.00918669	4	1	0	-	1	0.51685133	0	-	2	0.36787944	3	0.30422126
Non-small cell lung cancer	14	0.01122064	4	0.25924026	0	-	2	0.94176453	0	-	0	-	0	-
Arachidonic acid metabolism	2	0.01191449	0	-	0	-	1	0.77880078	0	-	0	-	0	-
Insulin signaling pathway	29	0.01529851	6	0.86070798	1	0.08981529	6	0.32627979	1	0.77880078	2	0.67705687	0	-
Adipocytokine signaling pathway	17	0.0181334	6	0.06925223	0	-	2	0.77880078	1	0.43171052	1	0.94176453	4	0.01144732
Tryptophan metabolism	1	0.021068	0	-	0	-	1	0.94176453	0	-	0	-	0	-
Ubiquitin mediated proteolysis	27	0.02328374	6	0.74826357	0	-	9	0.00514361	0	-	0	-	3	0.61878339
Complement and coagulation cascades	3	0.03019738	0	-	0	-	1	0.77880078	0	-	0	-	0	-
Melanogenesis	21	0.03651617	5	0.65050909	0	-	3	0.94176453	2	0.00918669	3	0.04460096	3	0.33959553
Type I diabetes mellitus	2	0.03688317	0	-	0	-	0	-	0	-	0	-	1	0.72614904
Basal transcription factors	9	0.03725385	3	0.22763769	0	-	2	0.48675226	0	-	1	0.62500227	1	0.96078944
Fc epsilon RI signaling pathway	17	0.04642115	4	0.69767633	0	-	4	0.30119421	0	-	0	-	1	0.69073433
Nucleotide sugars metabolism	3	0.04929168	2	0.00621991	0	-	0	-	0	-	0	-	0	-

KEGG Pathway	miR-139		miR-10b		miR-99a		miR-145		miR-706		miR-125b		miR-130a	
	# of Genes	p-value												
MAPK signaling pathway	4	0.60049558	3	0.03579311	1	0.82695913	14	0.00015532	11	0.0141223	18	1.5887E-05	13	0.18451952
Axon guidance	3	0.30727874	2	0.06142121	0	-	12	1.7519E-08	3	0.96078944	5	0.54335087	10	0.01191449
O-Glycan biosynthesis	1	0.67032005	0	-	0	-	0	-	2	0.18086579	4	0.00067554	4	0.52729242
Focal adhesion	7	0.00111378	1	0.94176453	1	0.99004983	8	0.062662	3	0.8436482	6	0.86070798	13	0.01657268
Colorectal cancer	5	0.00010622	0	-	2	0.0071546	6	0.00373503	3	0.54881164	3	0.87809543	9	0.0008251
Glioma	1	0.84366482	0	-	2	0.00108086	3	0.2780373	0	-	2	0.89583414	11	0.0694E-09
Renal cell carcinoma	3	0.03688317	0	-	0	-	3	0.36421898	0	-	3	0.63762815	8	0.00075409
TGF-beta signaling pathway	2	0.55432728	0	-	0	-	9	4.6557E-07	1	0.81873075	4	0.4538448	14	8.9876E-10
Regulation of actin cytoskeleton	1	0.63128365	1	0.88692044	0	-	8	0.10752843	8	0.0926125	6	0.99004983	15	0.0043831
Chronic myeloid leukemia	0	-	0	-	0	-	5	0.01640777	1	0.98019867	3	0.73344696	10	1.2373E-05
ErbB signaling pathway	2	0.52729242	1	0.61878339	1	0.57694981	3	0.57694981	2	0.85214379	3	0.89583414	9	0.0009491
GnRH signaling pathway	2	0.62500227	1	0.68386141	1	0.63128365	4	0.2671353	5	0.06203851	5	0.2143811	9	0.00334597
Oxidative phosphorylation	0	-	0	-	0	-	0	-	1	0.55432728	1	0.33959553	0	-
Wnt signaling pathway	3	0.41065575	0	-	1	0.86070798	8	0.00647375	4	0.72614904	4	0.86935824	9	0.09926125
Prostate cancer	3	0.10126646	0	-	2	0.00918669	4	0.20804518	2	0.81873075	4	0.4538448	11	1.275E-05
Adherens junction	4	0.00172937	0	-	1	0.4965853	11	1.0342E-13	2	1	4	0.26447726	5	0.21013607
Long-term potentiation	2	0.31663677	0	-	1	0.43171052	3	0.30422126	1	0.86935824	4	0.16863815	7	0.00341356
Glycan structures - biosynthesis 1	2	0.77880078	0	-	2	0.02815585	1	0.58274825	5	0.13806924	7	0.0395575	4	0.83527021
mTOR signaling pathway	1	0.95122942	0	-	1	0.33959553	3	0.16529889	2	0.67705687	4	0.07136127	8	1.5264E-05
Pancreatic cancer	0	-	0	-	0	-	4	0.09536916	0	-	4	0.25410696	8	0.00123091
Acute myeloid leukemia	0	-	1	0.42741493	1	0.38674102	2	0.78662786	2	0.77880078	3	0.44485807	7	0.00125578
Neuroactive ligand-receptor interaction	3	0.90483742	2	0.3753111	1	0.81873075	2	0.20804518	5	0.90483742	2	0.082085	2	0.02472353
Melanoma	1	0.77880078	1	0.52204578	1	0.47711392	3	0.37908304	2	0.96078944	2	0.77880078	7	0.00767337
Autoimmune thyroid disease	0	-	0	-	0	-	0	-	0	-	0	-	0	-
T cell receptor signaling pathway	3	0.12245643	1	0.67032005	0	-	3	0.67705687	1	0.76337949	1	0.51685133	8	0.01499558
Non-small cell lung cancer	0	-	0	-	0	-	3	0.16529889	0	-	2	0.94176453	8	1.5264E-05
Arachidonic acid metabolism	0	-	0	-	0	-	0	-	1	0.96078944	1	0.77880078	0	-
Insulin signaling pathway	3	0.37157669	0	-	1	0.83527021	6	0.10228421	2	0.86070798	6	0.32627979	11	0.00621991
Adipocytokine signaling pathway	0	-	0	-	1	0.47711392	1	0.97044553	1	0.96078944	2	0.77880078	7	0.00767337
Tryptophan metabolism	0	-	0	-	0	-	0	-	0	-	1	0.94176453	0	-
Ubiquitin mediated proteolysis	3	0.31981902	2	0.06457035	0	-	2	0.92311635	1	0.47711392	9	0.00514361	8	0.13806924
Complement and coagulation cascades	1	0.77880078	0	-	0	-	1	0.97044553	0	-	1	0.77880078	1	0.53794444
Melanogenesis	2	0.64403642	0	-	2	0.01484637	3	0.7344696	5	0.06925223	3	0.94176453	9	0.00416933
Type I diabetes mellitus	0	-	0	-	0	-	0	-	0	-	0	-	1	0.72614904
Basal transcription factors	1	0.78662786	0	-	0	-	2	0.30119421	1	0.85214379	2	0.48675226	1	0.71177032
Fc epsilon RI signaling pathway	0	-	0	-	0	-	2	0.95122942	2	0.96078944	4	0.30119421	6	0.07280286
Nucleotide sugars metabolism	0	-	0	-	0	-	1	0.28365403	0	-	0	-	1	0.52204578

4 Discussion of Methods

4.1 Cell culture experiments

To observe murine brown adipogenesis in vitro, different cell models with different characteristics were chosen.

4.1.1 Cell models

iBACs (kindly provided by Patrick Seale) were chosen to represent brown adipogenesis, known for a strong induction of *Ucp1* mRNA levels during adipogenesis and the ability of further β -adrenergic stimulation, functionally comparable to brown adipose tissue with slight restriction in mRNA amounts and fold changes during β -adrenergic stimulation¹¹⁰ (see details in discussion of results). Experiments with iBACs were focused on *Ucp1* mRNA as the classical brown marker gene, endogenous miR-26a levels and exogenous modulation of miR-26a (overexpression and inhibition).

For observations of possible brown adipogenesis in white adipocytes the classical cell lines **3T3-L1** and **3T3-F442A** were chosen. Despite their popularity and establishment in white adipogenesis research, function and comparability to in vivo has to be challenged in respect of karyotype⁸⁵ and other consequences arising from the applied method of immortalization (serial passaging and selection of susceptible clones)¹¹⁰. Experiments were focused on enhancement of *Ucp1* mRNA upon different treatments during differentiation of 3T3-L1 cells (see discussion of differentiation) and upon overexpression of miR-26a in both white cell lines.

4.1.2 Differentiation of cells

iBACs were proliferated and differentiated according to provider's protocols estimating intervals for change of medium (as well as amount) and the percentage of confluence for applying the induction cocktails (day 0). Obviously definition of day 0 has an effect on fold changes of *Ucp1* mRNA levels during differentiation. Differentiation of cells in experiments was accompanied by fast changes of pH-levels (color of medium) compared to 3T3-L1 cell lines, indicating a faster cell

metabolism demanding higher volume of media. Certain quantities of media require distinct intervals of renewal (pH levels, nutrients) and affect the application time of segregated hormones, thereby having effect on adipocyte differentiation. For experiments in white adipocytes (**3T3-L1** cells), the effect of two induction cocktail components (dexamethasone and IBMX), known for their effects on *C/ebps*¹⁵⁸ and in further consequence on brown adipogenesis²⁴, were tested due to *Ucp1* mRNA's inducibility. For examination of possible further effects on *Ucp1*, permanent *Ppar γ* ⁵⁴ activation with rosiglitazone and β -adrenergic stimulations (permanent or once) with norepinephrine was investigated³⁸. Effect of norepinephrine was not tested in **3T3-F442A** cells but could lead to further insights, considering these cells as a fast proliferating cell model (where metabolism is faster than in 3T3-L1 cells) – what rather resembles the behavior of brown adipocytes.

4.1.3 Transfection of adipocytes

Consequently a Standard Operation Protocol (SOP) for "Transfection", established by the "RNA Biology Group" in hMADS cells¹⁹⁶ was adapted to new murine cell lines. Transfection was always performed before 100% confluence (at least 24 h) with an established transfection reagent in two distinct concentrations following the established SOP. Another SOP for transfection by electroporation (procedure was kindly guided by Ariane Klatzer), was tested but did not improve efficiency of established procedure.

Two distinct concentrations (5 nM and 25 nM) of oligonucleotides for overexpression or inhibition of miR-26a were used in **iBACs**. High (25 nM) concentrations of oligonucleotides resulted in a 60-fold overexpression and a 0.2-fold (20% of NTC) down regulation of miR-26a levels at day 2 of differentiation (3 days after transfection). The low (5 nM) concentration transfection protocol was not tested upon miR-26a levels at day 2. The transfection reagent solely was tested on iBACs and did not have an effect on mortality rate in all used concentrations, while the confluence states at the time of transfection seemed to have an effect. Increased mortality rates were observed at earlier time points of transfection (the lower confluence, the higher mortality).

For transfection of **3T3-L1** and **-F442A** cells only the low concentration protocol (5 nM) was used leading to an 28-fold overexpression of miR-26a in 3T3-L1 cells at

day 0 (2 days after transfection) and in 3T3-F442A only 2-fold at day 2 (4 days after transfection). In comparison to iBACs miR-26a levels (after overexpression) are rather low in 3T3-L1 cells but very low in -F442As, although levels are from different days of differentiation. A higher oligonucleotides transfection efficiency for further experiments could possibly increase miR-26a levels without effecting mortality rate significantly, thereby increasing the effect of inhibition or overexpression of miR-26a. 3T3-F442As represented a cell line that allowed to observe the action of miR-26a effects independent from rosiglitazone.

4.1.4 Quantitative real time RT-PCR

Each experiment (both cell lines) was measured on one plate in 3 technical replicates.

For **iBACs** several housekeeping genes were tested, *Hmbs* showed most constant behavior in all conditions and was used in all experiments. All observed mRNA levels of genes were in trustable measuring range and results were fed to statistical analysis.

As known from literature *Ucp1* mRNA levels in white adipocytes (in vivo) are rather low²⁰⁸, often followed by big error bars. In vitro research of *Ucp1* mRNA levels in white **3T3-L1** or **-F442A** cells was not found in literature and observed *Ucp1* mRNA levels in experiments showed a "tipping behavior" at the limit of detection. To solve this detection limit problem, 8-fold amounts of cDNA were used for quantitative real time RT-PCR leading signal raise during quantification, thereby reaching a more confident detection range, indicated by values and graphs of technical triplicates (smaller variances).

Finally, for normalization of target genes *TFII β* and in some rare cases *Hmbs* were used.

4.1.5 Statistics to analyze biological replicates

In case of 3 biological replicates t-tests were performed for experiments. Means of technical replicates of each biological replicate were used for determination of p-values (all used cell lines).

Usually, two sided, paired, two sample t-tests are used to determine significance of biological replicates, which did not lead to significant p-values in experiments. Observing biological replicates in detail, fold changes (target to non targeting

control) were conserved but amounts of mRNA levels distinguished in biological replicates (offset). This led to the idea to feed statistic post processing (t-testing) with fold changes instead of two values (target and non targeting control). Nevertheless, two sided, paired, one sample t-tests are uncommon but used²¹³ and under given circumstances it was possible to show effects of micro RNAs, which are known by nature to be less effective and probably shifted by effects during transfection and differentiation (also see discussion above) leading to different offsets (bias) in biological replicates¹⁸⁵.

4.2 Microarray

The setup for microRNA microarrays analysis is multifunctional and could be post processed in many ways. Some properties and following effects are described below:

1. Two biological conditions were compared (WAT vs. BAT and WAT vs. cold exposed WAT) in order to explore simultaneous differential expressions of BAT and cold exposed WAT (referenced to WAT).
2. Each condition was labeled twice (plus dye swap) with labeling kits of different sensitivities. By choice of filtering, a wide (union of sets) or small (intersection of sets) range of intensities could be chosen, while a small range is considered as conservative.
3. Six samples for each group were available in the WAT vs. cold exposed WAT (WATce) condition. Pooling of control samples was done in two ways, testing reproducibility of results and improving confidence of a rather small sample size compared to WAT-BAT hybridization (30 samples per group).
4. One setup was performed by Michael Karbiener using an older version of the established miRNA chip, composing less miRNA candidates. For this reason filtering for one present value was performed in the WAT-BAT setup.

Obviously there are many possibilities for filtering, receiving different results related to the chosen focus. In this approach the aim was to reveal differential expression in WAT-BAT, and WAT-WATce, leading to novel miRNA candidates with potential involvement in the distinction between white and brown adipocytes. Performing different setups in different ways may result in a lower number but higher confidence of candidates. Finally results were transferred to an online

prediction tool (DIANA-miRPath)¹⁸⁸ to find putative pathways and targets effected by differential expressed miRNA candidates.

5 Discussion of Results

5.1 Murine cell models in brown adipogenesis

As shown in literature, isolated brown adipocytes, immortalized by SV40 large T antigen is a valid in vitro model for brown adipogenesis¹¹⁰, functionally also reflected by increasing *Ucp1* mRNA levels during adipogenesis and upon β -adrenergic stimulation of in **iBACs** adipocytes. Fold changes of mRNA levels during adipogenesis and upon β -adrenergic stimulation are related to samples of different individuals and procedures (also see discussion of methods and differentiation) during whole processing. Experiments show stronger induction of *Ucp1* mRNA levels upon β -adrenergic stimulation (8 fold) than described in literature (3-5 fold). Levels of *Ucp1* mRNA from mature iBACs adipocytes were described to reach 70 % of levels in BAT in vivo samples, while mature iBACs from experiments reached 14% of BAT in vivo values.

3T3-L1 and -F442A cells are not published to express *Ucp1*, probably because of low values of mRNA, close to detection limits and the expectation to have no brown adipogenesis in white adipocytes. Nevertheless there are published experiments in primary cultures from the purest white depot (epididymal) demonstrating to promote *Pgc-1a*, mitochondriogenesis and also a norepinephrine augmentable *Ucp1* expression under chronic treatment with rosiglitazone during differentiation⁵⁴. In experiments with 3T3-L1 cells, induction of *Ucp1* mRNA was close to significance ($p=0.0528$) with chronic treatment with the *Ppar γ* agonist rosiglitazone, while 40 h β -adrenergic stimulation showed no significant effect in any case. Interestingly, chronic rosiglitazone treatment upon long β -adrenergic stimulation with norepinephrine showed an effect in one biological replicate.

Although results are not significant some are promising or are almost significant, initializing further investigations for brown adipogenesis in white 3T3-L1 cells. Further experiments were motivated by published observations of other groups as well as established knowledge:

1. Mitochondrial biogenesis in 3T3-L1 cells upon 24 and 48 h of rosiglitazone indicating vital plasticity (at least) of mitochondria in 3T3-L1 cells¹¹⁸.

2. The involvement of *C/ebps* in brown adipogenesis²⁴ and their activation by Dexamethasone and IBMX¹⁵⁸, two typical components of induction cocktails for 3T3-L1 cells.
3. *Ucp1* mRNA levels of BAT from cold-exposed (4 °C) *C/ebpβ*^{-/-} mice are significantly higher than in wild type mice¹⁶¹, confirming (2)
4. *C/ebpβ* is able to reprogram white 3T3-L1 cells, expressing brown marker genes¹⁶⁴.
5. Experiments with primary cultures from the purest white depot (epididymal) showed promotion of *Pgc-1a*, mitochondriogenesis and also a norepinephrine augmentable *Ucp1* expression under chronic treatment of rosiglitazone during differentiation⁵⁴ (mentioned for initial experiments).

This led to repetition of initial experiments where dexamethasone and IBMX were omitted for differentiation. As these two components are involved in brown adipogenesis but also in general effects during adipogenesis, a weaker state of differentiation was observed via microscopy, nevertheless *Ucp1* mRNA was measurable with quantitative real time RT-PCR (also see discussion of methods). Retrospectively it would have been interesting not to omit both components and to observe discrete effects of each component. Nevertheless, results revealed significant increase of *Ucp1* mRNA upon chronic *Pparγ* activation by rosiglitazone, no effect upon 40h of β-adrenergic stimulation (in any case) but strong effects upon long β-adrenergic stimulation. Obviously, β-adrenergic stimulation in white 3T3-L1 cells is rather to recruit brown in white (brite) adipocytes during days. Fast recruitment upon short stimulation is probably not detectable because of low (or probably lack of) endogenous basal population of brite adipocytes in 3T3-L1 cells²¹⁴.

5.2 Endogenous miR-26a levels in murine brown adipogenesis

To observe a correlation of brown adipogenesis and miR-26a, endogenous miR-26a levels were observed during brown adipogenesis of iBACs. As expected from another study¹⁹⁶ on brite (brown in white) adipocytes performed by Michael Karbiener from the "RNA Biology Group", an increase in miR-26a levels during adipogenesis should occur. Endogenous levels of brown adipocytes (**iBACs**)

fulfilled expectations in three biological replicates and even reached higher fold changes during adipogenesis in brown (iBACs) compared to brite (hMADS) adipocytes. β -adrenergic stimulation, the typical activation and recruitment signal for brown adipocytes, also significantly increased endogenous miR-26a levels, as expected from experiments in vitro (hMADS) and in vivo upon CL treatment and cold exposure of mice¹⁹⁶. Obviously miR-26a is involved in brown adipogenesis of brite and brown adipocytes and β -adrenergic stimulation, conserved in human and mouse.

Finally, two interesting effects concerning latency were made:

1. Levels of miR-26a seem to increase already after 2 h (standard was 4 h) of β -adrenergic stimulation.
2. At least 26 h after β -adrenergic stimulation, levels of miR-26a had returned to basal.

To investigate endogenous miR-26a levels in white adipocytes, one biological replicate of **3T3-L1** cells was exposed upon long term (8 days) or short term (40h) β -adrenergic stimulation. For the assessment of brown adipogenesis, *Ucp1* was analyzed. Short term stimulation showed an increase of endogenous miR-26a levels while long term stimulation did not. This result is contradictory in comparison of *Ucp1* controls which showed large variance, probably a consequence of unintended β -adrenergic stimulation of control cells (long term β -adrenergic stimulation). Two points strengthen this suspect:

1. Controls of both experiments were performed in one 12-well and should reproduce similar levels of *Ucp1* and miR-26a. Controls showed 3-fold changes in *Ucp1* mRNA and 3.5-fold changes in miR-26 levels in two technical replicates.
2. *Ucp1* mRNA level of control sample (long term stimulation) is nearly equal to short term stimulation sample, indicating an unintended short stimulation in controls of long term stimulation.

Assuming equal levels in both controls, further interpretations of effect could be done by statistical analysis or crossing out one control. Best would be to perform further biological replicates to be able to compare experiments and probably calculate significance.

5.3 Exogenous modulation of miR-26a levels in murine adipogenesis

For exogenous miR-26a modulation, overexpression was performed in iBACs, 3T3-L1 and -F442A. Inhibition of miR-26a was performed only in iBACs because experiments in white adipocytes were expected to show no effect. To quantify effect of modulation, *Ucp1* mRNA was measured.

Overexpression of miR-26a showed no effect in white 3T3-L1 and -F442A adipocytes (probably because of weak transfection, see discussion of methods), while an effect of miR-26a on *Ucp1* levels was shown in brown iBAC adipocytes. Obviously, miR-26a is not only able to elevate *Ucp1* mRNA levels in white human adipocytes¹⁹⁶, but also to enforce its high levels in brown murine adipocytes. An effect on *Pgc-1a* could not be shown.

Inhibition of miR-26a in iBACs showed neither significance on *Ucp1* nor on *Pgc-1a* levels. At least there are three of four biological replicates showing significance (*Ucp1* mRNA), while one replicate showed completely opposite effects, as if NTC and target sample were switched.

5.4 Global miRNA signatures in murine adipose tissue

So far it was shown that the miR-193b-365 cluster²¹⁵ is important for lineage determination of brown adipocytes. 37 miRNAs were found to be differentially expressed by global miRNA profiling, and miR-193 was one of them showing upregulation in both setups (WAT-BAT and WAT-WATce). Although miR-26a is known for promoting brown adipogenesis¹⁹⁶, micro array showed a very weak down regulation in BAT (0.85 fold) and cold exposed WAT (0.96 fold) compared to WAT. Finally, 6 of 13 (up-regulated) and 14 of 23 (down-regulated) candidates were available in databases of DIANA miRPath¹⁸⁸ resulting in putative miR-26a targeted pathways, some also known to be related to brown adipogenesis (oxidative phosphorylation, Wnt-signaling, insulin signaling pathway) or β -adrenergic stimulation (axon guidance, MAPK signaling pathway, oxidative phosphorylation, insulin signaling pathway)³⁸.

6 Literature

1. WHO. WHO | Obesity and overweight (Fact sheet N°311). *WHO Fact sheets*. 2011. Available at: <http://www.who.int/mediacentre/factsheets/fs311/en/index.html>.
2. Wang J, Hu D, Sun Y, u. a. Obesity criteria for identifying metabolic risks. *Asia Pac J Clin Nutr*. 2009;18(1):105–113.
3. Hsieh SD, Muto T. Metabolic syndrome in Japanese men and women with special reference to the anthropometric criteria for the assessment of obesity: Proposal to use the waist-to-height ratio. *Prev Med*. 2006;42(2):135–139.
4. Vazquez G, Duval S, Jacobs DR Jr, Silventoinen K. Comparison of body mass index, waist circumference, and waist/hip ratio in predicting incident diabetes: a meta-analysis. *Epidemiol Rev*. 2007;29:115–128.
5. Welborn TA, Dhaliwal SS. Preferred clinical measures of central obesity for predicting mortality. *Eur J Clin Nutr*. 2007;61(12):1373–1379.
6. Chan RSM, Woo J. Prevention of overweight and obesity: how effective is the current public health approach. *Int J Environ Res Public Health*. 2010;7(3):765–783.
7. Kissebah AH, Krakower GR. Regional adiposity and morbidity. *Physiol. Rev*. 1994;74(4):761–811.
8. Gesta S, Tseng Y-H, Kahn CR. Developmental origin of fat: tracking obesity to its source. *Cell*. 2007;131(2):242–256.
9. Kissebah AH, Krakower GR. Regional adiposity and morbidity. *Physiol. Rev*. 1994;74(4):761–811.
10. World Health Organization: Geneva, Switzerland, 2003. *Diet, Nutrition and the Prevention of Chronic Diseases*. Available at: http://whqlibdoc.who.int/trs/who_trs_916.pdf.
11. Hossain P, Kavar B, El Nahas M. Obesity and diabetes in the developing world--a growing challenge. *N. Engl. J. Med*. 2007;356(3):213–215.
12. O A. WHO :: Global Database on Body Mass Index. Available at: <http://apps.who.int/bmi/index.jsp>. Zugegriffen März 23, 2012.
13. Guh DP, Zhang W, Bansback N, u. a. The incidence of co-morbidities related to obesity and overweight: a systematic review and meta-analysis. *BMC Public Health*. 2009;9:88.
14. Murugan AT, Sharma G. Obesity and respiratory diseases. *Chron Respir Dis*. 2008;5(4):233–242.
15. Schelbert KB. Comorbidities of obesity. *Prim. Care*. 2009;36(2):271–285.

16. Ting SMS, Nair H, Ching I, Taheri S, Dasgupta I. Overweight, obesity and chronic kidney disease. *Nephron Clin Pract.* 2009;112(3):c121–127; discussion c127.
17. American Institute for Cancer Research. *Food, Nutrition, Physical Activity, and the Prevention of Cancer: a Global Perspective.* Washington, DC, USA: World Cancer Research Fund and American Institute for Cancer Research; 2007. Available at: <http://eprints.ucl.ac.uk/4841/1/4841.pdf>.
18. Gesta S, Tseng Y-H, Kahn CR. Developmental origin of fat: tracking obesity to its source. *Cell.* 2007;131(2):242–256.
19. Neary MT, Batterham RL. Gut hormones: implications for the treatment of obesity. *Pharmacol. Ther.* 2009;124(1):44–56.
20. Heneghan HM, Miller N, Kerin MJ. Role of microRNAs in obesity and the metabolic syndrome. *Obes Rev.* 2010;11(5):354–361.
21. Rosen ED, MacDougald OA. Adipocyte differentiation from the inside out. *Nat. Rev. Mol. Cell Biol.* 2006;7(12):885–896.
22. Cinti S. Between brown and white: Novel aspects of adipocyte differentiation. *Ann Med.* 2011. Available at: <http://www.ncbi.nlm.nih.gov/pubmed/21254898>. Zugegriffen Januar 27, 2011.
23. Sethi JK, Vidal-Puig AJ. Thematic review series: adipocyte biology. Adipose tissue function and plasticity orchestrate nutritional adaptation. *J. Lipid Res.* 2007;48(6):1253–1262.
24. Hansen JB, Kristiansen K. Regulatory circuits controlling white versus brown adipocyte differentiation. *Biochem. J.* 2006;398(2):153–168.
25. Boulant JA. Role of the preoptic-anterior hypothalamus in thermoregulation and fever. *Clin. Infect. Dis.* 2000;31 Suppl 5:S157–161.
26. Imai-Matsumura K, Matsumura K, Nakayama T. Involvement of ventromedial hypothalamus in brown adipose tissue thermogenesis induced by preoptic cooling in rats. *Jpn. J. Physiol.* 1984;34(5):939–943.
27. Imai-Matsumura K, Nakayama T. The central efferent mechanism of brown adipose tissue thermogenesis induced by preoptic cooling. *Can. J. Physiol. Pharmacol.* 1987;65(6):1299–1303.
28. Bieber LL, Pettersson B, Lindberg O. Studies on norepinephrine-induced efflux of free fatty acid from hamster brown-adipose-tissue cells. *Eur. J. Biochem.* 1975;58(2):375–381.
29. Fain JN, Jacobs MD, Clement-Cormier YC. Interrelationship of cyclic AMP, lipolysis, and respiration in brown fat cells. *Am. J. Physiol.* 1973;224(2):346–351.

30. Kuusela P, Nedergaard J, Cannon B. Beta-adrenergic stimulation of fatty acid release from brown fat cells differentiated in monolayer culture. *Life Sci.* 1986;38(7):589–599.
31. Nedergaard J, Lindberg O. Norepinephrine-stimulated fatty-acid release and oxygen consumption in isolated hamster brown-fat cells. Influence of buffers, albumin, insulin and mitochondrial inhibitors. *Eur. J. Biochem.* 1979;95(1):139–145.
32. Fain JN, Reed N, Saperstein R. The isolation and metabolism of brown fat cells. *J. Biol. Chem.* 1967;242(8):1887–1894.
33. Nedergaard J, Cannon B, Lindberg O. Microcalorimetry of isolated mammalian cells. *Nature.* 1977;267(5611):518–520.
34. Prusiner SB, Cannon B, Lindberg O. Oxidative metabolism in cells isolated from brown adipose tissue. 1. Catecholamine and fatty acid stimulation of respiration. *Eur. J. Biochem.* 1968;6(1):15–22.
35. Klaus S, Casteilla L, Bouillaud F, Ricquier D. The uncoupling protein UCP: a membraneous mitochondrial ion carrier exclusively expressed in brown adipose tissue. *Int. J. Biochem.* 1991;23(9):791–801.
36. Klingenberg M, Echtay KS. Uncoupling proteins: the issues from a biochemist point of view. *Biochim. Biophys. Acta.* 2001;1504(1):128–143.
37. Nedergaard J, Golozoubova V, Matthias A, u. a. UCP1: the only protein able to mediate adaptive non-shivering thermogenesis and metabolic inefficiency. *Biochim. Biophys. Acta.* 2001;1504(1):82–106.
38. Cannon B, Nedergaard J. Brown adipose tissue: function and physiological significance. *Physiol. Rev.* 2004;84(1):277–359.
39. Nedergaard J, Cannon B. The changed metabolic world with human brown adipose tissue: therapeutic visions. *Cell Metab.* 2010;11(4):268–272.
40. Cannon B, Nedergaard J. Brown adipose tissue: function and physiological significance. *Physiol. Rev.* 2004;84(1):277–359.
41. Cinti S. The Adipose Organ. In: Fantuzzi G, Mazzone T, hrsg. *Adipose Tissue and Adipokines in Health and Disease.* Totowa, NJ: Humana Press; 1999:3–19. Available at: http://www.springerlink.com/index/10.1007/978-1-59745-370-7_1. Zugegriffen Februar 27, 2012.
42. Cinti S. The adipose organ. *Prostaglandins Leukot. Essent. Fatty Acids.* 2005;73(1):9–15.
43. Frontini A, Cinti S. Distribution and development of brown adipocytes in the murine and human adipose organ. *Cell Metab.* 2010;11(4):253–256.

44. Greenberg AS, Egan JJ, Wek SA, u. a. Perilipin, a major hormonally regulated adipocyte-specific phosphoprotein associated with the periphery of lipid storage droplets. *J. Biol. Chem.* 1991;266(17):11341–11346.
45. Cinti S, Cigolini M, Bosello O, Björntorp P. A morphological study of the adipocyte precursor. *J. Submicrosc. Cytol.* 1984;16(2):243–251.
46. Cinti S, Cigolini M, Gazzanelli G, Bosello O. An ultrastructural study of adipocyte precursors from epididymal fat pads of adult rats in culture. *J. Submicrosc. Cytol.* 1985;17(4):631–636.
47. Tang W, Zeve D, Suh JM, u. a. White fat progenitor cells reside in the adipose vasculature. *Science.* 2008;322(5901):583–586.
48. Cinti S, Zancanaro C, Sbarbati A, u. a. Immunoelectron microscopical identification of the uncoupling protein in brown adipose tissue mitochondria. *Biol. Cell.* 1989;67(3):359–362.
49. Rial E, González-Barroso MM. Physiological regulation of the transport activity in the uncoupling proteins UCP1 and UCP2. *Biochim. Biophys. Acta.* 2001;1504(1):70–81.
50. Collins S, Surwit RS. The beta-adrenergic receptors and the control of adipose tissue metabolism and thermogenesis. *Recent Prog. Horm. Res.* 2001;56:309–328.
51. Cinti S, Canello R, Zingaretti MC, u. a. CL316,243 and cold stress induce heterogeneous expression of UCP1 mRNA and protein in rodent brown adipocytes. *J. Histochem. Cytochem.* 2002;50(1):21–31.
52. Casteilla L, Muzzin P, Revelli JP, Ricquier D, Giacobino JP. Expression of beta 1- and beta 3-adrenergic-receptor messages and adenylate cyclase beta-adrenergic response in bovine perirenal adipose tissue during its transformation from brown into white fat. *Biochem. J.* 1994;297 (Pt 1):93–97.
53. Cinti S, Morrioni M. Brown adipocyte precursor cells: a morphological study. *Ital J Anat Embryol.* 1995;100 Suppl 1:75–81.
54. Petrovic N, Walden TB, Shabalina IG, u. a. Chronic peroxisome proliferator-activated receptor gamma (PPARgamma) activation of epididymally derived white adipocyte cultures reveals a population of thermogenically competent, UCP1-containing adipocytes molecularly distinct from classic brown adipocytes. *J. Biol. Chem.* 2010;285(10):7153–7164.
55. Atit R, Sgaier SK, Mohamed OA, u. a. Beta-catenin activation is necessary and sufficient to specify the dorsal dermal fate in the mouse. *Dev. Biol.* 2006;296(1):164–176.
56. Timmons JA, Wennmalm K, Larsson O, u. a. Myogenic gene expression signature establishes that brown and white adipocytes originate from distinct cell lineages. *Proc. Natl. Acad. Sci. U.S.A.* 2007;104(11):4401–4406.

57. Seale P, Bjork B, Yang W, et al. PRDM16 controls a brown fat/skeletal muscle switch. *Nature*. 2008;454(7207):961–967.
58. Barbatelli G, Murano I, Madsen L, et al. The emergence of cold-induced brown adipocytes in mouse white fat depots is determined predominantly by white to brown adipocyte transdifferentiation. *Am. J. Physiol. Endocrinol. Metab.* 2010;298(6):E1244–1253.
59. Tosh D, Slack JMW. How cells change their phenotype. *Nat. Rev. Mol. Cell Biol.* 2002;3(3):187–194.
60. Granneman JG, Li P, Zhu Z, Lu Y. Metabolic and cellular plasticity in white adipose tissue I: effects of beta3-adrenergic receptor activation. *Am. J. Physiol. Endocrinol. Metab.* 2005;289(4):E608–616.
61. Himms-Hagen J, Melnyk A, Zingaretti MC, et al. Multilocular fat cells in WAT of CL-316243-treated rats derive directly from white adipocytes. *Am. J. Physiol., Cell Physiol.* 2000;279(3):C670–681.
62. Barbatelli G, Morroni M, Vinesi P, Cinti S, Michetti F. S-100 protein in rat brown adipose tissue under different functional conditions: a morphological, immunocytochemical, and immunochemical study. *Exp. Cell Res.* 1993;208(1):226–231.
63. Cinti S, Frederich RC, Zingaretti MC, et al. Immunohistochemical localization of leptin and uncoupling protein in white and brown adipose tissue. *Endocrinology*. 1997;138(2):797–804.
64. Cancellato R, Zingaretti MC, Sarzani R, Ricquier D, Cinti S. Leptin and UCP1 genes are reciprocally regulated in brown adipose tissue. *Endocrinology*. 1998;139(11):4747–4750.
65. Bachman ES, Dhillon H, Zhang C-Y, et al. betaAR signaling required for diet-induced thermogenesis and obesity resistance. *Science*. 2002;297(5582):843–845.
66. Walden TB, Hansen IR, Timmons JA, Cannon B, Nedergaard J. Recruited versus nonrecruited molecular signatures of brown, „brite“ and white adipose tissues. *Am J Physiol Endocrinol Metab.* 2011. Available at: <http://www.ncbi.nlm.nih.gov/pubmed/21828341>. Zugegriffen August 22, 2011.
67. Seale P, Bjork B, Yang W, et al. PRDM16 controls a brown fat/skeletal muscle switch. *Nature*. 2008;454(7207):961–967.
68. Walden TB, Timmons JA, Keller P, Nedergaard J, Cannon B. Distinct expression of muscle-specific microRNAs (myomirs) in brown adipocytes. *J. Cell. Physiol.* 2009;218(2):444–449.
69. Seale P, Kajimura S, Spiegelman BM. Transcriptional control of brown adipocyte development and physiological function--of mice and men. *Genes Dev.* 2009;23(7):788–797.

70. Farmer SR. Molecular determinants of brown adipocyte formation and function. *Genes Dev.* 2008;22(10):1269–1275.
71. Cousin B, Cinti S, Morrioni M, u. a. Occurrence of brown adipocytes in rat white adipose tissue: molecular and morphological characterization. *J. Cell. Sci.* 1992;103 (Pt 4):931–942.
72. Guerra C, Koza RA, Yamashita H, Walsh K, Kozak LP. Emergence of brown adipocytes in white fat in mice is under genetic control. Effects on body weight and adiposity. *J. Clin. Invest.* 1998;102(2):412–420.
73. Xue Y, Petrovic N, Cao R, u. a. Hypoxia-independent angiogenesis in adipose tissues during cold acclimation. *Cell Metab.* 2009;9(1):99–109.
74. Laplante M, Sell H, MacNaul KL, u. a. PPAR-gamma activation mediates adipose depot-specific effects on gene expression and lipoprotein lipase activity: mechanisms for modulation of postprandial lipemia and differential adipose accretion. *Diabetes.* 2003;52(2):291–299.
75. Fukui Y, Masui S, Osada S, Umesono K, Motojima K. A new thiazolidinedione, NC-2100, which is a weak PPAR-gamma activator, exhibits potent antidiabetic effects and induces uncoupling protein 1 in white adipose tissue of KKAY obese mice. *Diabetes.* 2000;49(5):759–767.
76. Carmona MC, Louche K, Lefebvre B, u. a. S 26948: a new specific peroxisome proliferator activated receptor gamma modulator with potent antidiabetes and antiatherogenic effects. *Diabetes.* 2007;56(11):2797–2808.
77. Sell H, Berger JP, Samson P, u. a. Peroxisome proliferator-activated receptor gamma agonism increases the capacity for sympathetically mediated thermogenesis in lean and ob/ob mice. *Endocrinology.* 2004;145(8):3925–3934.
78. Rong JX, Qiu Y, Hansen MK, u. a. Adipose mitochondrial biogenesis is suppressed in db/db and high-fat diet-fed mice and improved by rosiglitazone. *Diabetes.* 2007;56(7):1751–1760.
79. Wilson-Fritch L, Nicoloso S, Chouinard M, u. a. Mitochondrial remodeling in adipose tissue associated with obesity and treatment with rosiglitazone. *J. Clin. Invest.* 2004;114(9):1281–1289.
80. Loncar D, Afzelius BA, Cannon B. Epididymal white adipose tissue after cold stress in rats. I. Nonmitochondrial changes. *J. Ultrastruct. Mol. Struct. Res.* 1988;101(2-3):109–122.
81. Rodeheffer MS, Birsoy K, Friedman JM. Identification of white adipocyte progenitor cells in vivo. *Cell.* 2008;135(2):240–249.
82. Gregoire FM, Smas CM, Sul HS. Understanding adipocyte differentiation. *Physiol. Rev.* 1998;78(3):783–809.
83. Rosen ED. The transcriptional basis of adipocyte development. *Prostaglandins Leukot. Essent. Fatty Acids.* 2005;73(1):31–34.

84. McGregor RA, Choi MS. microRNAs in the regulation of adipogenesis and obesity. *Curr. Mol. Med.* 2011;11(4):304–316.
85. Lafontan M. Historical perspectives in fat cell biology: the fat cell as a model for the investigation of hormonal and metabolic pathways. *Am. J. Physiol., Cell Physiol.* 2012;302(2):C327–359.
86. Pairault J, Green H. A study of the adipose conversion of suspended 3T3 cells by using glycerophosphate dehydrogenase as differentiation marker. *Proc. Natl. Acad. Sci. U.S.A.* 1979;76(10):5138–5142.
87. Otto TC, Lane MD. Adipose development: from stem cell to adipocyte. *Crit. Rev. Biochem. Mol. Biol.* 2005;40(4):229–242.
88. Ailhaud G. Early adipocyte differentiation. *Biochem. Soc. Trans.* 1996;24(2):400–402.
89. Cornelius P, MacDougald OA, Lane MD. Regulation of adipocyte development. *Annu. Rev. Nutr.* 1994;14:99–129.
90. Grégoire FM, Johnson PR, Greenwood MR. Comparison of the adipoconversion of preadipocytes derived from lean and obese Zucker rats in serum-free cultures. *Int. J. Obes. Relat. Metab. Disord.* 1995;19(9):664–670.
91. MacDougald OA, Lane MD. Transcriptional regulation of gene expression during adipocyte differentiation. *Annu. Rev. Biochem.* 1995;64:345–373.
92. Cryer A. Tissue lipoprotein lipase activity and its action in lipoprotein metabolism. *Int. J. Biochem.* 1981;13(5):525–541.
93. Goldberg IJ. Lipoprotein lipase and lipolysis: central roles in lipoprotein metabolism and atherogenesis. *J. Lipid Res.* 1996;37(4):693–707.
94. Amri EZ, Dani C, Doglio A, et al. Adipose cell differentiation: evidence for a two-step process in the polyamine-dependent Ob1754 clonal line. *Biochem. J.* 1986;238(1):115–122.
95. Amri EZ, Dani C, Doglio A, Grimaldi P, Ailhaud G. Coupling of growth arrest and expression of early markers during adipose conversion of preadipocyte cell lines. *Biochem. Biophys. Res. Commun.* 1986;137(2):903–910.
96. Aratani Y, Kitagawa Y. Enhanced synthesis and secretion of type IV collagen and entactin during adipose conversion of 3T3-L1 cells and production of unorthodox laminin complex. *J. Biol. Chem.* 1988;263(31):16163–16169.
97. Weiner FR, Shah A, Smith PJ, Rubin CS, Zern MA. Regulation of collagen gene expression in 3T3-L1 cells. Effects of adipocyte differentiation and tumor necrosis factor alpha. *Biochemistry.* 1989;28(9):4094–4099.
98. Brown MS, Goldstein JL. The SREBP pathway: regulation of cholesterol metabolism by proteolysis of a membrane-bound transcription factor. *Cell.* 1997;89(3):331–340.

99. Paulauskis JD, Sul HS. Cloning and expression of mouse fatty acid synthase and other specific mRNAs. Developmental and hormonal regulation in 3T3-L1 cells. *J. Biol. Chem.* 1988;263(15):7049–7054.
100. Spiegelman BM, Frank M, Green H. Molecular cloning of mRNA from 3T3 adipocytes. Regulation of mRNA content for glycerophosphate dehydrogenase and other differentiation-dependent proteins during adipocyte development. *J. Biol. Chem.* 1983;258(16):10083–10089.
101. Weiner FR, Smith PJ, Wertheimer S, Rubin CS. Regulation of gene expression by insulin and tumor necrosis factor alpha in 3T3-L1 cells. Modulation of the transcription of genes encoding acyl-CoA synthetase and stearyl-CoA desaturase-1. *J. Biol. Chem.* 1991;266(35):23525–23528.
102. Garcia de Herreros A, Birnbaum MJ. The acquisition of increased insulin-responsive hexose transport in 3T3-L1 adipocytes correlates with expression of a novel transporter gene. *J. Biol. Chem.* 1989;264(33):19994–19999.
103. Fève B, Emorine LJ, Briend-Sutren MM, u. a. Differential regulation of beta 1- and beta 2-adrenergic receptor protein and mRNA levels by glucocorticoids during 3T3-F442A adipose differentiation. *J. Biol. Chem.* 1990;265(27):16343–16349.
104. Fève B, Emorine LJ, Lasnier F, u. a. Atypical beta-adrenergic receptor in 3T3-F442A adipocytes. Pharmacological and molecular relationship with the human beta 3-adrenergic receptor. *J. Biol. Chem.* 1991;266(30):20329–20336.
105. Guest SJ, Hadcock JR, Watkins DC, Malbon CC. Beta 1- and beta 2-adrenergic receptor expression in differentiating 3T3-L1 cells. Independent regulation at the level of mRNA. *J. Biol. Chem.* 1990;265(10):5370–5375.
106. Lai E, Rosen OM, Rubin CS. Dexamethasone regulates the beta-adrenergic receptor subtype expressed by 3T3 L1 preadipocytes and adipocytes. *J. Biol. Chem.* 1982;257(12):6691–6696.
107. Wang H, Scott RE. Inhibition of distinct steps in the adipocyte differentiation pathway in 3T3 T mesenchymal stem cells by dimethyl sulphoxide (DMSO). *Cell Prolif.* 1993;26(1):55–66.
108. Wier ML, Scott RE. Regulation of the terminal event in cellular differentiation: biological mechanisms of the loss of proliferative potential. *J. Cell Biol.* 1986;102(5):1955–1964.
109. Prins JB, O’Rahilly S. Regulation of adipose cell number in man. *Clin. Sci.* 1997;92(1):3–11.
110. Klein J, Fasshauer M, Klein HH, Benito M, Kahn CR. Novel adipocyte lines from brown fat: a model system for the study of differentiation, energy metabolism, and insulin action. *Bioessays.* 2002;24(4):382–388.
111. Kahn BB, Flier JS. Obesity and insulin resistance. *J. Clin. Invest.* 2000;106(4):473–481.

112. Michael M, Winnay J, Peroni O, et al. *Mice with a fat-specific insulin receptor knockout are normoglycemic and are protected from obesity*. San Diego, USA: Endocrine Society; 1999.
113. Green H, Meuth M. An established pre-adipose cell line and its differentiation in culture. *Cell*. 1974;3(2):127–133.
114. Green H, Kehinde O. Spontaneous heritable changes leading to increased adipose conversion in 3T3 cells. *Cell*. 1976;7(1):105–113.
115. Tang Q-Q, Otto TC, Lane MD. Mitotic clonal expansion: a synchronous process required for adipogenesis. *Proc. Natl. Acad. Sci. U.S.A.* 2003;100(1):44–49.
116. Mandrup S, Lane MD. Regulating adipogenesis. *J. Biol. Chem.* 1997;272(9):5367–5370.
117. Rosen ED, Walkey CJ, Puigserver P, Spiegelman BM. Transcriptional regulation of adipogenesis. *Genes Dev.* 2000;14(11):1293–1307.
118. Wilson-Fritch L, Burkart A, Bell G, et al. Mitochondrial biogenesis and remodeling during adipogenesis and in response to the insulin sensitizer rosiglitazone. *Mol. Cell. Biol.* 2003;23(3):1085–1094.
119. Klein J, Fasshauer M, Ito M, et al. beta(3)-adrenergic stimulation differentially inhibits insulin signaling and decreases insulin-induced glucose uptake in brown adipocytes. *J. Biol. Chem.* 1999;274(49):34795–34802.
120. Klein J, Fasshauer M, Benito M, Kahn CR. Insulin and the beta3-adrenoceptor differentially regulate uncoupling protein-1 expression. *Mol. Endocrinol.* 2000;14(6):764–773.
121. Fasshauer M, Klein J, Ueki K, et al. Essential role of insulin receptor substrate-2 in insulin stimulation of Glut4 translocation and glucose uptake in brown adipocytes. *J. Biol. Chem.* 2000;275(33):25494–25501.
122. Fasshauer M, Klein J, Kriauciunas KM, et al. Essential role of insulin receptor substrate 1 in differentiation of brown adipocytes. *Mol. Cell. Biol.* 2001;21(1):319–329.
123. Klein J, Fasshauer M, Ueki K, et al. *Disruption of the p85a gene differentially alters metabolic responses to insulin in a brown adipocyte model*. Toronto, Canada: Endocrine Society; 2000.
124. Rosen ED, Hsu C-H, Wang X, et al. C/EBPalpha induces adipogenesis through PPARgamma: a unified pathway. *Genes Dev.* 2002;16(1):22–26.
125. Rangwala SM, Lazar MA. Transcriptional control of adipogenesis. *Annu. Rev. Nutr.* 2000;20:535–559.
126. Rosen ED, Sarraf P, Troy AE, et al. PPAR gamma is required for the differentiation of adipose tissue in vivo and in vitro. *Mol. Cell.* 1999;4(4):611–617.

127. Barak Y, Nelson MC, Ong ES, et al. PPAR gamma is required for placental, cardiac, and adipose tissue development. *Mol. Cell.* 1999;4(4):585–595.
128. Jones JR, Barrick C, Kim K-A, et al. Deletion of PPARgamma in adipose tissues of mice protects against high fat diet-induced obesity and insulin resistance. *Proc. Natl. Acad. Sci. U.S.A.* 2005;102(17):6207–6212.
129. Imai T, Takakuwa R, Marchand S, et al. Peroxisome proliferator-activated receptor gamma is required in mature white and brown adipocytes for their survival in the mouse. *Proc. Natl. Acad. Sci. U.S.A.* 2004;101(13):4543–4547.
130. Lehmann JM, Moore LB, Smith-Oliver TA, et al. An antidiabetic thiazolidinedione is a high affinity ligand for peroxisome proliferator-activated receptor gamma (PPAR gamma). *J. Biol. Chem.* 1995;270(22):12953–12956.
131. Tai TA, Jennermann C, Brown KK, et al. Activation of the nuclear receptor peroxisome proliferator-activated receptor gamma promotes brown adipocyte differentiation. *J. Biol. Chem.* 1996;271(47):29909–29914.
132. Teruel T, Hernandez R, Benito M, Lorenzo M. Rosiglitazone and retinoic acid induce uncoupling protein-1 (UCP-1) in a p38 mitogen-activated protein kinase-dependent manner in fetal primary brown adipocytes. *J. Biol. Chem.* 2003;278(1):263–269.
133. Foellmi-Adams LA, Wyse BM, Herron D, Nedergaard J, Kletzien RF. Induction of uncoupling protein in brown adipose tissue. Synergy between norepinephrine and pioglitazone, an insulin-sensitizing agent. *Biochem. Pharmacol.* 1996;52(5):693–701.
134. Pisani DF, Djedaini M, Beranger GE, et al. Differentiation of human adipose-derived stem cells into „brite“ (brown-in-white) adipocytes. *Frontiers in Endocrinology.* 2011;2(87):1–9.
135. Elabd C, Chiellini C, Carmona M, et al. Human Multipotent Adipose-derived Stem Cells Differentiate into Functional Brown Adipocytes. *Stem Cells.* 2009. Available at: <http://www.ncbi.nlm.nih.gov/pubmed/19697348>.
136. Kelly LJ, Vicario PP, Thompson GM, et al. Peroxisome proliferator-activated receptors gamma and alpha mediate in vivo regulation of uncoupling protein (UCP-1, UCP-2, UCP-3) gene expression. *Endocrinology.* 1998;139(12):4920–4927.
137. Wilson-Fritch L, Nicoloso S, Chouinard M, et al. Mitochondrial remodeling in adipose tissue associated with obesity and treatment with rosiglitazone. *J. Clin. Invest.* 2004;114(9):1281–1289.
138. Wilson-Fritch L, Burkart A, Bell G, et al. Mitochondrial biogenesis and remodeling during adipogenesis and in response to the insulin sensitizer rosiglitazone. *Mol. Cell. Biol.* 2003;23(3):1085–1094.

139. Guan H-P, Ishizuka T, Chui PC, Lehrke M, Lazar MA. Corepressors selectively control the transcriptional activity of PPARgamma in adipocytes. *Genes Dev.* 2005;19(4):453–461.
140. Hondares E, Mora O, Yubero P, u. a. Thiazolidinediones and rexinoids induce peroxisome proliferator-activated receptor-coactivator (PGC)-1alpha gene transcription: an autoregulatory loop controls PGC-1alpha expression in adipocytes via peroxisome proliferator-activated receptor-gamma coactivation. *Endocrinology.* 2006;147(6):2829–2838.
141. Rocchi S, Picard F, Vamecq J, u. a. A unique PPARgamma ligand with potent insulin-sensitizing yet weak adipogenic activity. *Mol. Cell.* 2001;8(4):737–747.
142. Rieusset J, Touri F, Michalik L, u. a. A new selective peroxisome proliferator-activated receptor gamma antagonist with antiobesity and antidiabetic activity. *Mol. Endocrinol.* 2002;16(11):2628–2644.
143. Berger JP, Petro AE, Macnaul KL, u. a. Distinct properties and advantages of a novel peroxisome proliferator-activated protein [gamma] selective modulator. *Mol. Endocrinol.* 2003;17(4):662–676.
144. Misra P, Chakrabarti R, Vikramadithyan RK, u. a. PAT5A: a partial agonist of peroxisome proliferator-activated receptor gamma is a potent antidiabetic thiazolidinedione yet weakly adipogenic. *J. Pharmacol. Exp. Ther.* 2003;306(2):763–771.
145. Umek RM, Friedman AD, McKnight SL. CCAAT-enhancer binding protein: a component of a differentiation switch. *Science.* 1991;251(4991):288–292.
146. Christy RJ, Kaestner KH, Geiman DE, Lane MD. CCAAT/enhancer binding protein gene promoter: binding of nuclear factors during differentiation of 3T3-L1 preadipocytes. *Proc. Natl. Acad. Sci. U.S.A.* 1991;88(6):2593–2597.
147. Ross SR, Graves RA, Greenstein A, u. a. A fat-specific enhancer is the primary determinant of gene expression for adipocyte P2 in vivo. *Proc. Natl. Acad. Sci. U.S.A.* 1990;87(24):9590–9594.
148. Birkenmeier EH, Gwynn B, Howard S, u. a. Tissue-specific expression, developmental regulation, and genetic mapping of the gene encoding CCAAT/enhancer binding protein. *Genes Dev.* 1989;3(8):1146–1156.
149. Brun RP, Kim JB, Hu E, Altiok S, Spiegelman BM. Adipocyte differentiation: a transcriptional regulatory cascade. *Curr. Opin. Cell Biol.* 1996;8(6):826–832.
150. Lane MD, Lin FT, MacDougald OA, Vasseur-Cognet M. Control of adipocyte differentiation by CCAAT/enhancer binding protein alpha (C/EBP alpha). *Int. J. Obes. Relat. Metab. Disord.* 1996;20 Suppl 3:S91–96.
151. Lin FT, Lane MD. Antisense CCAAT/enhancer-binding protein RNA suppresses coordinate gene expression and triglyceride accumulation during differentiation of 3T3-L1 preadipocytes. *Genes Dev.* 1992;6(4):533–544.

152. Lin FT, Lane MD. CCAAT/enhancer binding protein alpha is sufficient to initiate the 3T3-L1 adipocyte differentiation program. *Proc. Natl. Acad. Sci. U.S.A.* 1994;91(19):8757–8761.
153. Freytag SO, Paielli DL, Gilbert JD. Ectopic expression of the CCAAT/enhancer-binding protein alpha promotes the adipogenic program in a variety of mouse fibroblastic cells. *Genes Dev.* 1994;8(14):1654–1663.
154. Linhart HG, Ishimura-Oka K, DeMayo F, u. a. C/EBPalpha is required for differentiation of white, but not brown, adipose tissue. *Proc. Natl. Acad. Sci. U.S.A.* 2001;98(22):12532–12537.
155. Hwang CS, Mandrup S, MacDougald OA, Geiman DE, Lane MD. Transcriptional activation of the mouse obese (ob) gene by CCAAT/enhancer binding protein alpha. *Proc. Natl. Acad. Sci. U.S.A.* 1996;93(2):873–877.
156. Kaestner KH, Christy RJ, Lane MD. Mouse insulin-responsive glucose transporter gene: characterization of the gene and trans-activation by the CCAAT/enhancer binding protein. *Proc. Natl. Acad. Sci. U.S.A.* 1990;87(1):251–255.
157. McKeon C, Pham T. Transactivation of the human insulin receptor gene by the CAAT/enhancer binding protein. *Biochem. Biophys. Res. Commun.* 1991;174(2):721–728.
158. Cao Z, Umek RM, McKnight SL. Regulated expression of three C/EBP isoforms during adipose conversion of 3T3-L1 cells. *Genes Dev.* 1991;5(9):1538–1552.
159. Wu Z, Bucher NL, Farmer SR. Induction of peroxisome proliferator-activated receptor gamma during the conversion of 3T3 fibroblasts into adipocytes is mediated by C/EBPbeta, C/EBPdelta, and glucocorticoids. *Mol. Cell. Biol.* 1996;16(8):4128–4136.
160. Tanaka T, Yoshida N, Kishimoto T, Akira S. Defective adipocyte differentiation in mice lacking the C/EBPbeta and/or C/EBPdelta gene. *EMBO J.* 1997;16(24):7432–7443.
161. Carmona MC, Hondares E, Rodríguez de la Concepción ML, u. a. Defective thermoregulation, impaired lipid metabolism, but preserved adrenergic induction of gene expression in brown fat of mice lacking C/EBPbeta. *Biochem. J.* 2005;389(Pt 1):47–56.
162. Rehnmark S, Antonson P, Xanthopoulos KG, Jacobsson A. Differential adrenergic regulation of C/EBP alpha and C/EBP beta in brown adipose tissue. *FEBS Lett.* 1993;318(3):235–241.
163. Manchado C, Yubero P, Viñas O, u. a. CCAAT/enhancer-binding proteins alpha and beta in brown adipose tissue: evidence for a tissue-specific pattern of expression during development. *Biochem. J.* 1994;302 (Pt 3):695–700.

164. Karamanlidis G, Karamitri A, Docherty K, Hazlerigg DG, Lomax MA. C/EBPbeta reprograms white 3T3-L1 preadipocytes to a Brown adipocyte pattern of gene expression. *J. Biol. Chem.* 2007;282(34):24660–24669.
165. Bartel DP. MicroRNAs: target recognition and regulatory functions. *Cell.* 2009;136(2):215–233.
166. Carthew RW, Sontheimer EJ. Origins and Mechanisms of miRNAs and siRNAs. *Cell.* 2009;136(4):642–655.
167. Krol J, Loedige I, Filipowicz W. The widespread regulation of microRNA biogenesis, function and decay. *Nat. Rev. Genet.* 2010;11(9):597–610.
168. Kim VN, Han J, Siomi MC. Biogenesis of small RNAs in animals. *Nat. Rev. Mol. Cell Biol.* 2009;10(2):126–139.
169. Diederichs S, Haber DA. Dual role for argonautes in microRNA processing and posttranscriptional regulation of microRNA expression. *Cell.* 2007;131(6):1097–1108.
170. Cheloufi S, Dos Santos CO, Chong MMW, Hannon GJ. A dicer-independent miRNA biogenesis pathway that requires Ago catalysis. *Nature.* 2010;465(7298):584–589.
171. Cifuentes D, Xue H, Taylor DW, u. a. A novel miRNA processing pathway independent of Dicer requires Argonaute2 catalytic activity. *Science.* 2010;328(5986):1694–1698.
172. Chiang HR, Schoenfeld LW, Ruby JG, u. a. Mammalian microRNAs: experimental evaluation of novel and previously annotated genes. *Genes Dev.* 2010;24(10):992–1009.
173. Ghildiyal M, Xu J, Seitz H, Weng Z, Zamore PD. Sorting of Drosophila small silencing RNAs partitions microRNA* strands into the RNA interference pathway. *RNA.* 2010;16(1):43–56.
174. Czech B, Zhou R, Erlich Y, u. a. Hierarchical rules for Argonaute loading in Drosophila. *Mol. Cell.* 2009;36(3):445–456.
175. Okamura K, Liu N, Lai EC. Distinct mechanisms for microRNA strand selection by Drosophila Argonautes. *Mol. Cell.* 2009;36(3):431–444.
176. Lai EC. microRNAs: runts of the genome assert themselves. *Curr. Biol.* 2003;13(23):R925–936.
177. Bartel DP. MicroRNAs: genomics, biogenesis, mechanism, and function. *Cell.* 2004;116(2):281–297.
178. O A. miRBase. Available at: <http://www.mirbase.org/>. Zugegriffen März 5, 2012.

179. Rhoades MW, Reinhart BJ, Lim LP, et al. Prediction of plant microRNA targets. *Cell*. 2002;110(4):513–520.
180. Lai EC. Predicting and validating microRNA targets. *Genome Biol*. 2004;5(9):115.
181. Jones-Rhoades MW, Bartel DP. Computational identification of plant microRNAs and their targets, including a stress-induced miRNA. *Mol. Cell*. 2004;14(6):787–799.
182. Bonnet E, Wuyts J, Rouzé P, Van de Peer Y. Detection of 91 potential conserved plant microRNAs in *Arabidopsis thaliana* and *Oryza sativa* identifies important target genes. *Proc. Natl. Acad. Sci. U.S.A.* 2004;101(31):11511–11516.
183. Lai EC. Micro RNAs are complementary to 3' UTR sequence motifs that mediate negative post-transcriptional regulation. *Nat. Genet.* 2002;30(4):363–364.
184. Bushati N, Cohen SM. microRNA functions. *Annu. Rev. Cell Dev. Biol.* 2007;23:175–205.
185. Eulalio A, Huntzinger E, Izaurralde E. Getting to the root of miRNA-mediated gene silencing. *Cell*. 2008;132(1):9–14.
186. Stark A, Brennecke J, Russell RB, Cohen SM. Identification of *Drosophila* MicroRNA targets. *PLoS Biol*. 2003;1(3):E60.
187. Ivanovska I, Cleary MA. Combinatorial microRNAs: working together to make a difference. *Cell Cycle*. 2008;7(20):3137–3142.
188. Papadopoulos GL, Alexiou P, Maragkakis M, Reczko M, Hatzigeorgiou AG. DIANA-mirPath: Integrating human and mouse microRNAs in pathways. *Bioinformatics*. 2009;25(15):1991–1993.
189. Xie H, Lim B, Lodish HF. MicroRNAs induced during adipogenesis that accelerate fat cell development are downregulated in obesity. *Diabetes*. 2009;58(5):1050–1057.
190. Gerin I, Bommer GT, McCoin CS, et al. Roles for miRNA-378/378* in adipocyte gene expression and lipogenesis. *Am. J. Physiol. Endocrinol. Metab.* 2010;299(2):E198–206.
191. Wang Q, Li YC, Wang J, et al. miR-17-92 cluster accelerates adipocyte differentiation by negatively regulating tumor-suppressor Rb2/p130. *Proc. Natl. Acad. Sci. U.S.A.* 2008;105(8):2889–2894.
192. Sun T, Fu M, Bookout AL, Kliewer SA, Mangelsdorf DJ. MicroRNA let-7 regulates 3T3-L1 adipogenesis. *Mol. Endocrinol.* 2009;23(6):925–931.
193. Qin L, Chen Y, Niu Y, et al. A deep investigation into the adipogenesis mechanism: profile of microRNAs regulating adipogenesis by modulating the canonical Wnt/beta-catenin signaling pathway. *BMC Genomics*. 2010;11:320.

194. Karbiener M, Fischer C, Nowitsch S, u. a. microRNA miR-27b impairs human adipocyte differentiation and targets PPARgamma. *Biochem. Biophys. Res. Commun.* 2009;390(2):247–251.
195. Karbiener M, Neuhold C, Opriessnig P, u. a. MicroRNA-30c promotes human adipocyte differentiation and co-represses PAI-1 and ALK2. *RNA Biol.* 2011;8(5). Available at: <http://www.ncbi.nlm.nih.gov/pubmed/21878751>. Zugegriffen Januar 31, 2012.
196. Karbiener M. Influence of Distinct MicroRNAs on White and Brown Adipogenesis in Human. 2011.
197. Xie H, Sun L, Lodish HF. Targeting microRNAs in obesity. *Expert Opin. Ther. Targets.* 2009;13(10):1227–1238.
198. Sun F, Wang J, Pan Q, u. a. Characterization of function and regulation of miR-24-1 and miR-31. *Biochem. Biophys. Res. Commun.* 2009;380(3):660–665.
199. Lin Q, Gao Z, Alarcon RM, Ye J, Yun Z. A role of miR-27 in the regulation of adipogenesis. *FEBS J.* 2009;276(8):2348–2358.
200. Karbiener M, Fischer C, Nowitsch S, u. a. microRNA miR-27b impairs human adipocyte differentiation and targets PPARgamma. *Biochem. Biophys. Res. Commun.* 2009;390(2):247–251.
201. Oskowitz AZ, Lu J, Penforis P, u. a. Human multipotent stromal cells from bone marrow and microRNA: regulation of differentiation and leukemia inhibitory factor expression. *Proc. Natl. Acad. Sci. U.S.A.* 2008;105(47):18372–18377.
202. Kim YJ, Hwang SJ, Bae YC, Jung JS. miR-21 Regulates Adipogenic Differentiation Through the Modulation of TGF-beta Signaling in Mesenchymal Stem Cells Derived from Human Adipose Tissue. *Stem Cells.* 2009. Available at: <http://www.ncbi.nlm.nih.gov/pubmed/19816956>.
203. Yang Z, Bian C, Zhou H, u. a. MicroRNA hsa-miR-138 inhibits adipogenic differentiation of human adipose tissue-derived mesenchymal stem cells through adenovirus EID-1. *Stem Cells Dev.* 2011;20(2):259–267.
204. Tang Y-F, Zhang Y, Li X-Y, u. a. Expression of miR-31, miR-125b-5p, and miR-326 in the adipogenic differentiation process of adipose-derived stem cells. *OMICS.* 2009;13(4):331–336.
205. Nedergaard J, Cannon B. The changed metabolic world with human brown adipose tissue: therapeutic visions. *Cell Metab.* 2010;11(4):268–272.
206. Chen J-F, Mandel EM, Thomson JM, u. a. The role of microRNA-1 and microRNA-133 in skeletal muscle proliferation and differentiation. *Nat. Genet.* 2006;38(2):228–233.
207. Sun L, Xie H, Mori MA, u. a. Mir193b-365 is essential for brown fat differentiation. *Nat. Cell Biol.* 2011;13(8):958–965.

208. Walden TB, Hansen IR, Timmons JA, Cannon B, Nedergaard J. Recruited versus nonrecruited molecular signatures of brown, „brite“ and white adipose tissues. *Am J Physiol Endocrinol Metab.* 2011. Available at: <http://www.ncbi.nlm.nih.gov/pubmed/21828341>. Zugegriffen August 22, 2011.
209. Golozoubova V, Cannon B, Nedergaard J. UCP1 is essential for adaptive adrenergic nonshivering thermogenesis. *Am. J. Physiol. Endocrinol. Metab.* 2006;291(2):E350–357.
210. Collins S, Yehuda-Shnaidman E, Wang H. Positive and negative control of Ucp1 gene transcription and the role of β -adrenergic signaling networks. *Int J Obes (Lond)*. 2010;34 Suppl 1:S28–33.
211. Scheideler M, Elabd C, Zaragosi L-E, u. a. Comparative transcriptomics of human multipotent stem cells during adipogenesis and osteoblastogenesis. *BMC Genomics*. 2008;9:340.
212. Wurmbach E, Yuen T, Sealfon SC. Focused microarray analysis. *Methods*. 2003;31(4):306–316.
213. Elabd C, Chiellini C, Carmona M, u. a. Human multipotent adipose-derived stem cells differentiate into functional brown adipocytes. *Stem Cells*. 2009;27(11):2753–2760.
214. Cannon B, Nedergaard J. Brown adipose tissue: function and physiological significance. *Physiol. Rev.* 2004;84(1):277–359.
215. Sun L, Xie H, Mori MA, u. a. Mir193b-365 is essential for brown fat differentiation. *Nat. Cell Biol.* 2011;13(8):958–965.